

デザイン・ガイド: TIDA-00366

電流、電圧、温度保護機能を搭載した強化絶縁型 3 相インバータのリファレンス・デザイン



概要

このリファレンス・デザインでは、強化絶縁型ゲート・ドライバ UCC21530、強化絶縁型アンプ AMC1301 と AMC1311、および TMS320F28027 MCU を使用して設計した最大定格 10kW の 3 相インバータのリファレンス・ソリューションを紹介します。MCU の内部 ADC と接続した AMC1301 を使用してモータ電流を測定し、ブートストラップ電源を使用して IGBT ゲート・ドライバを駆動することで、システム・コストを低減しています。このインバータは、過負荷、短絡、グラウンド・フォルト、DC バス低電圧および過電圧、IGBT モジュール過熱に対する保護を備えています。

設計リソース

TIDA-00366	デザイン・フォルダ
UCC21530, AMC1311	プロダクト・フォルダ
AMC1301, OPA320	プロダクト・フォルダ
TLC372, TLV1117-33	プロダクト・フォルダ
TLV70450, REF2033	プロダクト・フォルダ
TL431B, SN74LVC1G11	プロダクト・フォルダ
SN74LVC1G32	プロダクト・フォルダ
LAUNCHXL-F28027	ツール・フォルダ
TIDA-00199	ツール・フォルダ

特長

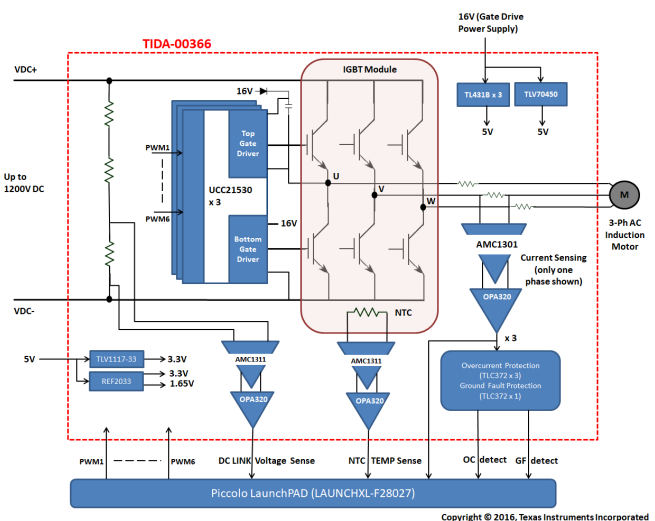
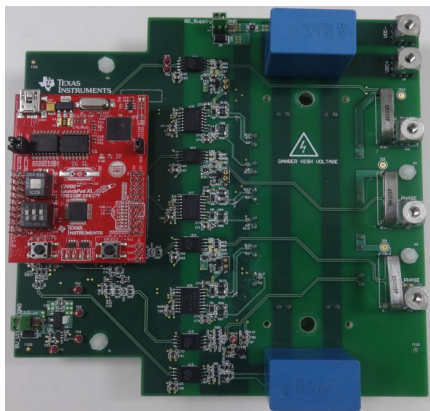
- AC 200V~690V の駆動に適した最大定格 10kW の強化絶縁型インバータ
- 4A ソースおよび 6A シンク出力電流を駆動可能なシンプルで効率的なゲート・ドライバ
- 広帯域幅 (200kHz 超) の強化絶縁型アンプによるインバータ電流、DC バス電圧、IGBT モジュール温度測定、MCU の内部 ADC を使用可能
- 較正済みの電流測定機能は、-25°C~85°C の全温度範囲にわたって±0.5% の精度を実現
- DC バスの低電圧、過電圧、過負荷、地絡、過熱に対する保護
- ハイサイド・ゲート・ドライバにブートストラップ・ベースの電源を使用し、電源要件の総コストを低減

アプリケーション

- 可変速 AC ドライブ
- 3 相 UPS
- 産業用電源
- 太陽光インバータ



E2E エキスパートに質問



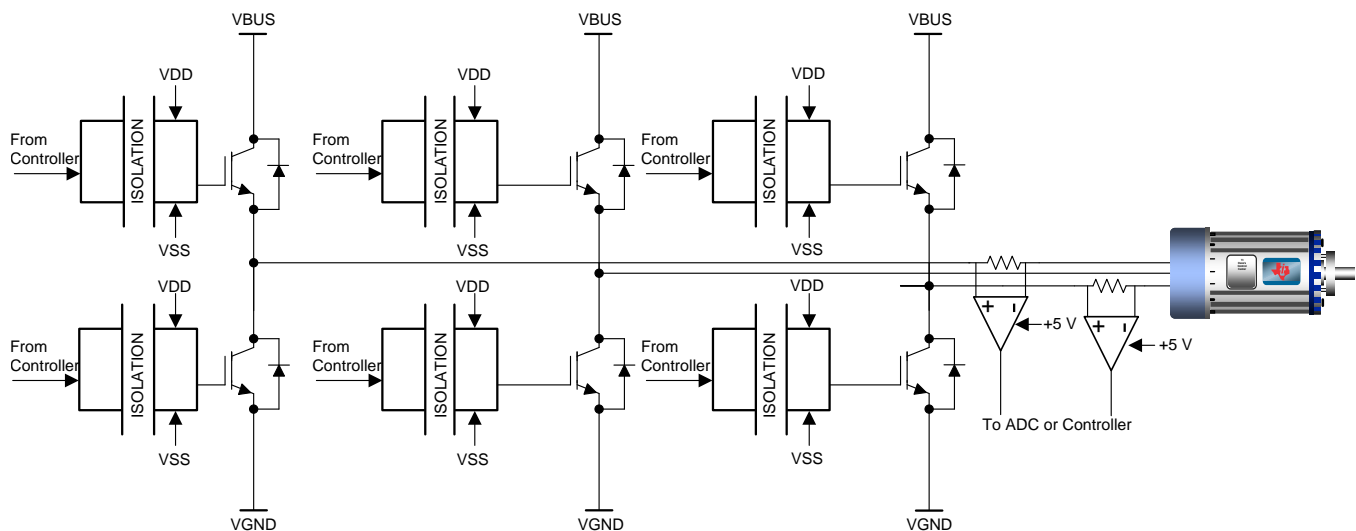


使用許可、知的財産、その他免責事項は、最終ページにあるIMPORTANT NOTICE (重要な注意事項)をご参照くださいますようお願いいたします。

1 System Description

Insulated gate bipolar transistors (IGBTs) are mostly used in three-phase inverters that have numerous applications like variable-frequency drives that control the speed of AC motors, uninterruptible power supply, solar inverters, and other similar inverter applications. IGBTs have advantages such as high input impedance as the gate is insulated, a rapid response ability, good thermal stability, simple driving circuit, good ability to withstand high voltage, snubber-less operation, and controllability of switching behavior to provide reliable short-circuit protection. The IGBT is a voltage-controlled device, which gives it the ability to turn on and off very quickly.

A typical application of a three-phase inverter using six isolated gate drivers is shown in [Figure 1](#). Note that each phase uses a high-side and a low-side IGBT switch to apply positive and negative high-voltage DC pulses to the motor coils in an alternating mode. The output voltage to the motor is controlled by pulse width modulation (PWM). The output voltage is an average of the peak or maximum voltage and the amount of time the transistor is turned on or off.



Copyright © 2016, Texas Instruments Incorporated

図 1. Three-Phase Inverter With Isolated Gate Drive

Apart from isolated gate-drivers for IGBTs, the three-phase inverters include DC bus voltage sensing, inverter current sensing, IGBT protection (like over-temperature, overload, ground fault, and so on).

There are many end applications such as HVAC, solar pumps, and appliances where cost is major concern without compromising the performance. High-end three-phase inverters use $\Sigma\Delta$ modulators for current sensing, which also asks for using expensive controllers with built-in SINC filters. Using an isolated amplifier enables interfacing with low-cost M4 core MCU or TI's Piccolo with a built-in SAR analog-to-digital converter (ADC). The overload protection can be implemented in external hardware, which reduces software complexity. The isolated gate drivers need different supplies for both high-side and low-side gate drivers. Instead of using expensive isolated supplies for powering the gate drivers, using a bootstrap power supply reduces BOM cost on the power supply and also reduces the board space.

DC-Link sensing is an important parameter in the motor control algorithm and is required to be sensed with an accuracy of 1%. The DC-link sensing circuits employ a high impedance voltage divider to scale the voltage to a lower level. However, this causes DC-link feedback signals to have high source impedance. A high impedance source will affect the gain error and offset error if it is in the same range as the input impedance of the isolated sensing amplifier. However, this error can be mitigated by using the AMC1311 which has very high input impedance in the giga ohm range. The high input impedance of the AMC1311 makes the effect of source impedance negligible.

2 Key System Specifications

表 1. Key System Specifications

PARAMETER	SPECIFICATION
DC bus input voltage	400 V to 1200 V
Gate driver supply voltage	16 V for low-side IGBT gate-driver, 15 V (bootstrapped) for high-side IGBT gate-driver
IGBT power module	Voltage rating: 1200 V Current rating: 50 A or more
Rated power capacity	10 kW
Inverter switching frequency	15 kHz (default); adjustable through software
Isolation	Reinforced (IEC61800-5)
Microcontroller	TMS320F28027
Operating ambient temperature	-25°C to 85°C
Motor	Three-phase 400-V AC induction motor
Power supply specification for MCU	3.3 V \pm 5%
Feedbacks	Current sensing, DC link voltage sensing, IGBT module temperature sensing
Current sensing accuracy	\pm 0.5%
DC-Link bus voltage sensing accuracy	\pm 1%
Protections	Overload, overvoltage, undervoltage, ground-fault, over-temperature
PCB	160 \times 156 mm, 4 layers, 2-oz. copper

3 Block Diagram

Figure 2 shows the system level block diagram for the TIDA-00366.

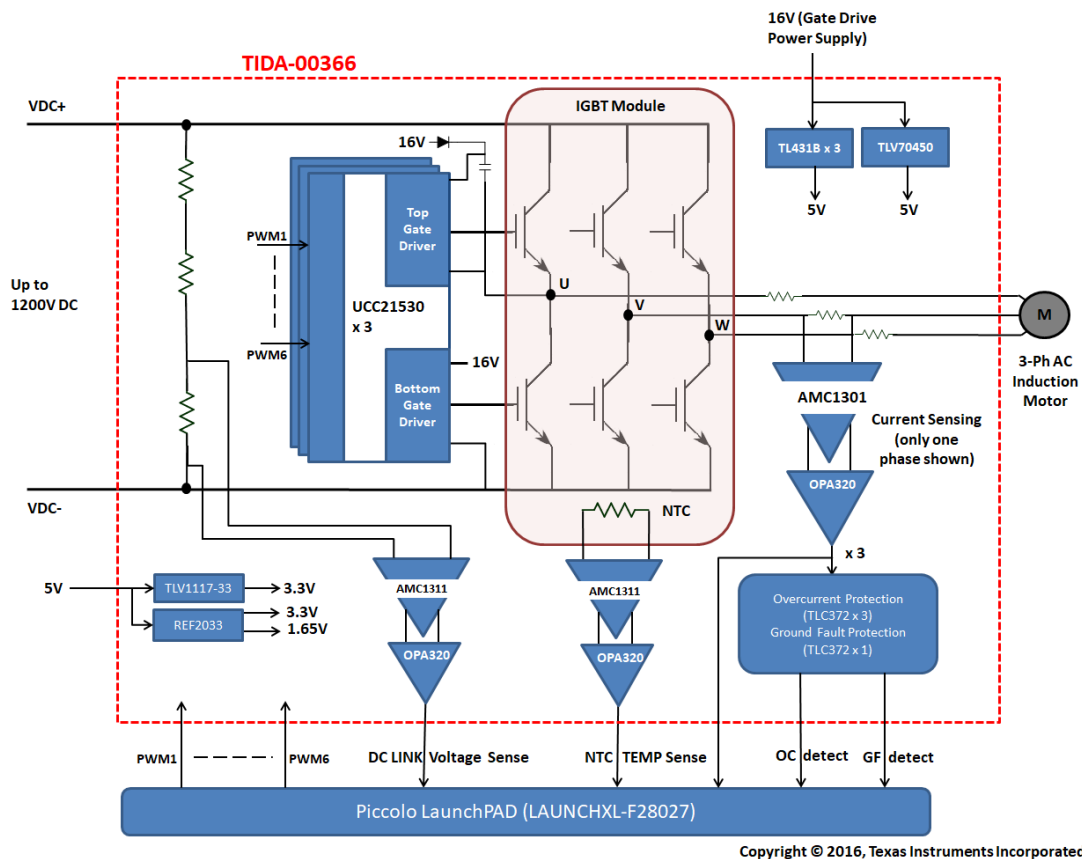


Figure 2. System Level Block Diagram for TIDA-00366

This design provides a reference solution for a three-phase inverter rated up to 10 kW. As shown in Figure 2, the design uses three reinforced isolated dual IGBT gate drivers (UCC21530) to drive six IGBTs. The IGBTs are integrated into a module along with a temperature sensor (NTC). The IGBTs inside the module are configured in half-bridge configurations. Each half-bridge is driven by two IGBT gate-drivers—top (high-side) and bottom (low-side). The design is interfaced with TI's Piccolo LaunchPad, LAUNCHXL-F28027 through two 20-pin connectors. The complementary PWM signals are generated from the LaunchPad. The three mid-points of IGBT half-bridges are connected to motor terminals. The board is designed to operate up to 1200-V DC for the inverter DC bus voltage.

Accurate phase current sensing with three-phase brushless motors is critical for motor drive performance, efficiency, and protection. This design uses in-phase current sensing using three 5-mΩ shunts and three reinforced isolated amplifiers (AMC1301). The benefits of using in-phase current sensing are:

1. constant motor current flowing through the shunt, independent of IGBT switching, and
2. easy detection of terminal-to-terminal short and terminal to GND short.

The voltage generated across the shunt is amplified using the reinforced isolated amplifier AMC1301. The output of the AMC1301 is signal conditioned and converted to a single-ended signal using the OPA320. Outputs of all the three channels are fed into microcontroller (MCU).

The inverter is designed to protect against overload, short circuit, ground fault, DC bus undervoltage and overvoltage, and IGBT module over-temperature. The DC bus voltage is dropped down using the resistor divider and fed to one more AMC1311 for sensing. The under- and overvoltage are programmed in the MCU using the sensed signal. Similarly, the signal from NTC (integrated into IGBT module) is sensed using the AMC1311, and the sensed signal is fed to the MCU for over-temperature protection. The overload, short-circuit, and ground fault protections are implemented using comparators TLC372, which use the current sensed from the three shunts.

The board is powered through two external power supplies: one 16 V and the other 5 V. The low-side IGBT gate-drivers are powered using 16 V, and high-side IGBT gate-drivers are powered using a bootstrapped supply generated from 16 V. The MCU, op amps, and comparators are powered using 3.3 V generated from a 5-V supply using the TLV1117-33. The design uses the TLV70450, TL431B, and REF2033 to generate other rails and references on the board.

Lower system cost is achieved by using the isolated amplifiers AMC1301 and AMC1311 to measure motor current, DC-Link voltage, and NTC voltage. The signals are interfaced with an internal ADC of the MCU. The system cost is also reduced by using a bootstrap power supply configuration for IGBT gate drivers.

3.1 Highlighted Products

3.1.1 UCC21530

The UCC21530 is an isolated dual-channel gate driver with a 4-A source and a 6-A sink peak current. It is designed to drive IGBTs and SiC MOSFETs up to 5 MHz with a best-in-class propagation delay and pulse-width distortion. The input side is isolated from the two output drivers by a 5.7-kV_{RMS} reinforced isolation barrier, with a minimum of 100-V/ns common-mode transient immunity (CMTI). Internal functional isolation between the two secondary-side drivers allows a working voltage of up to 1850-V DC. An enable pin pulled low shuts down both outputs simultaneously and allows normal operation when left open or pulled high. As a fail-safe measure, primary-side logic failures force both outputs low. The device accepts VDD supply voltages up to 25 V. A wide input VCCI range from 3 to 18 V makes the driver suitable for interfacing with both analog and digital controllers.

3.1.2 AMC1311

The AMC1311 device is a precision, high-impedance input isolated amplifier with an output separated from the input circuitry by an isolation barrier that is highly resistant to magnetic interference. This barrier is certified to provide reinforced galvanic isolation of up to 7 kV_{PEAK} according to VDE V 0884-11 and UL1577. Used in conjunction with isolated power supplies, this device prevents noise currents on a high common-mode voltage line from entering the local ground and interfering with or damaging sensitive circuitry. The high-impedance input of the AMC1311 device is optimized for connection to high-voltage resistive divider circuits or other voltage signal sources with high output resistance. The excellent performance of the device supports accurate voltage or temperature sensing and control in closed-loop systems. The integrated common-mode overvoltage and missing high-side supply voltage detection features of the AMC1311 device simplify system-level design and diagnostics.

- 2-V high impedance input voltage range optimized for isolated voltage measurement
- Low offset error and drift: ± 1.6 mV at 25°C, ± 21 μ V/°C
- Fixed gain: 1
- Very low gain error and drift: $\pm 0.3\%$ at 25°C, ± 60 ppm/°C
- Very low nonlinearity and drift: 0.05%, 1 ppm/°C

3.1.3 AMC1301

The AMC1301 is a precision isolation amplifier with an output separated from the input circuitry by an isolation barrier that is highly resistant to magnetic interference. The input of the AMC1301 is optimized for direct connection to shunt resistors or other low-voltage level signal sources. The excellent performance of the device supports accurate current control resulting in system-level power saving and, especially in motor control applications, lower torque ripple.

- ± 250 -mV input voltage range optimized for current measurement using shunt resistors
- Low offset error and drift: ± 200 μ V at 25°C, ± 3 μ V/°C
- Fixed gain: 8.2
- Very low gain error and drift: $\pm 0.3\%$ at 25°C, ± 50 ppm/°C
- Very low nonlinearity and drift: 0.03%, 1 ppm/°C

3.1.4 OPA320

The OPA320 is precision, low-power, single-supply op amp optimized for very low noise. Operated from a voltage range from 1.8 to 5.5 V, the device is well-suited for driving ADCs. With a typical offset voltage of 40 μ V and very low drift over temperature (1.5 μ V/°C typical), it is very well suited for applications like control loop and current sensing in motor control.

3.1.5 TLC372 (Q-Version)

The TLC372 consists of two independent voltage comparators, each designed to operate from a single power supply (3- to 16-V range). The outputs are open-drain configurations and can be connected to achieve positive-logic wired-AND relationships. The TLC372Q is characterized for operation from -40°C to 125°C . The typical response time of comparators for the switching is 200 ns.

3.1.6 TLV1117-33 (I-Version)

The TLV1117 is a positive low-dropout voltage regulator designed to provide up to 800 mA of output current. The internal circuitry is designed to operate down to 1-V input-to-output differential. Dropout voltage is specified at a maximum of 1.3 V at 800 mA, decreasing at lower load currents. With excellent line and load regulations, the device is available in multiple packages and works for a temperature range from -40°C to 125°C .

3.1.7 TLV70450

The TLV70450 is a 5-V LDO with ultralow quiescent current and operates over a wide operating input voltage of 2.5 to 24 V. The device is an excellent choice for industrial applications that undergo large line transients. The TLV70450 is available in a 3-mm \times 3-mm SOT23-5 package, which is ideal for cost-effective board manufacturing.

3.1.8 REF2033

The REF2033 offers excellent temperature drift (8 ppm/°C, max) and initial accuracy (0.05%) on both the V_{REF} and V_{BIAS} outputs while operating at a quiescent current less than 430 μ A. In addition, the V_{REF} and V_{BIAS} outputs track each other with a precision of 6 ppm/°C (max) across the temperature range of -40°C to 85°C . All these features increase the precision of the signal chain and decrease board space, while reducing the cost of the system as compared to a discrete solution. Extremely low dropout voltage of only 10 mV allows operation from very low input voltages.

3.1.9 TL431B (Q-Version)

The TL431 is a three-terminal adjustable shunt regulator with specified ranges for thermal stability over temperature. The output voltage can be set to any value between V_{REF} (approximately 2.5 V) and 36 V, with two external resistors. Active output circuitry provides a very sharp turn-on characteristic, making these devices excellent replacements for Zener diodes in many applications. The "B-grade" version comes with initial tolerances (at 25°C) of 0.5% and TL431BQ devices are characterized for operation from –40°C to 125°C.

3.1.10 SN74LVC1G11

The SN74LVC1G11 performs the Boolean function $Y = A \cdot B \cdot C$ or $Y = \overline{(\overline{A} + \overline{B} + \overline{C})}$ in positive logic. With a supply range from 1.65 to 5.5 V and availability in multiple packages, this AND gate is characterized for operation from –40°C to 125°C.

3.1.11 SN74LVC1G32

The SN74LVC1G32 is a single 2-input positive-OR gate which performs the Boolean function $Y = A + B$ or $Y = \overline{(\overline{A} \cdot \overline{B})}$ in positive logic. The device is available in a variety of packages, including the ultra-small DPW package with a body size of 0.8 × 0.8 mm.

4 System Design Theory

4.1 DC Bus Voltage Input

The TIDA-00366 is designed to operate for a DC bus voltage up to 1200 V. The DC bus voltage can be applied to the TIDA-00366 at terminals J7 (VDC+) and J9 (VDC-). To keep the board compact and cost optimized, the bulk capacitors are not provided on the board. Most of the ripple current is expected to be sourced from external capacitors. Two polyester capacitors (C89 and C90 with value of 5 μ F/1300 V each) are used across the DC bus to suppress high frequency noise as shown in [Fig. 3](#).

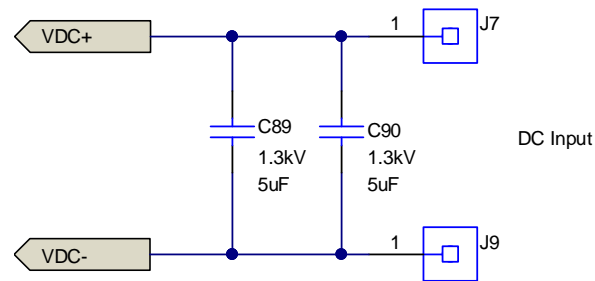


Fig. 3. DC Input

4.1.1 Bleeder Resistors

As shown in [Fig. 4](#), a series combination of five 100-k Ω resistors is connected across the DC bus terminals. The purpose of these bleeder resistors is to discharge the electric charge stored in the filter capacitors when the DC bus voltage is turned off for safety reasons. It eliminates the possibility of a leftover charge causing electric shock. The total current taken by these bleeder resistor when DC bus voltage is connected is $1200 \text{ V}/500 \text{ k}\Omega = 2.4 \text{ mA}$.

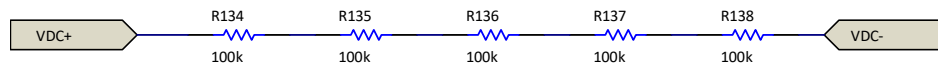


Fig. 4. Bleeder Resistors

4.2 Inverter Stage

The three-phase inverter is designed to operate from the DC bus voltage up to 1200 V. This design uses an IGBT module instead of discrete IGBTs.

4.2.1 IGBT Module

This reference design is intended to support various makes of IGBT modules so a commonly used footprint of IGBT module is selected. The power stage is designed to deliver up to 10 kW. The power stage is supplied with 800-V DC replicating high DC bus voltage during regeneration. Considering the safety factor and switching spikes, IGBTs were selected with the voltage rating equal to 1200 V. The current rating of the IGBT depends on the peak winding current. The three-phase inverter bridge is switched such that the sinusoidal current is injected into the motor windings.

- Motor rating (P_{OUT}) = 10 kW
- Line-to-line voltage (V_{LL}) = 415-V AC
- Power factor considered = 0.9
- Typical motor efficiency $\eta_{MOTOR} = 85\%$

The current through the winding is calculated using 式 1.

$$I_{LL(RMS)} = \frac{P_{OUT}}{\eta_{MOTOR} \times V_{LL} \times \sqrt{3} \times \cos \Phi} = \frac{10 \text{ kW}}{0.85 \times 415 \times \sqrt{3} \times 0.9} = 18.18 \text{ A}_{RMS} \quad (1)$$

The peak value of the winding current is calculated in 式 2.

$$\sqrt{2} \times I_{LL(RMS)} = \sqrt{2} \times 18.18 = 25.7 \text{ A}_{PEAK} \tag{2}$$

Considering an overloading of 200%, the peak winding current would be ~51 A. For this reference design, the following IGBT module is used. It has a continuous collector current carrying capacity of 85 A at TC = 25°C and a peak current capacity of 100 A.

The selection of IGBT module with a built-in NTC Thermistor is preferred to avoid thermal breakdown of the IGBT. This IGBT temperature rise information is routed to the MCU to take necessary action.

図 5 shows the connections for IGBT module and shunts connected in-phase for current sensing.

The design uses the MIXA60W1200TED (from IXYS). Other modules with the same layout footprint and similar specifications can also be used.

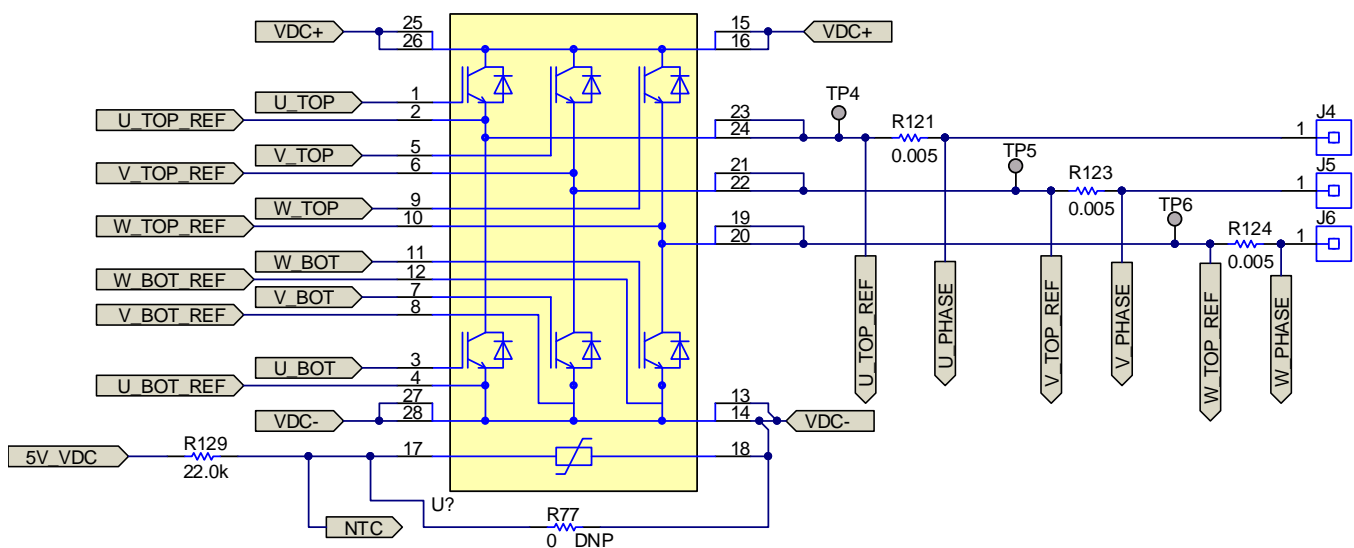


図 5. IGBT Module Connections

図 6 shows the grounding scheme used in the design. The reference points (U_BOT_REF, V_BOT_REF, and W_BOT_REF) are connected together to VDC- through 0-Ω resistors R133, R139, and R140 respectively. They are also connected with the GND1 (ground for a 16-V gate-drive power supply) through one more 0-Ω resistor R142. The placements of these shorting links are important in the layout. 図 88 and 図 89 show the placements in the layout.

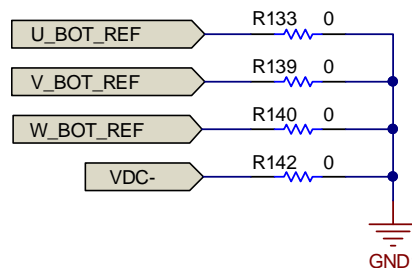


図 6. Grounding Scheme

4.3 Isolated IGBT Gate Driver

注: The TIDA-00366 is designed for a three-phase inverter, but this section explains the circuits and components for one channel (U-Phase) only. The same explanation is applicable to two other channels (V-Phase and W-Phase).

A three-phase inverter application uses six power switches (IGBTs in this case). To drive these switches, six totally independent gate drivers are required. Also, with a high-voltage operation, it is necessary to have enough isolation between primary and secondary side of the gate-driver. The UCC21530 is an isolated dual-channel gate driver with a 4-A source and a 6-A sink peak current. It is designed to drive power MOSFETs, IGBTs, and SiC MOSFETs up to 5 MHz with best-in-class propagation delay and pulse width distortion. The input side is isolated from the two output drivers by a 5.7-kV_{RMS} reinforced isolation barrier, with a minimum of 100-V/ns common mode transient immunity (CMTI). Internal functional isolation between the two secondary-side drivers allows a working voltage of up to 1850-V_{MAX} DC. The internal structure of the UCC21530 is shown in 図 7.

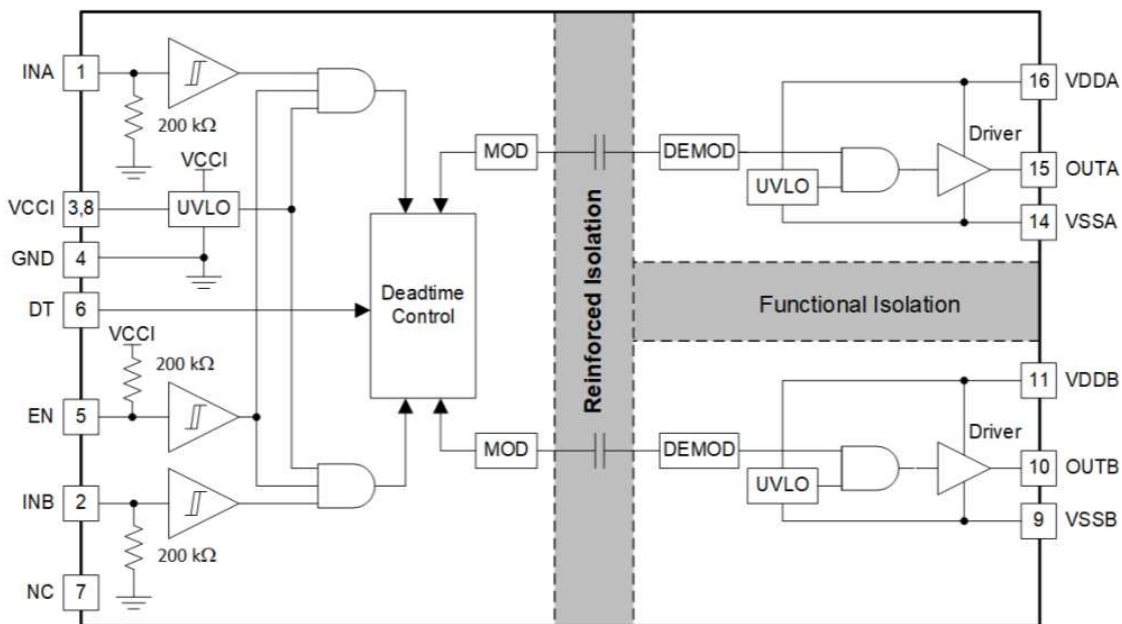


図 7. Functional Block Diagram of UCC21530

This driver can be configured as two low-side drivers, two high-side drivers, or a half-bridge driver with programmable dead time (DT). An enable pin pulled low shuts down both outputs simultaneously and allows normal operation when left open or pulled high. As a fail-safe measure, primary-side logic failures force both outputs low. The device accepts VDD supply voltages up to 25 V. A wide input VCCI range from 3 to 18 V makes the driver suitable for interfacing with both analog and digital controllers. All the supply voltage pins have undervoltage lockout (UVLO) protection. With all these advanced features, the UCC21530 enables high efficiency, high power density, and robustness in a wide variety of power applications. Fig 8 shows the circuit for the UCC21530 and associated components implemented for half-bridge configuration for a three-phase inverter.

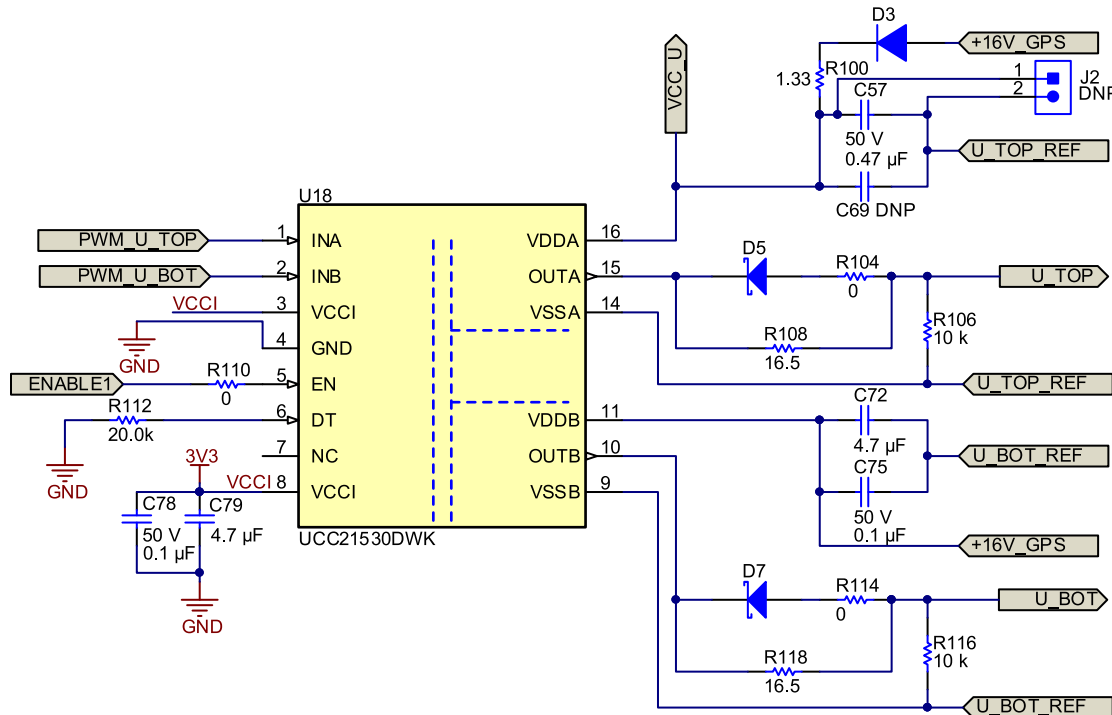


図 8. Gate Driver UCC21530 and Related Components and Circuits

4.3.1 Control Supply for Primary Side

VCCI pins (Pin 3 and Pin 8) are supplied with 3.3 V generated using the TLV1117-33 (as explained in 4.11.1). C78 (0.1 μF) and C79 (4.7 μF) are used as local decoupling capacitors for VCCI pins.

4.3.2 PWM Inputs

The PWM signals "PWM_U_TOP" and "PWM_U_BOT" are generated from LaunchPad with a dead time of 1.4 μs.

4.3.3 Dead Time Control

The UCC21530 has a programmable dead time function using the DT pin. Tying DT to VCCI disables the DT feature and allows the outputs to overlap. Placing a resistor R112 between DT and GND adjusts dead time according to 式 3.

$$DT(\text{in ns}) = 10 \times R_{DT}(\text{in k}\Omega) \tag{3}$$

A 20-k Ω resistor is connected between DT pin and GND pin sets the dead time to 200 ns as per 式 3. This resistor must be selected for 1% tolerance to prevent any drift in the dead time. For this design, the dead time is controlled using MCU.

4.3.4 Enable (EN) Signal for Gate Drivers

The EN pin is used to enable the gate drivers. It disables both driver outputs if asserted low and enables if set high or left open. The EN pin is only functional when VCCI stays above the UVLO threshold. Tie this pin to VCCI if it is not used to achieve better noise immunity. In this design, the EN pin is generated as explained in 4.9.

4.3.5 Supply for Low-Side Gate Drivers

The low-side gate drivers for all three channels are powered using 16V_GPS, which is supplied externally from connector J8 as shown in 図 9. Diode D12 is used for reverse-polarity protection for this supply and C88 (10 μ F) is used as decoupling capacitor for the same. R141 is used as shorting link for connecting the GND1 (ground for 16V_GPS) and VDC-. The placement of this shorting link in layout is shown in 図 88.

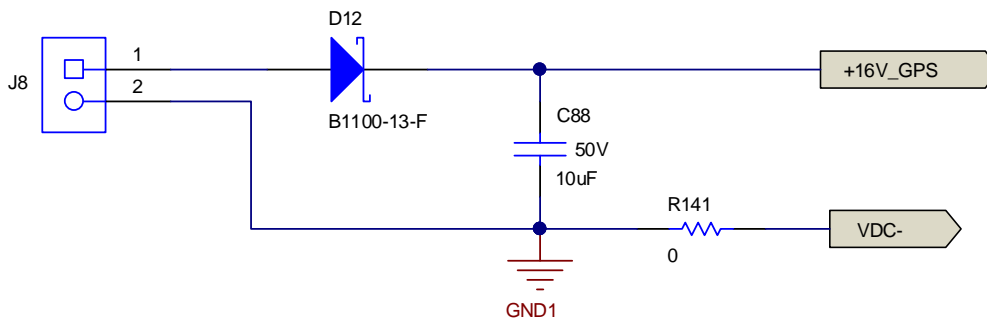


図 9. Gate Driver Power Supply

As shown in 図 8, VDDB is secondary-side power for driver B. It is supplied with 16V_GPS and locally decoupled to VSSB using low ESR/ESL capacitors C75 (0.1 μ F) and C72 (4.7 μ F) located as close to the device as possible. VSSB is ground for secondary-side driver B and ground reference for secondary side B channel.

4.3.6 Bootstrap Power Supply for High-Side Gate Drivers

One of the most widely used methods to supply power to the high-side drive circuitry of a gate driver IC is the bootstrap power supply. The bootstrap power supply consists of a bootstrap diode and a bootstrap capacitor (with an optional series resistor). This method has the advantage of being both simple and low cost. The maximum voltage that the bootstrap capacitor (V_{BS}) can reach is dependent on the elements of the bootstrap circuit. Consider the voltage drop across R_{BOOT} , V_F of the bootstrap diode, and the drop across the low-side switch ($V_{CE(ON)}$ or V_{FP} , depending on the direction of current flow through the switch).

4.3.6.1 Selection of Bootstrap Capacitor (C_{BOOT})

The bootstrap capacitor must be sized to have more than enough energy to drive the gate of the IGBT high without depleting the bootstrap capacitor more than 10%. A good guideline is to size C_{BOOT} to be at least ten times as large as the equivalent IGBT gate capacitance (C_g). C_g must be calculated based on the voltage driving the high-side gate of the IGBT (V_{GE}) and the gate charge of the IGBT (Q_g). V_{GE} is approximately the bias voltage supplied to VDD after subtracting the forward voltage drop of the bootstrap diode D3 (V_{DBOOT}). In this design example, the estimated V_{GE} is approximately 15 V, as 式 4 shows.

$$V_{GE} \approx V_{DD} - V_{DBOOT} = 16 \text{ V} - 1 \text{ V} = 15 \text{ V} \quad (4)$$

The IGBT module in this reference design has a specified Q_g of 0.165 μC . The equivalent gate capacitance of the IGBT can be calculated as 式 5 shows.

$$C_g = \frac{Q_g}{V_{GE}} = \frac{0.165 \mu\text{C}}{15 \text{ V}} = 0.011 \mu\text{F} \quad (5)$$

After estimating the value for C_g , C_{BOOT} must be sized to at least ten times larger than C_g , as 式 6 shows.

$$C_{BOOT} \geq 10 \times C_g = 10 \times 0.011 \mu\text{F} = 0.11 \mu\text{F} \quad (6)$$

For this reference design, a 0.47- μF capacitor has been chosen for the bootstrap capacitor.

4.3.6.2 Selection of Bootstrap Diode

The voltage that the bootstrap diode encounters is the same as the full DC bus voltage (in this case a maximum of 1200-V DC). The bootstrap diode voltage rating must be greater than the DC bus rail voltage. The bootstrap diode must be a fast recovery diode to minimize the recovery charge and thereby the charge that feeds from the bootstrap capacitor to the 16-V supply. The diode must be able to carry a pulsed peak current of 11.28 A (as per 式 11). However, the average current is much smaller and depends on the switching frequency and the gate charge requirement of the high-side IGBT. This TIDA-00366 reference design uses a 1300-V, 1-A, fast recovery diode BYG23T-M3.

The bootstrap diode power dissipation (P_{DBOOT}) can be estimated based on the switching frequency, diode forward voltage drop, and the switching frequency of the PWM signal (f_{SW}). In this reference design, the switching frequency has been set to 15 kHz. 式 7 calculates the estimated power loss for the bootstrap diode.

$$P_{DBOOT} = \frac{1}{2} \times Q_g \times f_{SW} \times V_{DBOOT} = \frac{1}{2} \times 0.165 \mu\text{C} \times 15 \text{ kHz} \times 1 \text{ V} = 1.2375 \text{ mW} \quad (7)$$

4.3.6.3 Selection of Current Limiting Resistor for Bootstrap Diode

Considering that having a 2-V(p-p) ripple on the bootstrap capacitor, the charge on the 0.47- μF capacitor is:

$$Q = C \times V = 0.47 \mu\text{F} \times 2 = 0.94 \mu\text{C} \quad (8)$$

For a capacitor charging period of 1.25 μs , the same charge is also represented as 式 9.

$$Q = 0.94 \mu\text{C} = I_{CH} \times 1.25 \mu\text{s} \quad (9)$$

This gives $I_{CH} = 0.752 \text{ A}$.

With a voltage drop across diode being 1 V, the R_{BOOT} is calculated as:

$$R_{BOOT} = \frac{V_{DBOOT}}{I_{CH}} = \frac{1}{0.752} = 1.329 \Omega \quad (10)$$

The TIDA-00366 uses R_{BOOT} value of 1.33 Ω .

With $R_{BOOT} = 1.33 \Omega$, the bootstrap diode current is calculated as 式 11.

$$I_{\text{DBOOT(pk)}} = \frac{V_{\text{DD}} - V_{\text{DBOOT}}}{R_{\text{BOOT}}} = \frac{16 - 1}{1.33} = 11.28 \text{ A} \quad (11)$$

The power dissipation capability of the bootstrap resistor is important. The bootstrap resistor must be able to withstand the short period of high power dissipation during the initial charging sequence of the bootstrap capacitor.

4.3.7 Gate Resistors

The gate current and the appropriate power of the voltage supply depend on the operating frequency, bias control voltages, and total gate charge. The total gate charge is published in IGBT datasheets, depending on gate control voltage. The gate charge necessary for switching is very important to establish the switching performance of IGBT. The lower the charge, the lower is the gate-drive current needed for a given switching time. The gate current can be controlled using external gate resistor between driver output and gate of IGBT. The value of the gate resistor determines the peak charge and discharge currents. The most classical way to influence the switching behavior of an IGBT is by selecting the gate resistors. The gate resistors can be different for the on and off switching process. In such cases, the turn-on gate resistor is denominated with $R_{G(on)}$ and turning off with $R_{G(off)}$ as shown in 図 10. The effective values of gate resistors become:

- Effective $R_{G(on)} = R_{Gon}$
- Effective $R_{G(off)} = R_{Gon} // R_{Goff}$

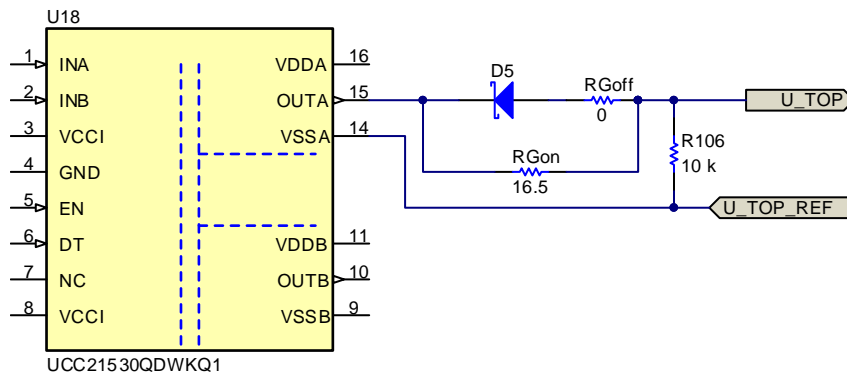


図 10. Gate Resistors

Depending on the gate resistor, both the voltage gradient (dv/dt) as well as the current gradient (di/dt) is modified. The higher the resistance of $R_{G(on)}$, the softer the switching of the IGBT (and correspondingly, the turn-off of the free-wheeling diode). As a consequence, however, the turn-on losses of the IGBT increase (and the recovery losses of free-wheeling diode decrease).

For the TIDA-00366, $R_{G(on)} = 16.5 \Omega$ and $R_{G(off)} = 0 \Omega$. With the internal gate resistance of 4Ω , the gate currents are calculated as:

- Source current = $16 \text{ V} / (16.5 + 4) \Omega = 780 \text{ mA}$
- Sink current = $16 \text{ V} / 4 \Omega = 4 \text{ A}$ approximately (considering zero on-resistance of diode)

Another important point to highlight is that 図 8 shows 10-k Ω resistors across the gate and emitter terminals of the IGBTs. These resistors are a safety precaution and are placed across these nodes to ensure that the IGBTs are not turned on if the UCC21530 is not in place or not properly soldered on the circuit board.

4.4 Isolated Current Sensing Circuit

注: The TIDA-00366 is designed for a three-phase inverter, but this section explains the circuits and components for one channel (U-Phase) only. The same explanation is applicable to other two channels (V-Phase and W-Phase).

The current sensing is done using three shunts in-phase with the inverter outputs. 4.4.1 explains the selection of shunt value.

4.4.1 Selection of Shunt Resistor for Inverter

As explained in 4.2.1, the peak winding current can go up to 51 A. Considering 50 A as the peak current (with some margin), the shunt value can be calculated as given in 式 12.

$$R_{\text{SHUNT}} = \frac{\pm 250 \text{ mV}}{\pm 50 \text{ A}} = 5 \text{ m}\Omega \quad (12)$$

where $\pm 250 \text{ mV}$ is the input voltage range for the AMC1301.

4.4.2 Reinforced Isolated Amplifier AMC1301

The AMC1301 is a precision isolation amplifier with an output separated from the input circuitry by an isolation barrier that is highly resistant to magnetic interference. The input of the AMC1301 is optimized for direct connection to shunt resistors. 図 11 shows the circuit and components related to the AMC1301.

VDD1 is the power supply and GND1 is ground for the hot side of the circuit, where the inputs VINP and VINN are coming directly from the 5-m Ω shunt resistor. VDD1 generation from the bootstrap supply is explained in 4.4.2.1. GND1 is connected to "U_TOP_REF" terminal, which is the mid-point of the connection between the top and bottom IGBT of the half-bridge. The capacitors C4 (4.7 μF) and C5 (0.1 μF) are used to decouple the VDD1 supply and must be kept very close to the VDD1 pin of the AMC1301 in the layout. For any noise filtering required by the user, a differential RC filter is provided (R10, R17, and C10). To test the TIDA-00366 no filtering is used so R10 = R17 = 0 Ω and C10 = DNP.

On the cold side, VDD2 is generated from an LDO TLV1117-33 as explained in 4.11.1. The capacitors C6 (4.7 μF) and C7 (0.1 μF) are used to decouple the VDD2 supply and must be kept very close to the VDD2 pin of the AMC1301 in the layout. The output of the AMC1301 is available on Pins VOUTP and VOUTN. A differential filter with a cutoff frequency of 95 kHz is connected at the output using R12 (4.7 k Ω), R15 (4.7 k Ω) and C11 (180 pF).

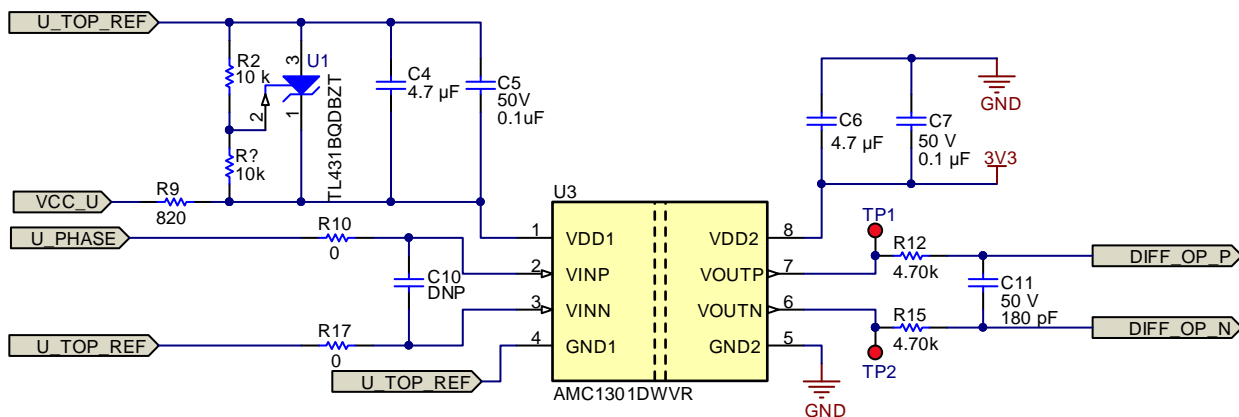


図 11. Reinforced Isolated Amplifier AMC1301

4.4.2.1 Primary-Side Supply Generation Using TL431B

The power supply for a high-side gate-driver is generated using the bootstrap circuit. The reference point for the high-side IGBT gate driver and related circuitry is "U_TOP_REF". The same reference is used for the current sensing circuit, and that is why it is necessary that the power supply for VDD1 for the AMC1301 is also generated from the same bootstrap supply. Figure 12 shows the power supply generation for VDD1 of the AMC1301 using the TL431B shunt regulator. The internal reference value for the TL431B is 2.5 V, which helps decide the output voltage.

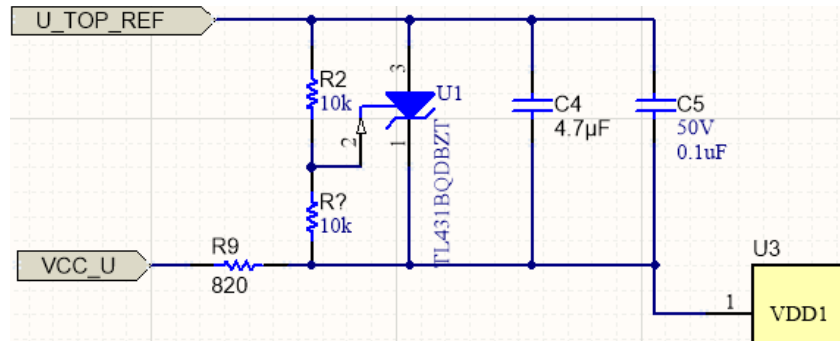


Figure 12. Power Supply Generation Using TL431B

4.4.3 Differential-to-Single-Ended Conversion Using OPA320

The output of the AMC1301 is differential and has a common-mode voltage of 1.4 V. To interface it with the MCU, the output of the AMC1301 needs to be converted to a single-ended form and must range between 0 to 3.3 V (because of the limitations from the MCU power supply).

4.4.3.1 Selection of Op Amp

The op-amp selection is an integral part of the signal chain for measuring the current, DC link voltage, and IGBT module temperature. For the op amp, consider the following parameters:

- *Offset voltage:* The offset voltage specification for the op amp adds into the overall measurement accuracy, so the lowest offset voltage is preferred for the op amp.
- *Offset voltage drift:* The signal chain accuracy is measured from a temperature range of -25°C to 85°C . The offset voltage drift must be low so as to get lowest error through the specified temperature range. If available, zero drift op-amps are preferred.
- *Rail-to-rail input and output:* The input and output of the op amp must go to both rails so as to use the full range of 1.65 V on both positive and negative cycles (when the output is interfaced with the MCU).
- *Input common-mode range:* The input of op-amp must be able to take a common-mode voltage of $V_{DD}/2$, which equals 1.65 V for this application.
- *Common-mode rejection ratio (CMRR):* The switching frequency of typical three-phase industrial inverter goes up to 16 to 20 kHz. The CMRR greater than 80 dB at 100 kHz (approximately five times the switching frequency of inverter) is generally preferred for such applications.

With these specifications, the cost of the op amp should be as low as possible. This design uses the OPA320 with the specifications shown in 表 2.

表 2. Key Specifications for OPA320

PARAMETER	VALUE
Supply voltage (V)	1.8 to 5.5 V
I_Q /GBW ratio	1.2 mA/20 MHz 60 $\mu\text{A}/\text{MHz}$
Noise at 1 kHz (nV/rtHz)	8 nV/rtHz
Rail-to-rail	RRIO Input extend $\pm 100\text{-mV}$ beyond rail V_{OUT} to $\pm 10\text{ mV}$
Zero crossover	Yes
Input bias max (pA)	1 pA max.
Offset voltage (mV)	100 μV , max.
Offset drift	0.5 $\mu\text{V}/^{\circ}\text{C}$
Packaging	SOT23-5, SOT23-6

Note that five single op amps are used to simplify the component placement in the PCB layout. Using the OPA320 ensures high precision and excellent signal linearity over the entire input common-mode range, making it ideal for driving sampling ADCs.

4.4.3.2 Calculation of Gain for the Amplifier

The AMC1301 datasheet has a specified linear full-scale range ($V_{INP} - V_{INN}$) of -250 to 250 mV . With a nominal gain of 8.2, the V_{OUT} range is -2.05 to 2.05 V . So, $V_{OUT(p-p)}$ for the AMC1301 = 4.10 V .

$V_{OUT(p-p)}$ required from the OPA320 = 3.24 V (the voltage output swing can go up to 30 mV close to both rails). This means the op amp must have a gain of 0.79 as calculated in 式 13.

$$\text{Op amp gain} = \frac{3.24}{4.10} = 0.79\text{ V/V} \tag{13}$$

4.4.3.3 Component Selections

The output of the AMC1301 is filtered using a differential filter (a combination of R12, R15, and C11) with a cutoff frequency of approximately 94 kHz.

The gain for the differential amplifier is calculated in 式 14.

$$\text{Differential amplifier gain} = \frac{R_F}{R_{IN}} = \frac{7.5 \text{ k}\Omega}{4.7 \text{ k}\Omega + 4.7 \text{ k}\Omega} = 0.7978 \text{ V/V} \quad (14)$$

図 13 shows the circuit for the differential amplifier to convert the differential output of the AMC1301 to single-ended to feed into the MCU. The output of the differential amplifier is routed through two paths—one going to the MCU pin (I_U) with an RC filter (cutoff frequency > 1 MHz and time delay of 150 ns) and the other going to the comparator for overload protection. Note that I_U also goes to the ground fault comparator as explained in 4.8.

If the delay created by the op-amp circuit is too high, then a bypass path is also given through the DNP resistor R18 to send the current sense signal to the comparator directly.

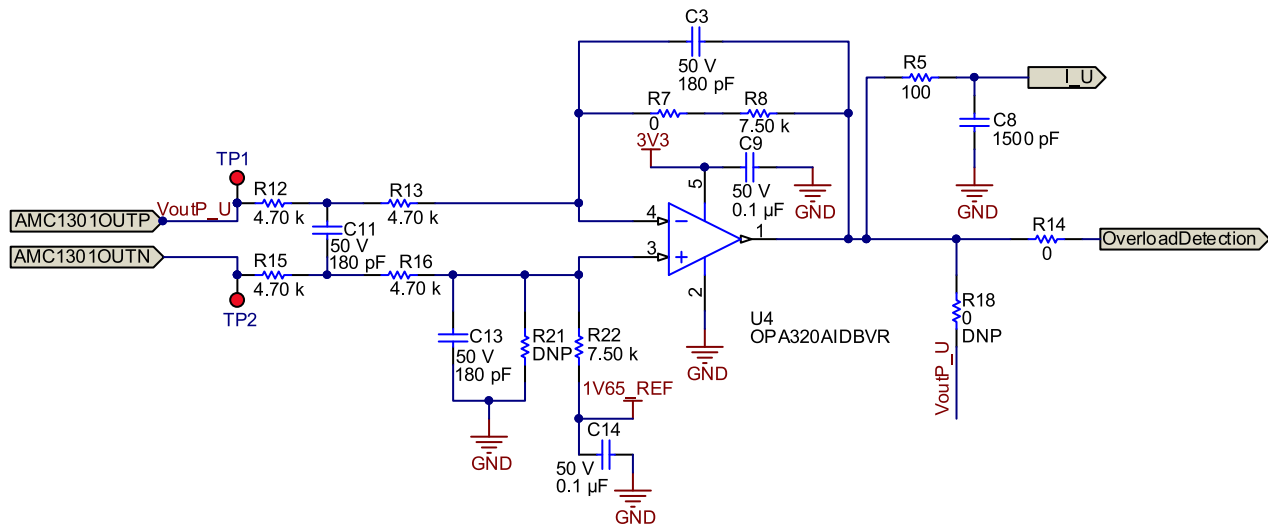



図 13. Differential-to-Single Ended Signal Conversion

4.5 DC Bus Voltage Sensing Circuit

The design implements undervoltage and overvoltage protections on the DC bus by measuring DC bus voltage. The DC bus input voltage is scaled down and fed to the MCU using the AMC1311 reinforced isolation amplifier, and op amp OPA320. The output of the OPA320 can directly drive an ADC input or can be further filtered before processed by the ADC.

To scale down the DC bus voltage, a resistor divider network is chosen considering the maximum voltage for the MCU ADC input as 3.3 V and the maximum DC bus voltage to be measured as 800 V.

To achieve better linearity and noise performance of the device, the allowable input voltage between the amplifier pin VINP and VINN is 2 V. The voltage divider resistor is selected such that input voltage to the amplifier is less than 2 V at maximum DC bus condition.

As shown in , five 200-kΩ resistors and a 2.49-kΩ resistor are used to drop the VDC signal.

注: The undervoltage for this design can be set at 400-V DC, hence anything below 400 V should not be measured. In that case, use two 200-V Zener diodes (currently DNP) connected in parallel with two 200-kΩ resistors.

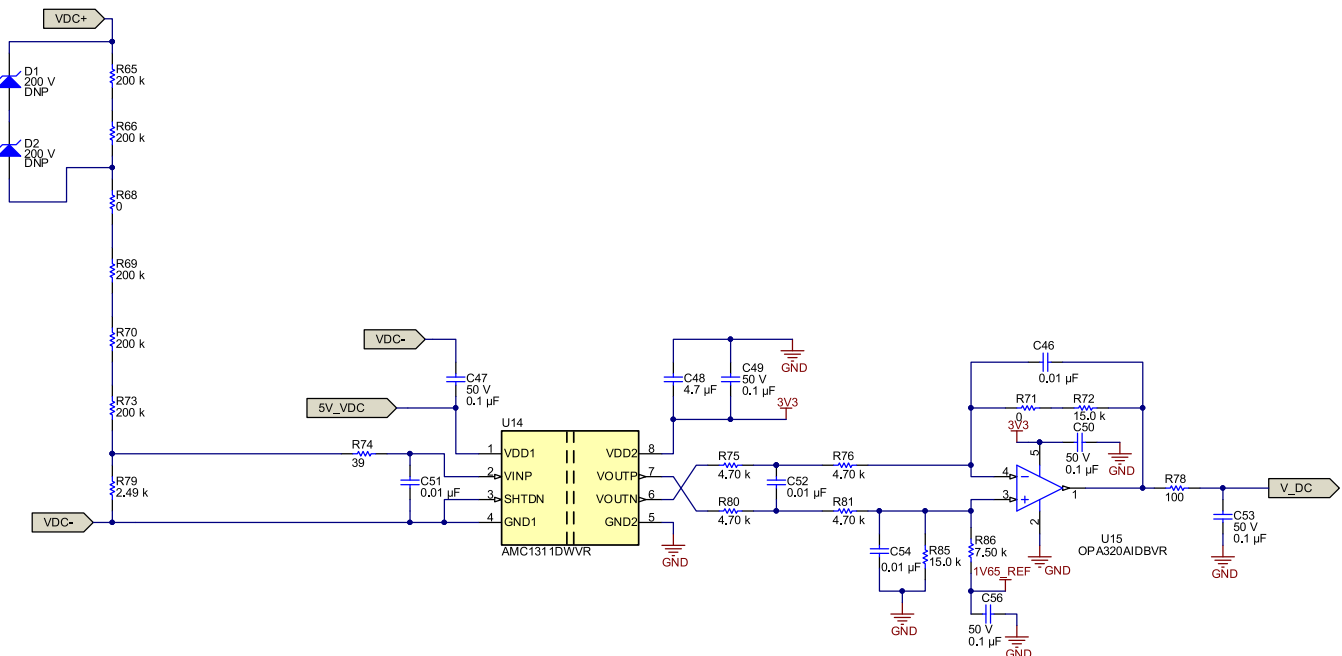


図 14. DC Bus Voltage Sensing Circuit

4.5.1 Calculation of Gain for Differential to Single Ended Conversion for Voltage Sensing

The AMC1311 data sheet has a specified linear full-scale range of 0 V to 2 V. With a nominal gain of 1, the VOUT range is 0 V to 2 V. So VOUT (P-P) for the AMC1311 is 2 V. VOUT (P-P) required from the OPA320 is 3 V (the voltage output swing can go up to 30 mV close to both the rails). The op amp must have a gain of 1.5, calculated as $Opamp\ Gain = 3/2 = 1.5\ V/V$.

4.5.2 Component Selections

The output of the AMC1311 is filtered using a differential filter (a combination of R75, R80, and C52) with a cutoff frequency of approximately 94 kHz. The gain for the differential amplifier is calculated in the following equation.

$$\text{Differential Amplifier Gain} = \frac{R_f}{R_n} = \frac{15 \text{ k}\Omega}{(4.7 \text{ k}\Omega + 4.7 \text{ k}\Omega)} = 1.5957 \text{ V / V} \quad (15)$$

4.6 NTC Temperature Sensing Circuit

The IGBT module used in this design has an integrated NTC thermistor. The characteristics of this NTC are shown in [Fig 15](#).

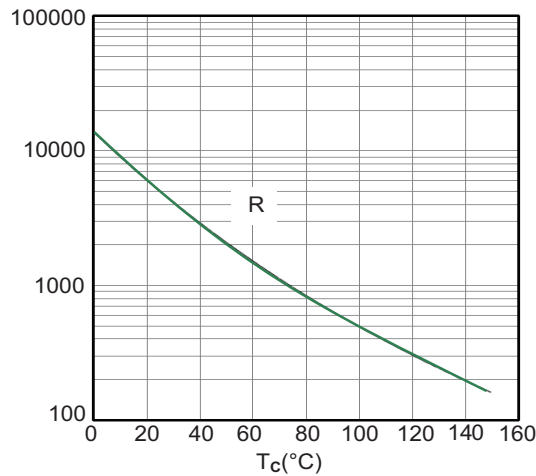


Fig 15. NTC Characteristics

The design implements over-temperature protection by sensing the NTC voltage and providing the signal to the MCU for shutting off the PWMs. The NTC is biased using one resistor R129 (22 kΩ) as shown in [Fig 5](#). The biased signal is given to the VINP pin of the AMC1311 as shown in [Fig 16](#). The sensed signal is filtered using a differential filter at the input of the AMC1311. The differential output of the AMC1311 is filtered and converted to single-ended signal by the OPA320 with the gain of 1.5. The output of the OPA320 is filtered using an RC filter (cutoff frequency = 16 kHz and RC delay = 10 μs) and fed to the MCU as a "MODULE_TEMP" signal.

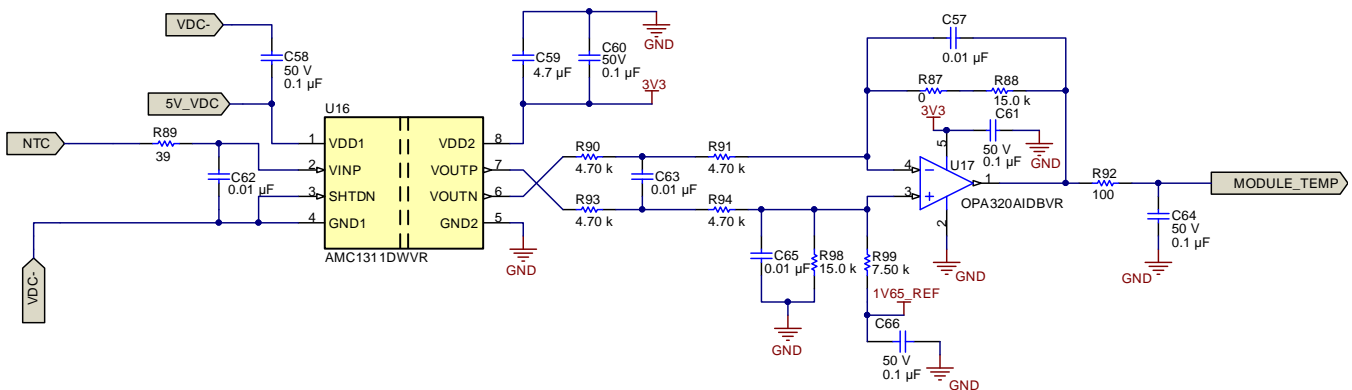


Fig 16. NTC Temperature Sensing Circuit

4.7 Overload (or Overcurrent) Protection

注: The TIDA-00366 is designed for a three-phase inverter, but this section explains the circuits and components for one channel (U-Phase) only. The same explanation is applicable to two other channels (V-Phase and W-Phase).

4.7.1 Selection of Comparators

A typical industrial drive needs to have overload protection to operate within 300 to 500 ns. The TLC372 helps reach this goal. The TLC372 is very low cost and a dual-channel comparator. It operates from a supply range from 3 to 16 V and has a typical response time of 200 ns.

4.7.2 Calculation of Threshold Levels

Considering $50 A_{PEAK}$ as the threshold for ground fault condition (which is ~200% of rated current), 表 3 shows the calculations that are used to select the resistors for setting the threshold on the comparators.

- $I_{SENSE(RMS)} = 35.4 A$
- $I_{SENSE(PEAK)} = 50 A$
- $R_{SHUNT} = 5 m\Omega$

表 3. Calculations of Threshold Levels for Overload Protection

PARAMETER	EQUATION	CALCULATED VALUE	UNIT
Input to AMC1301 (peak)	$I_{SENSE(PEAK)} \times R_{SHUNT}$	250	mV
Output of AMC1301 (peak)	Input to AMC1301 \times 8.2	2.05	V
Output of op-amp stage (peak)	Output of AMC1301 \times 0.7978	1.63549	V
With VDD for TLC372 = 3.3 V, the reference mid-point value is $(3.3 V/2) = 1.65 V$			
High threshold	$1.65 V +$ Output of op-amp stage (peak)	3.28549	V
Low threshold	$1.65 V -$ Output of op-amp stage (peak)	0.01451	V

4.7.3 Calculation of Resistors for Setting the Threshold

The high threshold is set by resistors R4 and R11, whereas the low threshold is set by resistors R11 and R19 as shown in 図 17. Assuming $R4 = R19 = 100 \Omega$, R11 is calculated as $R11 = 10.7 k\Omega$.

As shown in 図 17, the input signal for the comparators (which is compared with threshold) is coming from the output of the op-amp stage. The TLC372 is open-drain output comparator, which needs a pullup resistor at the output. R1 serves that purpose. C1 (0.1 μF) is used as decoupling capacitor for the TLC372. C2 (0.1 μF) is used as local decoupling for the threshold generating resistor divider network.

The OVERLOAD signal generated from all the three channels is combined together. It is given to the MCU as well as to the ENABLE logic gate input for further processing.

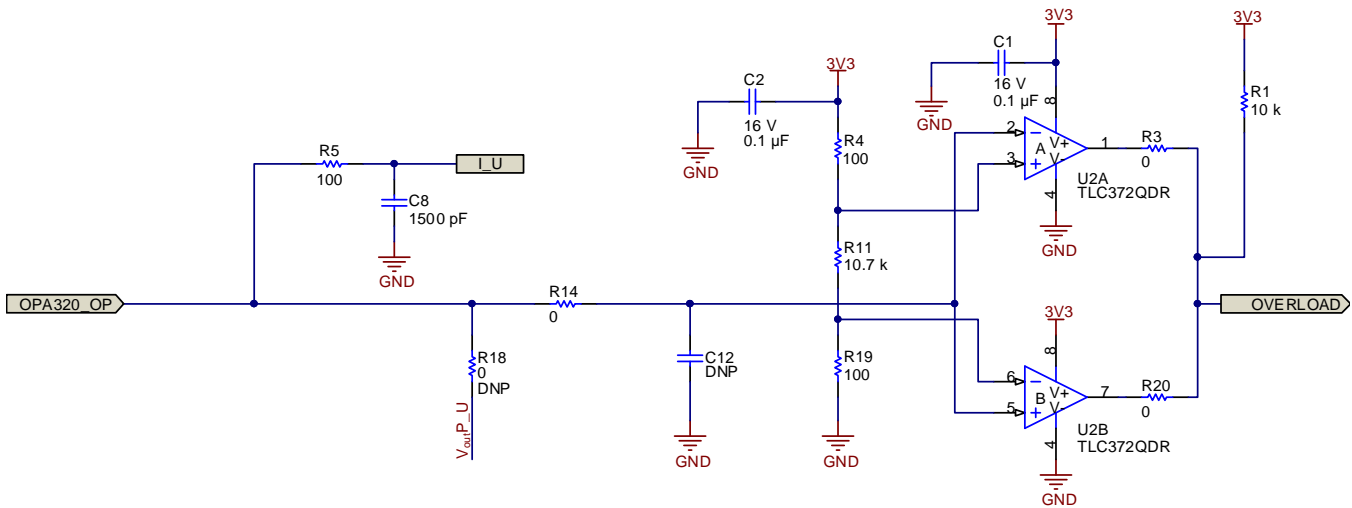


図 17. Overload Protection Circuit

4.8 Ground Fault Protection

4.8.1 Selection of Comparator

A typical industrial drive needs to have ground fault protection to operate within 300 to 500 ns. To reach this goal, the TLC372 is selected. The TLC372 is very low-cost and dual channel comparator. It operates from a supply range from 3 to 16 V and has typical response time of 200 ns.

4.8.2 Calculation of Threshold Levels

Considering $5 A_{PEAK}$ as threshold for ground fault condition (which is ~20% imbalance), the following calculations are used to select the resistors for setting the threshold on the comparators.

- $I_{SENSE(RMS)} = 3.54 A$
- $I_{SENSE(PEAK)} = 5 A$
- $R_{SHUNT} = 5 m\Omega$

表 4. Calculations of Threshold Levels for Ground Fault Protection

PARAMETER	EQUATION	CALCULATED VALUE	UNIT
Input to AMC1301 (peak)	$I_{SENSE(PEAK)} \times R_{SHUNT}$	25	mV
Output of AMC1301 (peak)	Input to AMC1301 \times 8.2	205	mV
Output of op-amp stage (peak)	Output of AMC1301 \times 0.7978	163.549	mV
With VDD for TLC372 = 3.3 V, the reference mid-point value is $(3.3 V/2) = 1.65 V$			
High threshold	$1.65 V + \text{Output of op-amp stage(peak)}$	1.813549	V
Low threshold	$1.65 V - \text{Output of op-amp stage(peak)}$	1.486451	V

4.8.3 Calculation of Resistors for Setting the Threshold

The high threshold is set by resistors R163, R165, and R166 as shown in [Fig. 18](#). Assuming R166 = 10 kΩ, the other two resistors are calculated as R163 + R165 = 8.2 kΩ.

The final values used in the schematic are R163 = 0 Ω, R165 = 8.2 kΩ, and R166 = 10 kΩ.

The low threshold is set by resistors R154, R155, and R158 as shown in [Fig. 18](#). Assuming R158 = 10 kΩ, the other two resistors are calculated as R154 + R155 = 12.2 kΩ.

The final values used in the schematic are R154 = 200 Ω, R155 = 12 kΩ, and R158 = 10 kΩ.

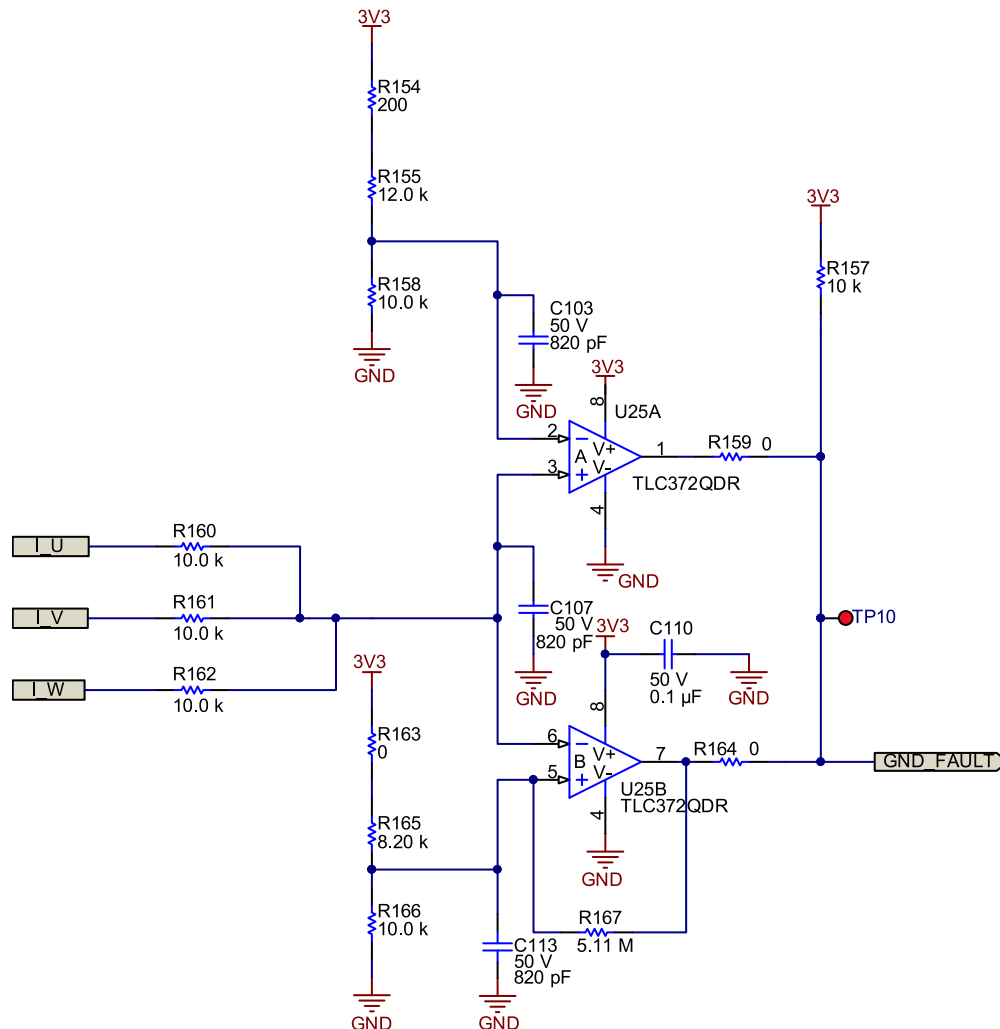


Fig. 18. Ground Fault Detection Circuit

As shown in [Fig. 18](#), the input signal for the comparators (which is compared with threshold) is coming from the output of three op-amp stages and summed together using three 10-kΩ resistors. The TLC372 is an open-drain output comparator, which needs a pullup resistor at the output. R157 serves that purpose. C110 (0.1 μF) is used as decoupling capacitor for the TLC372. C103, C107, and C113 (all equal to 820 pF) are used as local decoupling for the threshold generating resistor divider networks and input signal.

The GND_FAULT signal generated from comparators is given to the MCU as well as to the ENABLE logic gate input for further processing.

4.9 Gate Logic for ENABLE Signal

The ENABLE signal for IGBT gate drivers disable both the driver outputs if asserted low, and enabled if set high or left open. The ENABLE signal for IGBT gate-drivers used on TIDA-00366 design is pulled LOW for the occurrence of following conditions:

1. If any of the three channels have overload condition (that is, OVERLOAD = LOW) OR
2. If earth fault condition has occurred (that is, GND_FAULT = LOW) OR
3. If "TRIP" signal is generated from the microcontroller by user (that is, TRIP = HIGH).

At the PWM startup, a sequence is required that can make the low-side IGBT turn on first so that the bootstrap configuration works properly. This also uses the TRIP signal as explained in 6.3. The logic truth table for generating the ENABLE signal is shown in 表 5.

表 5. Truth Table for Enable Logic

STATE	MCUCntrl	TRIP (A)	GND_FAULT (B)	OVERLOAD (C)	ENABLE (Y)
0	1	X	X	X	1
1	0	0	0	0	0
1	0	0	0	1	0
2	0	0	1	0	0
3	0	0	1	1	0
4	0	1	0	0	0
5	0	1	0	1	0
6	0	1	1	0	0
7	0	1	1	1	1

To fulfill all these conditions, the circuit shown in 図 19 is used to implement the ENABLE logic.

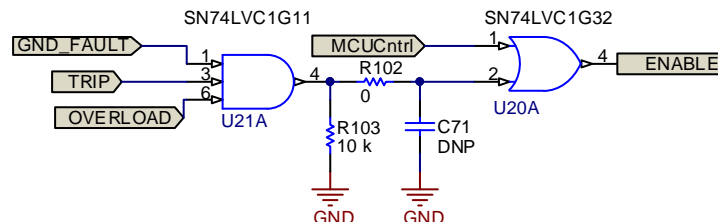


図 19. ENABLE Logic Generation

R103 (10 kΩ) is a pull-down resistor for the output of the AND gate just to make it connected to ground when not driven with the inputs. Also, the RC filter (R102 and C71) is used to set up a delay, required by the user.

When the board is powered up and PWM is not turned on, the "OVERLOAD" and "GND_FAULT" signals will be active low, which will make the ENABLE to go low as per 表 5. If the ENABLE signal is low, the gate-drivers are disabled. To come out of this situation, the ENABLE signal is pulled "High" by making the MCUCntrl signal high for a short duration of time.

4.10 Connectors to Connect C2000 Piccolo LaunchPad

表 6 shows the pinout for C2000 Piccolo LaunchPad. The highlighted pins are used for connecting the TIDA-00366 board.

表 6. C2000 LaunchPad Pinout

MUX VALUE						MUX VALUE			
			3.3 V	1		5 V			
			ADCINA6	2	2	GND			
TZ2	SDAA	SCIRXDA	GPIO28	3	3	ADCINA7			
TZ3	SCLA	SCITXDA	GPIO29	4	4	ADCINA3			
RSVD	RSVD	COMP2OUT	GPIO34	5	5	ADCINA1			
			ADCINA4	6	6	ADCINA0			
	SCITXDA	SPICLK	GPIO18	7	7	ADCINB1			
			ADCINA2	8	8	ADCINB3			
			ADCINB2	9	9	ADCINB7			
			ADCINB4	10	10	NC			
MUX VALUE				J6 PIN	J2 PIN	MUX VALUE			
RSVD	RSVD	EPWM1A	GPIO0			GND			
COMP10 UT	RSVD	EPWM1B	GPIO1	2	2	GPIO19	SPISTEA	SCIRXDA	ECAP1
RSVD	RSVD	EPWM2A	GPIO2	3	3	GPIO12	TZ1	SCITXDA	RSVD
COMP20 UT	RSVD	EPWM2B	GPIO3	4	4	NC			
RSVD	RSVD	EPWM3A	GPIO4	5	5	RESET number			
ECAP1	RSVD	EPWM3B	GPIO5	6	6	GPIO16 and GPIO32	SPISIMOA or SDAA	RSVD or EPWMSYNCI	TZ2 or ADCSOCA
TZ2 or ADCSOC A	RSVD or EPWMSYN CI	SPISIMOA or SDAA	GPIO16 and GPIO32	7	7	GPIO17 and GPIO33	SPISOMIA or SCLA	RSVD or EPWMSYN CO	TZ3 or ADCSOCB
TZ3 or ADCSOC B	RSVD or EPWMSYN CO	SPISOMIA or SCLA	GPIO17 and GPIO33	8	8	GPIO6	EPWM4A	EPWMSYNCI	EPWMSYN CO
			NC	9	9	GPIO7	EPWM4B	SCIRXDA	RSVD
			NC	10	10	ADCINB6			

On the TIDA-00366 board, two 20-pin connectors are used to connect with the C2000 LaunchPad as shown in [Fig. 20](#) and [Fig. 21](#). The PWM signals for the inverter are generated using the LAUNCHXL-F28027 board. The PWM signals generated from the MCU are filtered using an RC filter with values of $R = 100 \Omega$ and $C = 10 \text{ pF}$. This corresponds to a cutoff frequency of 159 MHz and an RC time delay of 1 ns. GND_FAULT and OVERLOAD signals are generated from their respective comparators and are connected to the MCU on GPIOs and also connected to a three-input AND gate as explained in Section 4.9 to generate the ENABLE signal for gate drivers. The TRIP signal is generated from the MCU in case the user wants to interrupt the PWM signals or if the GND_FAULT and OVERLOAD signals need to be latched.

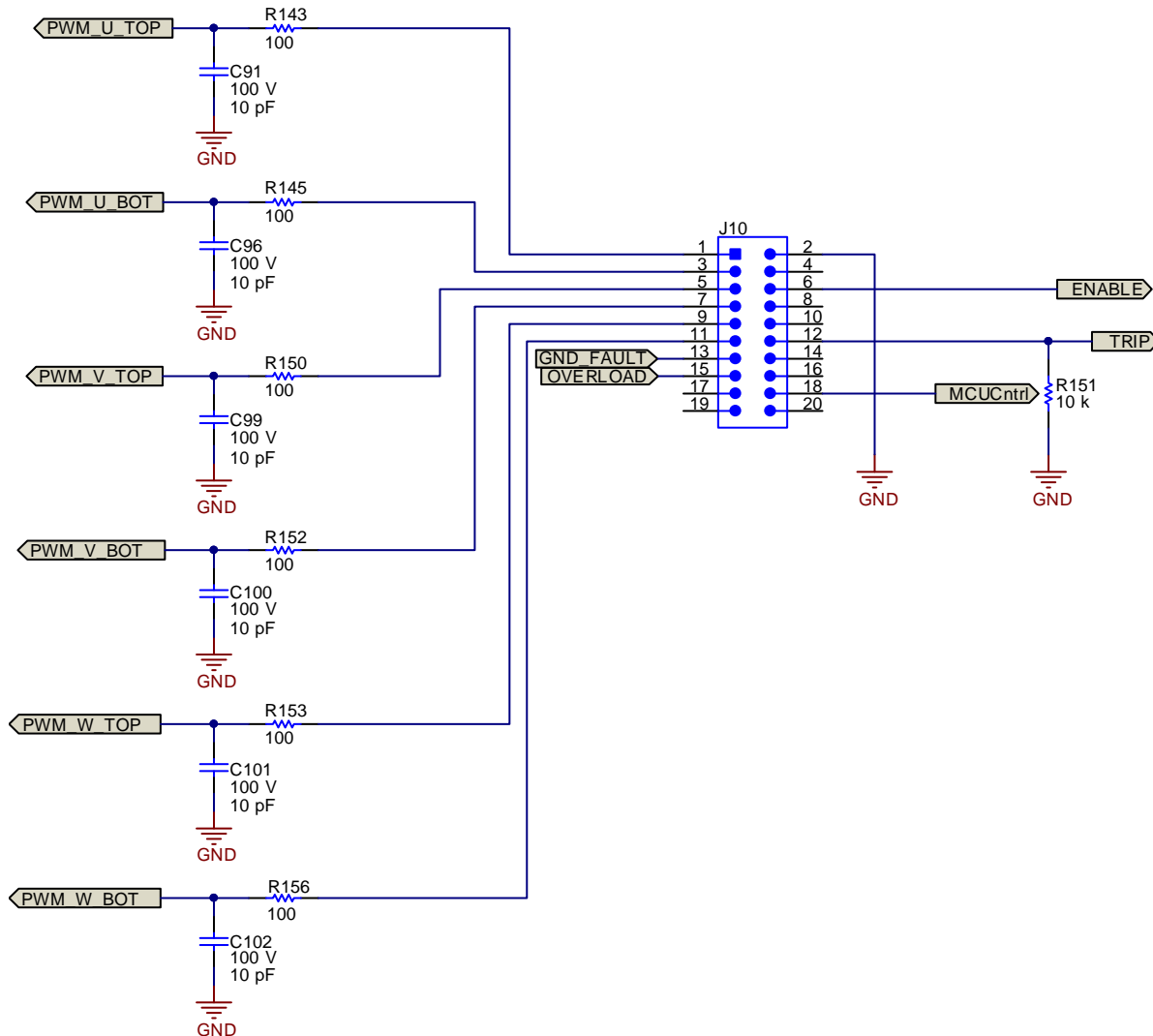
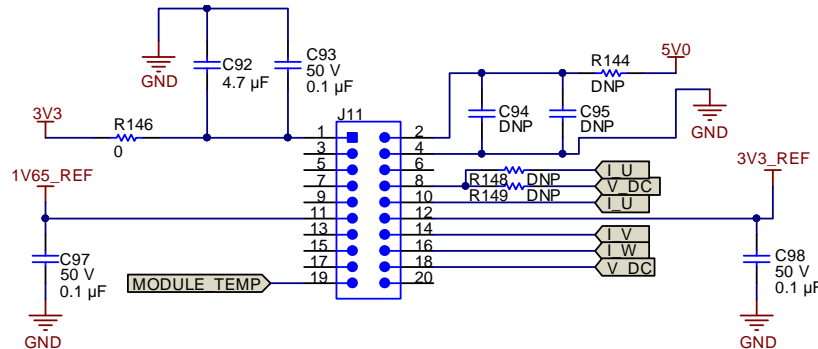


Fig. 20. 20-Pin Connector to Connect With Connectors J6 and J2 on LAUNCHXL-F28027

The 3.3-V supply generated using the TLV1117-33 supplies the LaunchPad as shown in 21. There is also a provision to power the MCU from external 5 V by populating components R144, C94, and C95 on the board. The sensed signals I_U, I_V, I_W, V_DC, and MODULE_TEMP are connected to ADC input pins after the RC filtering (for aliasing). 1V65_REF and 3V3_REF are also provided to ADCs for any ratiometric measurements.



21. 20-Pin Connector to Connect With Connectors J1 and J5 on LAUNCHXL-F28027

4.11 Power Supplies

As explained in the system block diagram in 3, the design uses two external supplies: 5 V for powering the cold side of the design, and 16 V for powering the isolated gate-drivers (near high-voltage side).

4.11.1 3.3-V Generation Using TLV1117-33

A 3.3-V supply is needed to power:

- VDD2 of AMC1301 (output side) used for all current measurement channels
- VDD2 of AMC1311 (output side) used for DC link voltage sensing and temperature sensing circuit
- VCCI of the UCC21530 (input side)
- VDD of the OPA320
- VDD of the TLC372 for overload as well as ground-fault detection circuit
- VCC of the SN74LVC1G11 AND gate
- VCC of the SN74LVC1G32 OR gate
- 3.3-V supply for LAUNCHXL-F28027 board through connector J2 (Pin 1)

To convert 5 V to 3.3 V, the TLV1117-33 is selected for the following reasons:

1. Input voltage range: 4.7 to 15 V (16-V absolute maximum rating)
2. Output current: up to 800 mA
3. Temperature range: -40°C to 125°C

The total current required to be supplied from the TLV1117-33 is ~ 205.87 mA ($3 \times \text{IDD2}$ of the AMC1301, or 3×4.4 mA = 13.2 mA; $2 \times \text{IDD2}$ of the AMC1311, or 2×5.3 mA = 10.6 mA; $3 \times \text{ICCI}$ of the UCC21530, or 3×2 mA = 6 mA; $5 \times \text{IDD}$ of the OPA320, or 5×1.85 mA = 9.25 mA; $4 \times \text{IDD}$ of the TLC372, or 4×400 μA = 1.6 mA; ICC of the SN74LVC1G11 = 10 μA ; ICC of the SN74LVC1G32 = 10 μA ; and a supply current of 150 mA for the LAUNCHXL-F28027 board).

Check the thermal stress on the LDO. The total power it has to dissipate is:

$$P_{LDO(max)} = (V_{LDO(IN)} - V_{LDO(OUT)}) \times i_{LDO(max)} = (5V - 3.3V) \times 190.67 \text{ mA} = 0.324139 \text{ W} \quad (16)$$

For package selection,

$$\theta_{JA(max)} = \frac{(T_J - T_A)}{P_{D(max)}} = \frac{(125^\circ\text{C} - 85^\circ\text{C})}{0.324139 \text{ W}} = 123.40^\circ\text{C} / \text{W} \quad (17)$$

The LDO must have a package with $\theta_{JA} \leq 123.40^\circ\text{C/W}$. Looking at 表 7 from the TLV1117-33 datasheet, all packages are suitable. The TIDA-00366 uses DCY package.

表 7. Thermal Information for TLV1117-33

THERMAL METRIC		TLV1117							UNIT
$R_{\theta JA}$	Junction-to-ambient thermal resistance	38.6	19.2	38.3	104.3	50.9	30.1	27.50	$^\circ\text{C/W}$

The schematic of 5-V to 3.3-V conversion using the LDO TLV1117-33 is shown in 図 22. Diode D13 is used for reverse polarity protection. C106 (10 μF) and C104 (0.1 μF) are the input capacitors. C108 (22 μF) and C109 (0.1 μF) are output capacitors. Output capacitor selection is critical for regulator stability. Larger COUT values benefit the regulator by improving transient response and loop stability. This device is designed to be stable with tantalum and aluminum electrolytic output capacitors having an ESR between 0.2 and 10 Ω. Although an input capacitor is not required for stability, a 10-μF capacitor placed between IN and GND counteracts reactive input sources and improves transient and noise performance. Higher value capacitors are necessary if large load transients with fast rise times are anticipated.

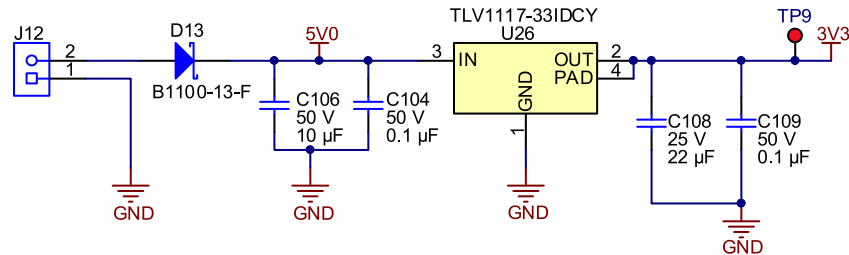


図 22. 3.3-V Generation From 5-V Input

4.11.2 5-V Generation Using TLV70450

A 5-V supply is needed to power VDD1 of the AMC1311 (input side) used for DC link voltage sensing and temperature sensing circuit.

To convert 16 V to 5 V, the TLV70450 is selected for the following reasons:

1. Input voltage range: 2.5 to 24 V
2. Output current: up to 150 mA
3. Temperature range: -40°C to 125°C

The total current required to be supplied from the TLV70450 is ~14.2 mA (7.1 mA for VDD1 of each AMC1311, used for the DC bus sense circuit and NTC module temperature sensing circuit).

Check the thermal stress on the LDO. The total power it has to dissipate is:

$$P_{LDO(max)} = (V_{LDO(IN)} - V_{LDO(OUT)}) \times I_{LDO(max)} = (16V - 5V) \times 14.2 \text{ mA} = 0.1562 \text{ W} \quad (18)$$

For package selection,

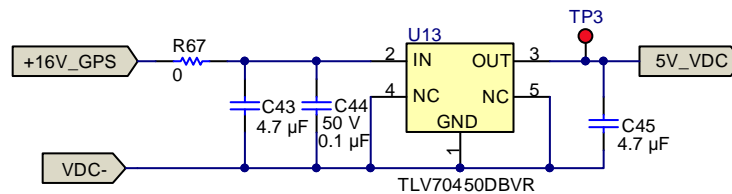
$$\theta_{JA(max)} = \frac{(T_J - T_A)}{P_{D(max)}} = \frac{(125^\circ\text{C} - 85^\circ\text{C})}{0.1562 \text{ W}} = 256.08^\circ\text{C} / \text{W} \quad (19)$$

The LDO must have a package with $\theta_{JA} \leq 256.08^\circ\text{C}/\text{W}$. Looking at 表 8 from the TLV70450 datasheet, DBV (SOT-23) package is suitable.

表 8. Thermal Information for TLV70433

THERMAL METRIC		TLV704	UNIT
R _{nJA}	Junction-to-ambient thermal resistance	213.1	°C/W

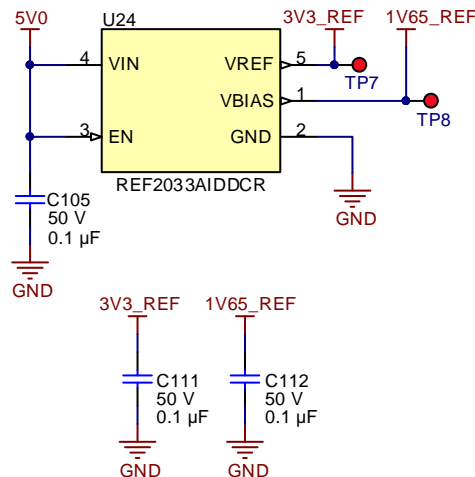
The schematic of the 16-V to 5-V conversion using the LDO TLV70450 is shown in 23. C43 (4.7 μ F) and C44 (0.1 μ F) are the input capacitors, and C45 (4.7 μ F) is output capacitor. Although an input capacitor is not required for stability, when a 0.1- μ F or larger capacitor is placed between IN and GND, it counteracts reactive input sources and improves transient and noise performance. Higher value capacitors are necessary if large load transients with fast rise times are anticipated. The TLV704 requires a 1- μ F or larger capacitor connected between OUT and GND for stability. Ceramic or tantalum capacitors can be used. Larger value capacitors result in better transient and noise performance.



23. 5-V Generation From 16-V Gate Drive Power Supply Input

4.11.3 3.3-V and 1.65-V Reference Generation Using REF2033

Applications with only a positive supply voltage often require additional stable voltage in the middle of the ADC input range to bias input bipolar signals. As explained in 4.4.2, the output of the AMC1301 is bipolar; hence the level shifting is required during the differential-to-single-ended op amp stage. The output of the op amp is interfaced with the MCU (which is operating with a 3.3-V power supply), so the level shifting of signal should be done at 1.65 V. 24 shows the reference voltage generation using the REF2033. The 0.1- μ F capacitors at input and outputs are for noise filtering.



24. 1.65-V and 3.3-V Reference Generation

5 Getting Started Hardware

This section explains the top and bottom views of the PCB for the TIDA-00366 showing all the different sections. It also explains the power supply requirement and connectors used to connect the external world.

5.1 TIDA-00366 PCB Overview

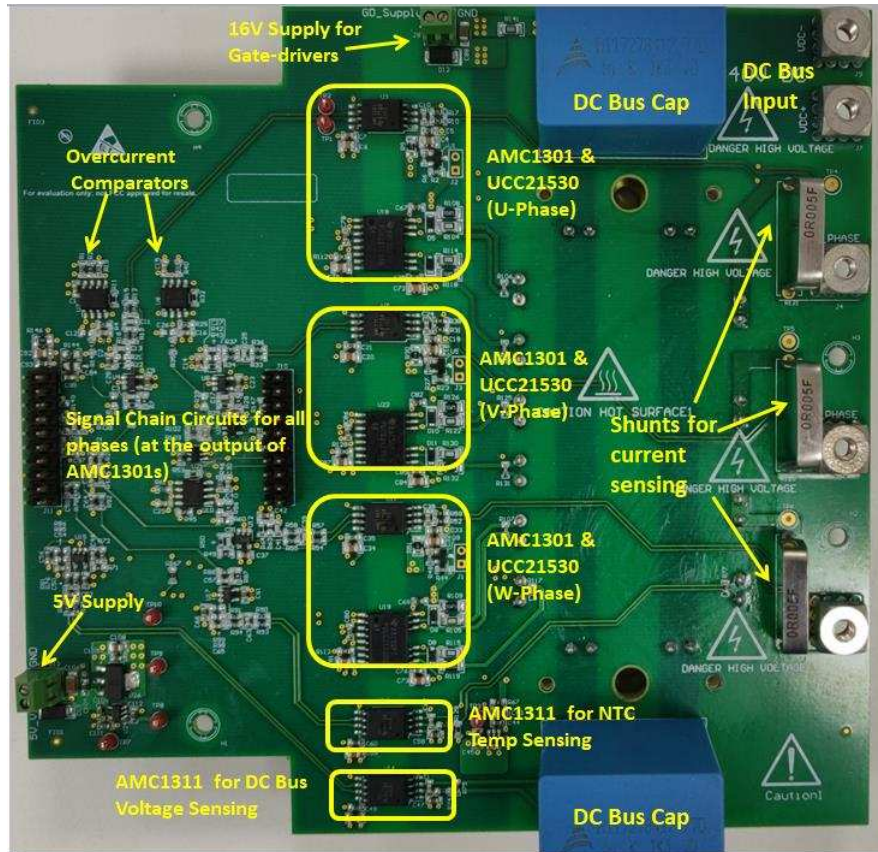


図 25. Top View of PCB for TIDA-00366

Figure 26 shows the bottom view of the TIDA-00366 PCB. The IGBT module is mounted on the bottom layer so it can connect with the heat sink as required by the output power levels.

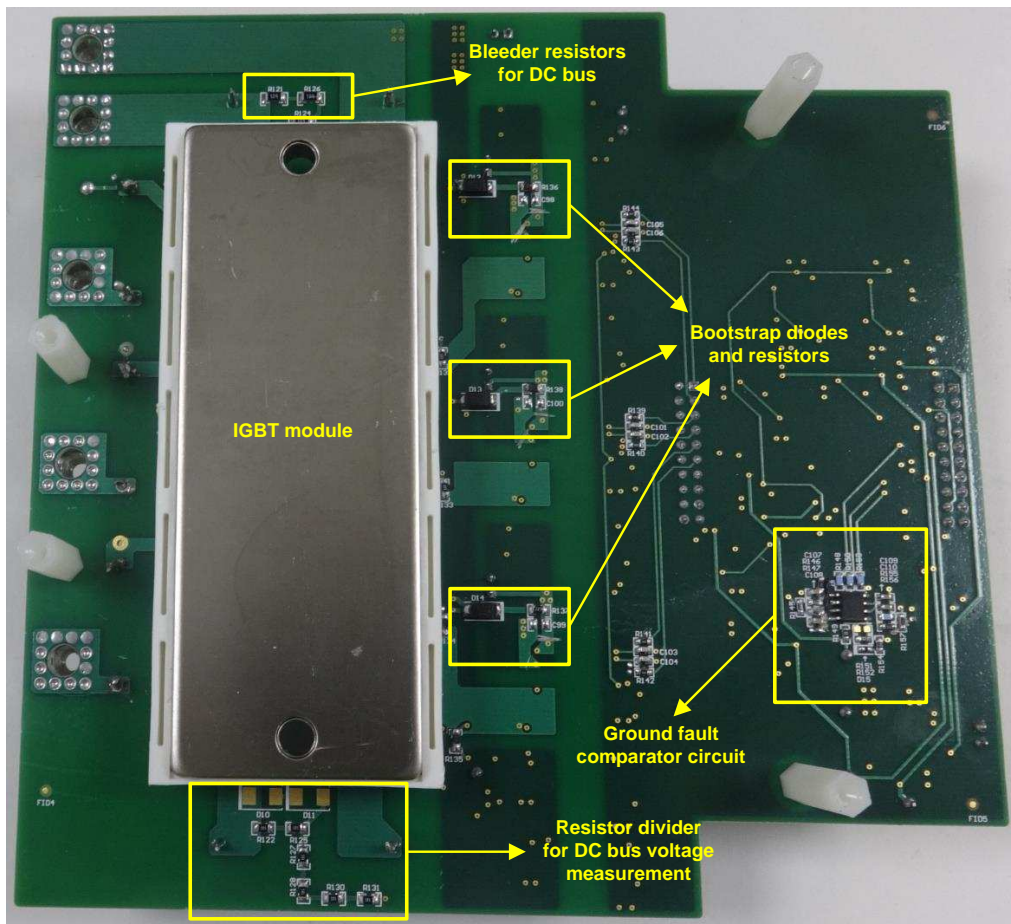


Figure 26. Bottom View of PCB for TIDA-00366

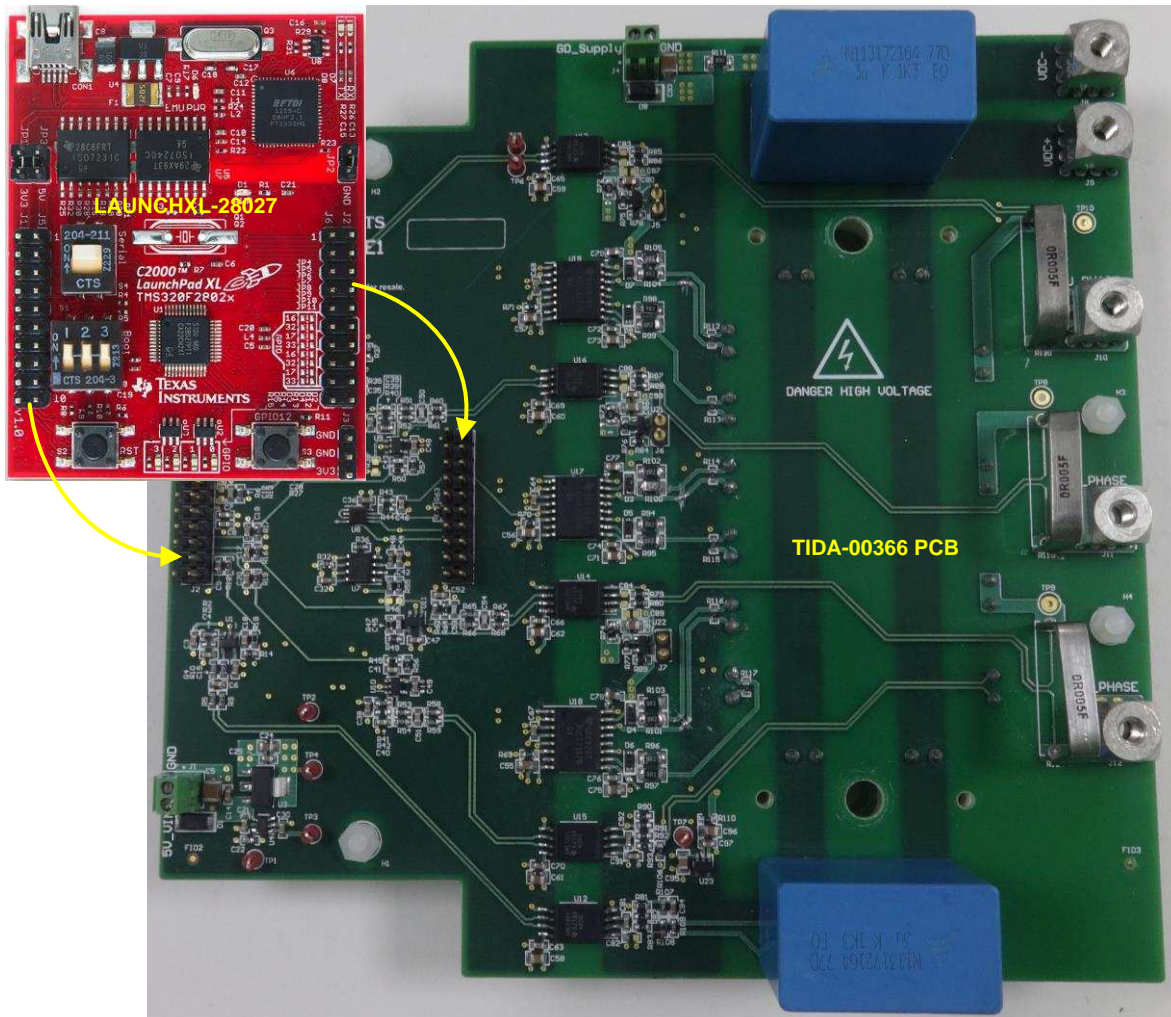
5.2 Connectors

Table 9 shows the connectors used on the TIDA-00366 PCB and their purposes.

Table 9. Connectors

CONNECTOR	PURPOSE
J1	To supply external isolated 16 V for W-Phase high-side gate driver if bootstrap configuration is not used
J2	To supply external isolated 16 V for U-Phase high-side gate driver if bootstrap configuration is not used
J3	To supply external isolated 16 V for V-Phase high-side gate driver if bootstrap configuration is not used
J4	U-Phase output for connecting to the motor
J5	V-Phase output for connecting to the motor
J6	W-Phase output for connecting to the motor
J7	VDC+ input
J8	16-V GD_Supply to power low-side gate drivers
J9	VDC- input
J10	To connect to J6-J2 of LAUNCHXL-F28027
J11	To connect to J1-J5 of LAUNCHXL-F28027
J12	5-V_VIN power supply to power MCU, op amps, low side of AMC1301 and comparators

☒ 27 shows how the LAUNCHXL-28027 can be mounted on connectors J10 and J11.



☒ 27. Connecting LAUNCHXL-F28027 Board to TIDA-00366 PCB

6 Test Data

6.1 Power Supplies

表 10 shows the measured values of voltage rails on the board.

表 10. Voltage Rails—Designed and Measured Values

RAIL NAME	FROM DEVICE	DESIGNED VALUE FOR THE RAIL (V)	MEASURED VALUE FOR THE RAIL (V)
5V VDC	TLV70450	5	5.025
3V3	TLV1117-33	3.3	3.2997
3V3_REF	REF2033	3.3	3.3
1V65_REF	REF2033	1.65	1.6501
16V GPS	Externally applied (for low-side IGBT gate-drivers)	16	16
VCC_U	Bootstrap supply (for high-side IGBT gate driver)	15	14.9
VCC_V	Bootstrap supply (for high-side IGBT gate driver)	15	14.89
VCC_W	Bootstrap supply (for high-side IGBT gate driver)	15	14.92
Supply for AMC1301	U Phase	5	5.017

6.1.1 Power Supply Rail Generated Using LDOs and References

図 28 and 図 29 show the voltage rail and ripple for 3V3 rail generated using the TLV1117-33. The ripple is much less than 10 mV(p-p).

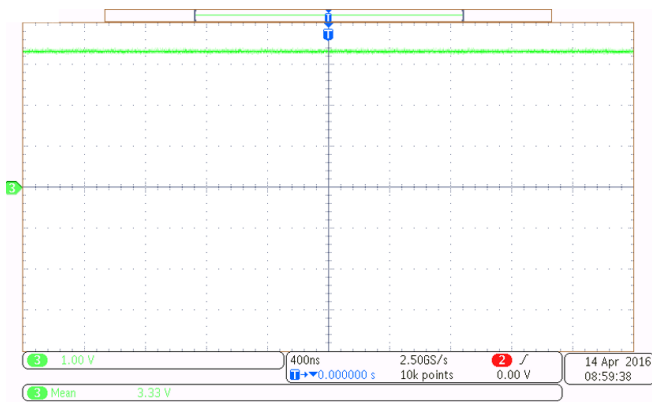


図 28. 3.3-V Rail Generated Using TLV1117-33

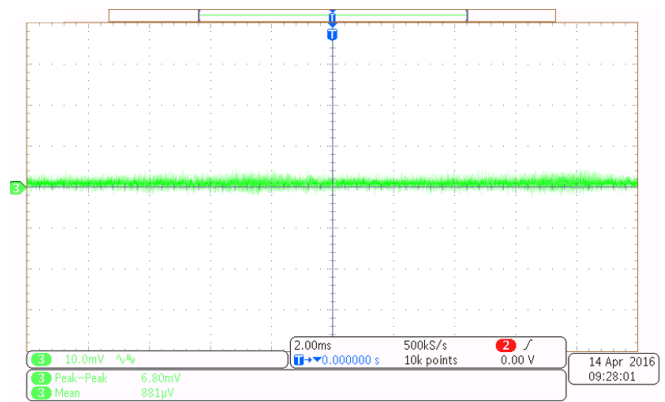
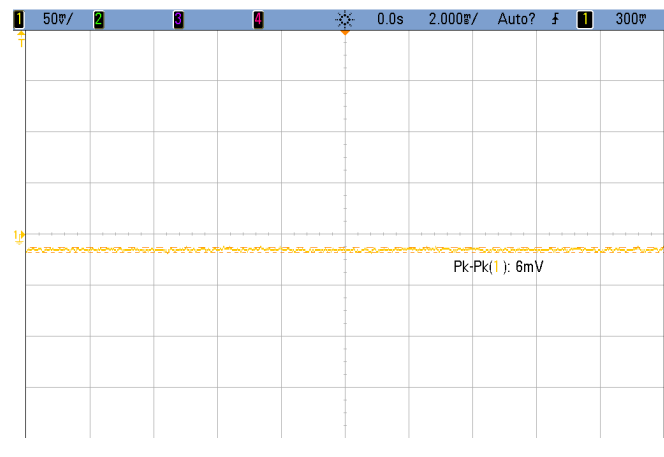


図 29. Ripple on 3.3-V Rail Generated Using TLV1117-33

☒ 30 and ☒ 31 show the voltage rail and ripple for the 5-V VDC rail generated using the TLV70450. The ripple is much less than 10 mV (p-p).



☒ 30. 5-V Rail Generated Using TLV70450

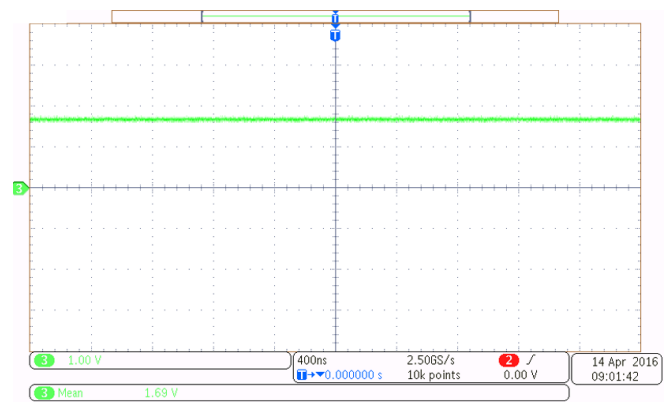


☒ 31. Ripple on 5-V Rail Generated Using TLV70450

☒ 32 and ☒ 33 show the voltage rails, 3V3 and 1V65 rails, respectively, generated using the REF2033.



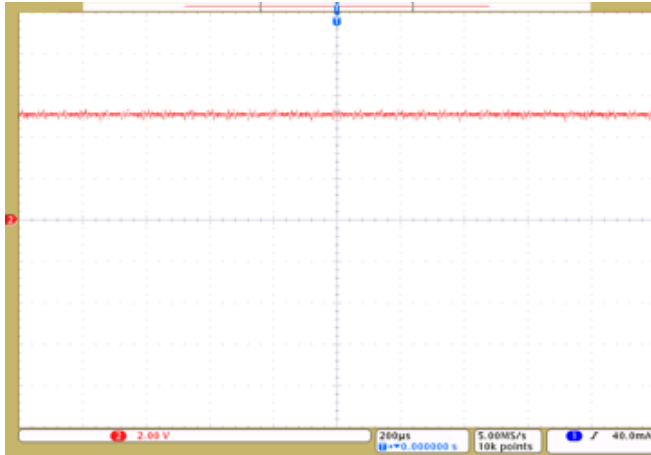
☒ 32. 3.3-V Rail Generated Using REF2033



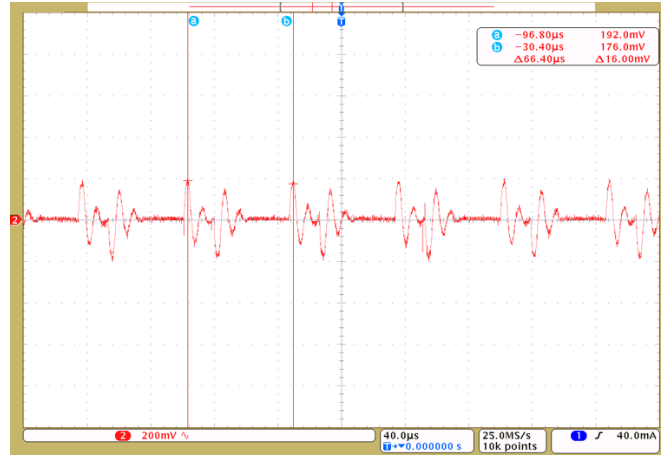
☒ 33. 1.65-V Rail Generated Using REF2033

6.1.2 Power Supply Rail for AMC1301

As explained in 4.4.2.1, 5-V rails for the hot side of the AMC1301 are generated from the bootstrap power supply using the TL431B. 34 and 35 show the 5-V rail and ripple on that rail, respectively. The peak-to-peak ripple value is less than 400 mV and the frequency is $(1/66.40 \mu\text{s}) = 15.040 \text{ kHz}$, which is exactly the switching frequency of the power stage.



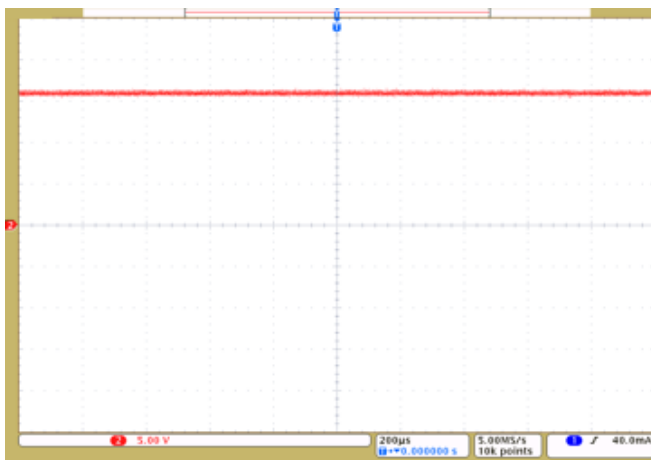
34. 5 V to Power Hot Side of AMC1301



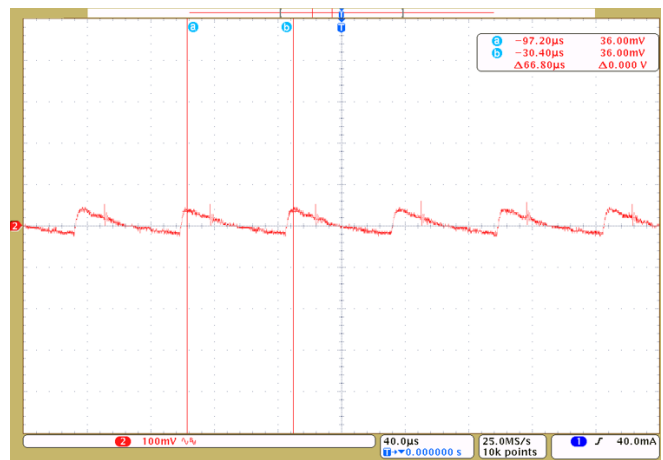
35. Ripple on 5 V to Power Hot Side of AMC1301

6.1.3 Power Supply Rail for Low-Side Gate Drivers

36 and 37 show the voltage rail and ripple for the 16-V rail, respectively, for the low-side gate driver. The peak-to-peak ripple value is 80 mV and the frequency is $(1/66.80 \mu\text{s}) = 14.97 \text{ kHz}$, which is near to the switching frequency of the power stage.



36. 16-V Rail for Low-Side Gate Driver



37. Ripple on 16-V Rail for Low-Side Gate Driver

6.1.4 Power Supply Rail for High-Side Gate Drivers (Bootstrap Supply)

Figure 38 and Figure 39 show the voltage rail and ripple for bootstrap supply, respectively, for the high-side gate driver. The peak-to-peak ripple voltage is 2.3 V while applying a VDC = 800 V on DC Bus.

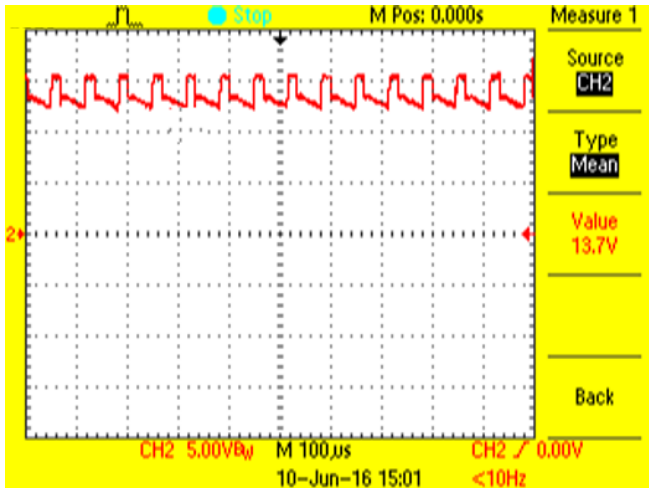


Figure 38. Bootstrap Power Supply for High-Side Gate Driver

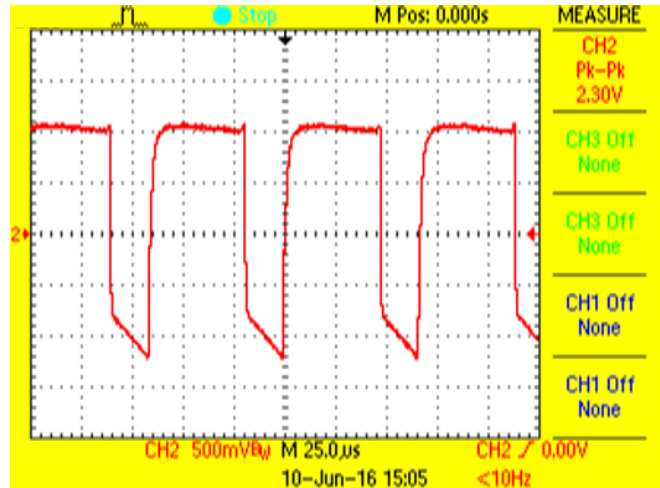


Figure 39. Ripple on Bootstrap Power Supply for High-Side Gate Driver

The bootstrap capacitor value plays a major role in deciding the ripple on the power supply. As an extended test, a bootstrap capacitor value of 1 µF is used and tested for ripple on the supply line. Figure 40 shows the reduced value of ripple with higher capacitance. The peak-to-peak ripple voltage is 1.5 V while applying a VDC = 800 V on the DC Bus.

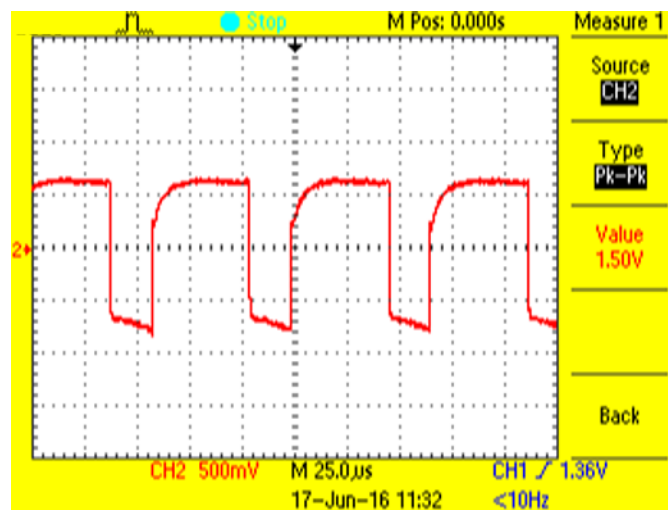


Figure 40. Bootstrap Ripple With 1-µF Capacitor for CBST

6.2 Gate Drive Signals and Waveforms

6.2.1 PWM Waveforms

Figure 41 and Figure 42 show PWM signal generated from the MCU and at the gate of IGBTs, respectively. The PWM frequency is 15 kHz.

注: Blue: High-side PWM signal, Red: Low-side PWM signal

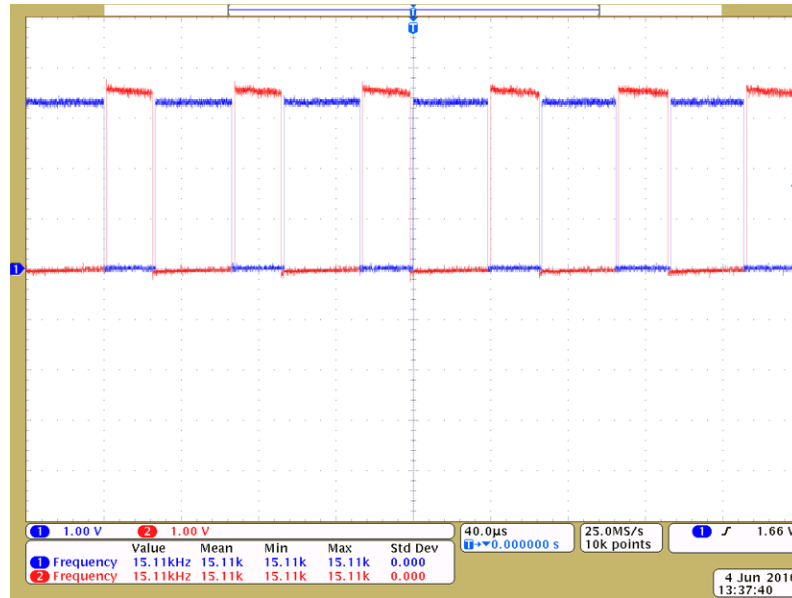


Figure 41. PWM Generated From MCU

注: Purple: High-side PWM signal, Green: Low-side PWM signal

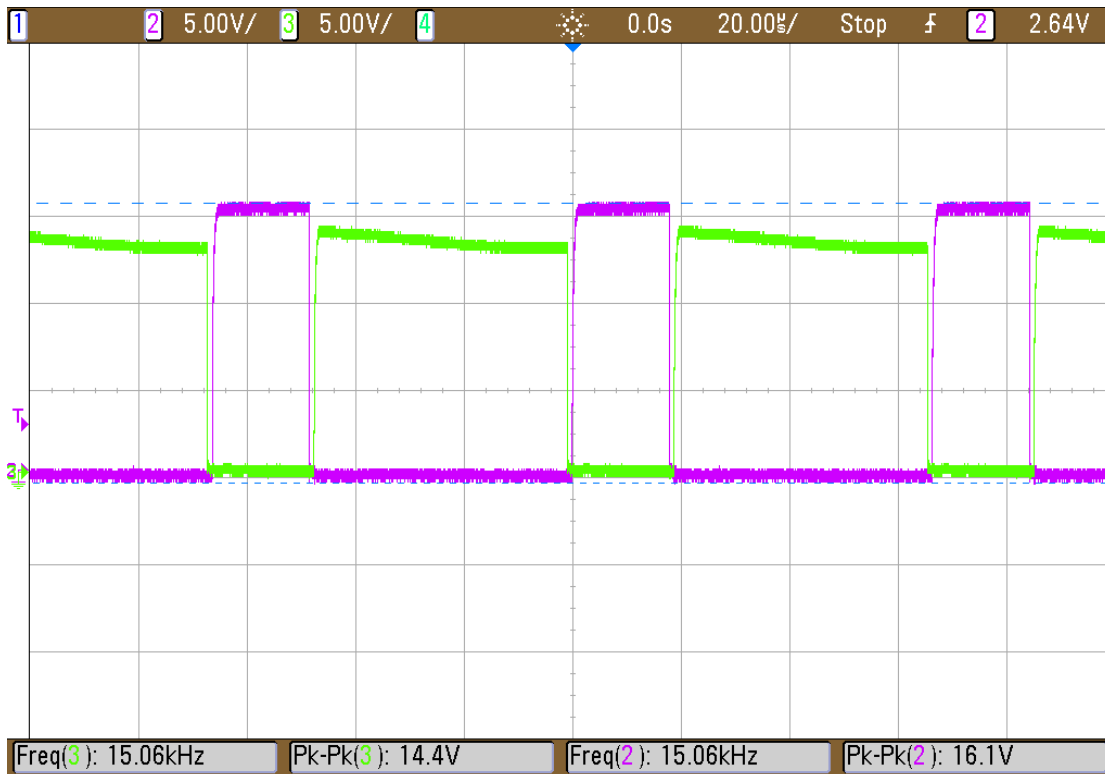
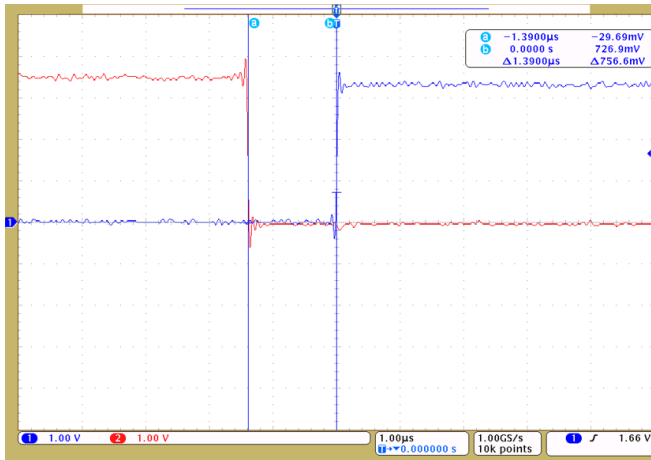


図 42. PWM at the Gate Driver Output

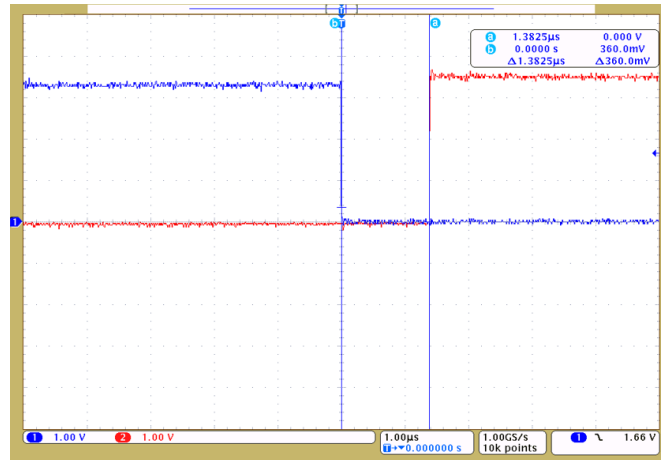
6.2.2 Dead Time Between High-Side and Low-Side PWM

For the PWM waveforms driving both high-side and low-side IGBT gates, it is important to have enough dead time to prevent shoot-through during the switching operation. The dead time is set to $\sim 1.4 \mu\text{s}$ as shown in 43, 44, 45, and 46.

注: Blue: High-side PWM signal, Red: Low-side PWM signal

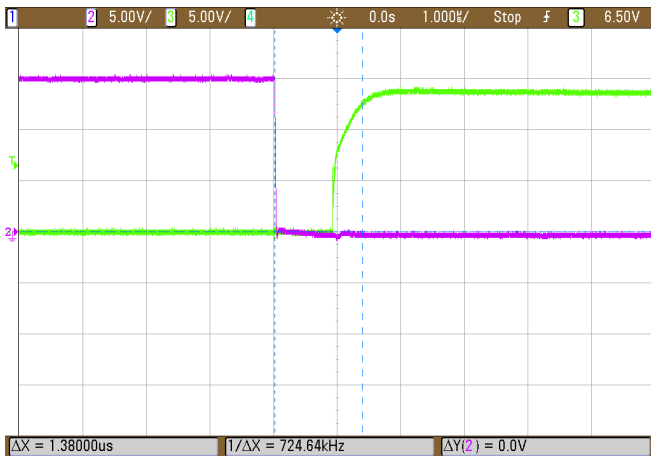


43. PWM From MCU—Dead Time (Rising Edge)

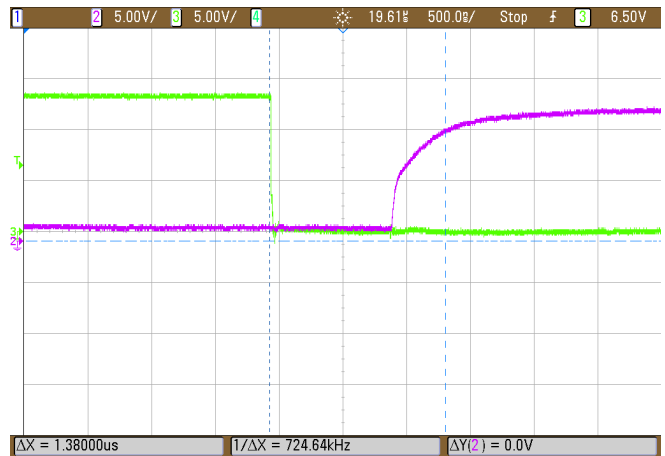


44. PWM From MCU—Dead Time (Falling Edge)

注: Purple: High-Side PWM Signal, Green: Low-Side PWM Signal

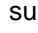
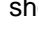


45. PWM at Gate Driver Output—Dead Time (Rising Edge)

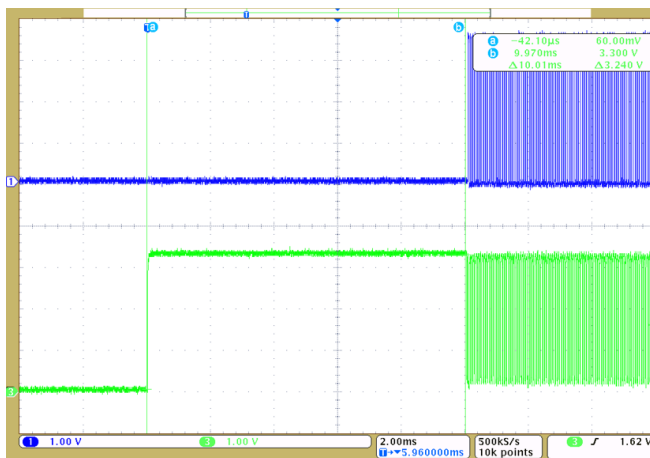


46. PWM at Gate Driver Output—Dead Time (Rising Edge)

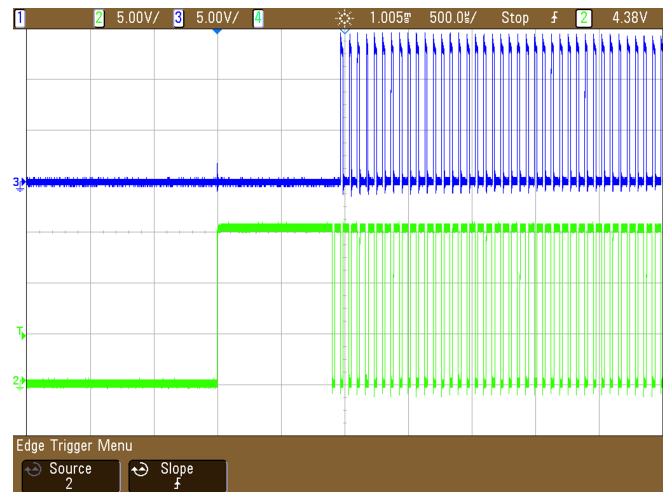
6.2.3 Startup Sequence

As explained in 4.3.6.3, the high-side gate drivers are powered using bootstrap configuration. This configuration needs a start-up sequence. When starting the application, the low-side IGBTs of half-bridge should always be turned on first, so that the bootstrap capacitor can recharge to the nominal value of the supply voltage. Otherwise, it may lead to uncontrolled switching and/or error detection.  47 and  48 show the startup sequence where low-side IGBT is turned on first for time of 10 ms and then high-side IGBT is turned on.

注: Blue: High-side PWM signal, Green: Low-side PWM signal


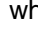


 47. Startup Sequence (PWM From MCU)



 48. Startup Sequence (PWM at Gate Driver Output)

6.2.4 UVLO for Gate Drivers

 49 and  50 show the undervoltage lockout for the IGBT gate drivers. The output PWM starts only when the power supply of the gate driver reaches a threshold as defined in the UCC21530 data sheet. The UVLO threshold measured during the testing of the TIDA-00366 is 13.87 V (for low-side gate driver) and 14.25 V (for high-side gate driver).

注: Blue: PWM signal from MCU, Red: VDDB supply, Green: PWM signal at the output of the gate driver

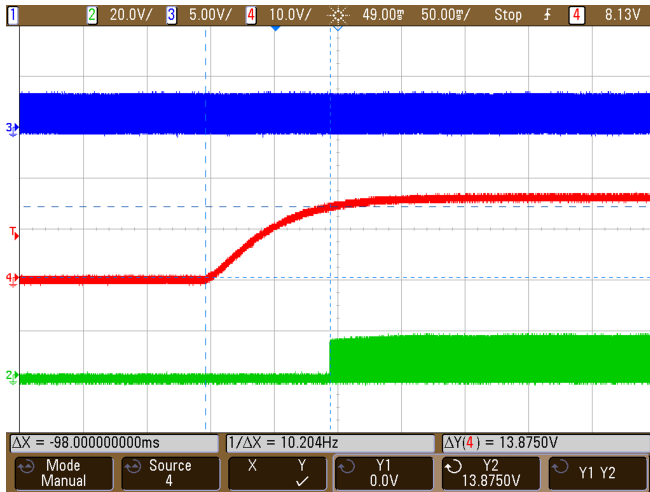


図 49. Low-Side Gate Driver UVLO

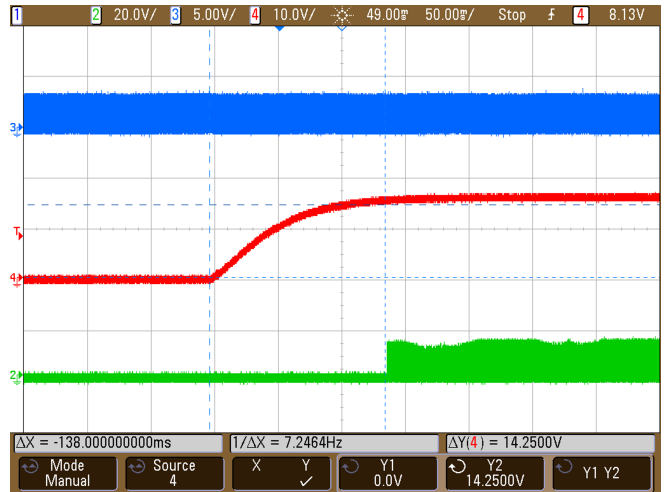
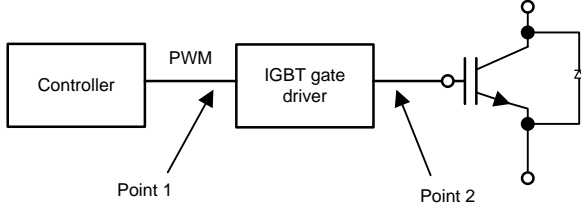
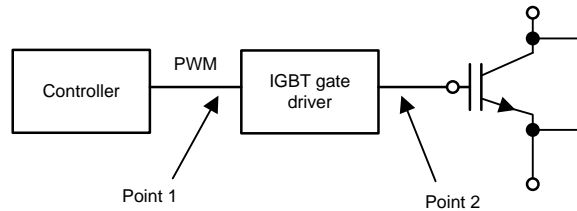


図 50. High-Side Gate Driver UVLO





6.2.5 PWM Signal Propagation Delay From Gate Drivers

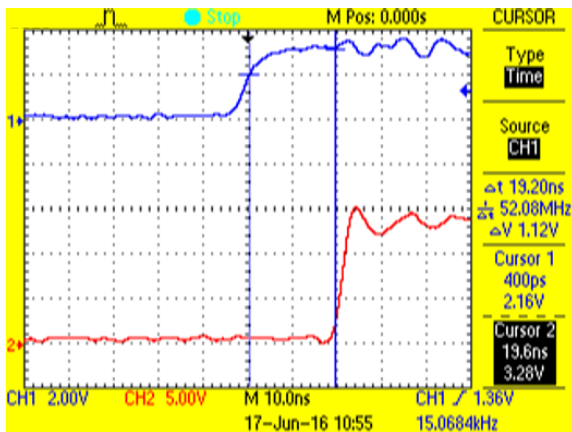
The user must know the propagation delay of the gate driver.  51 shows the line diagram where the measurements are taken for the propagation delay.



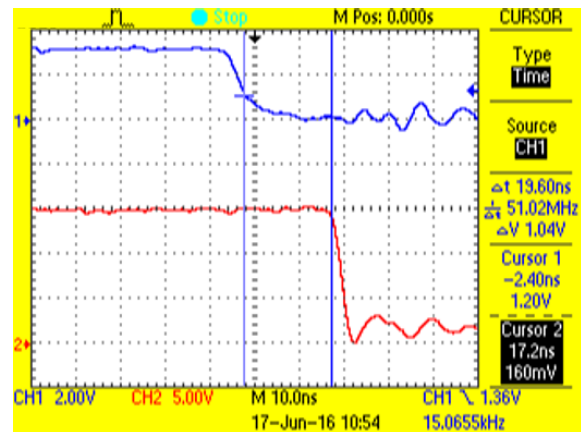
Copyright © 2016, Texas Instruments Incorporated


 51. Propagation Delay Measurement Points

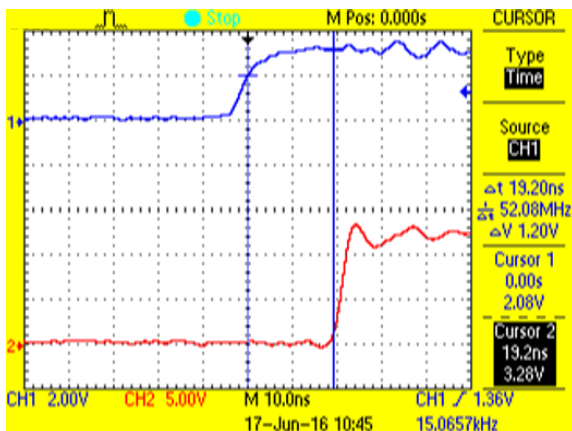
 52,  53,  54, and  55 show the propagation delays measured for the low-side and high-side gate drivers at rising and falling edges. For these figures, the blue waveform is the input of the gate driver and the red waveform is the output of the gate driver. The measured propagation delay is ~19 ns. The UCC21530 datasheet specifies the propagation delay of 19 ns (typical).



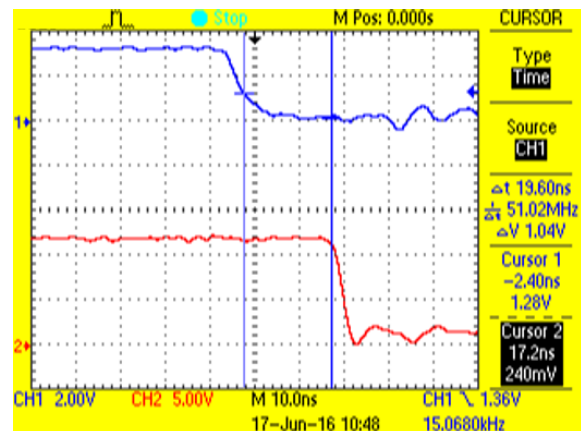
 52. Propagation Delay—Low-Side Gate Driver (Rising Edge)



 53. Propagation Delay—Low-Side Gate Driver (Falling Edge)



 54. Propagation Delay—High-Side Gate Driver (Rising Edge)



 55. Propagation Delay—High-Side Gate Driver (Falling Edge)

6.2.6 Sink/Source Current From Gate Drivers

Figure 56, Figure 57, and Figure 58 show the source and sink currents delivered by the UCC21530. The test conditions are:

- $R_{G(on)} = 16.5 \Omega$
- $R_{G(off)} = 0 \Omega$
- IGBT module = MIXA60W1200TED (from IXYS)
- Gate charge (Q_G) = 0.165 μC
- Internal resistance = 4 Ω
- Input capacitance $C_{IES} = 3.6 \text{ nF}$

注: For sake of measuring the current, $R_{G(off)}$ is changed to 0.5 Ω . The actual circuit uses $R_{G(off)} = 0 \Omega$ only.

注: Blue: Gate driving PWM Waveform, Red: Voltage across gate resistor

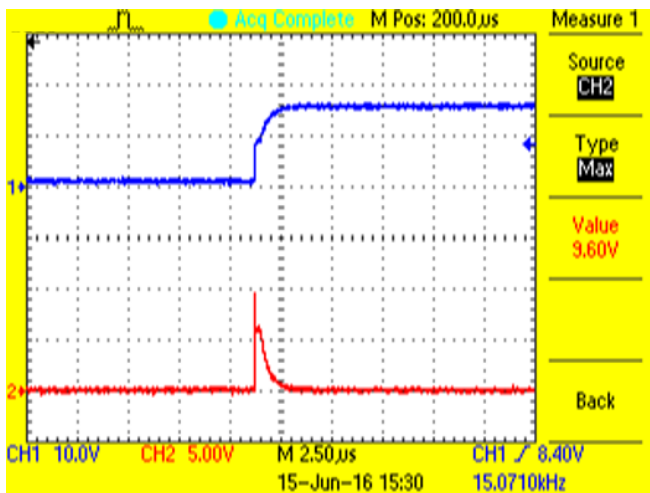


Figure 56. Source Current From Gate Driver

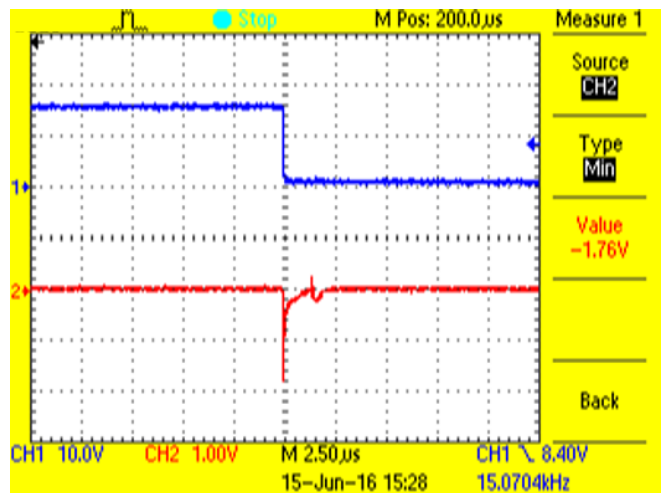


Figure 57. Sink Current to Gate Driver

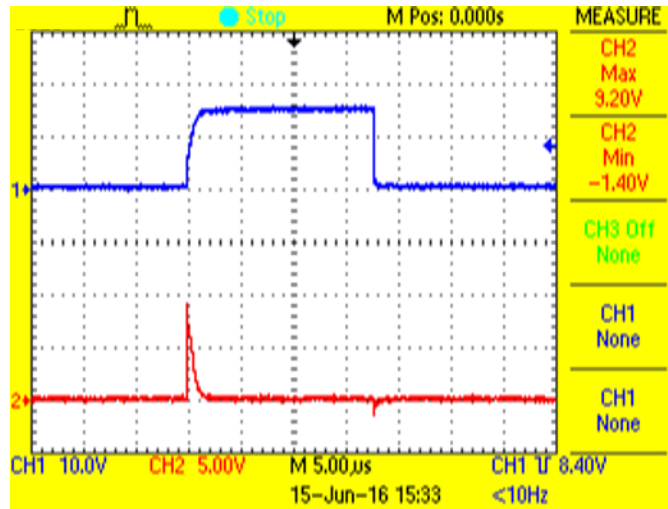


図 58. Source and Sink Current

6.2.7 dv/dt Measurement

With the test conditions specified in 6.2.6, the measured dv/dt for the falling edge (図 59) and rising edge (図 60) is $744 \text{ V}/180 \text{ ns} = 4.133 \text{ kV}/\mu\text{s}$ at $V_{DC} = 800 \text{ V}$.

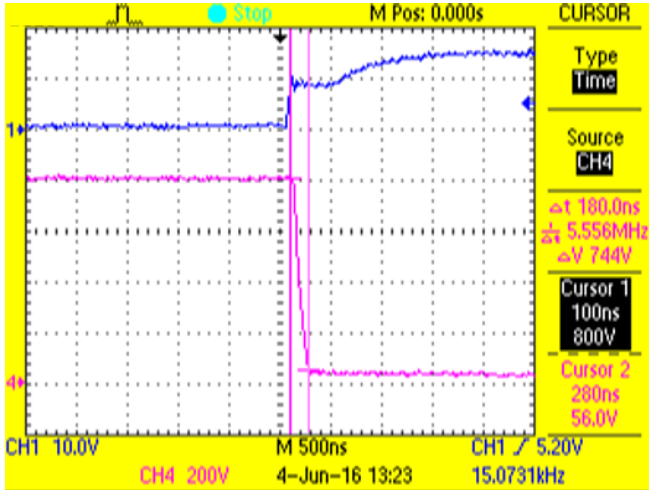


図 59. dv/dt During Sourcing

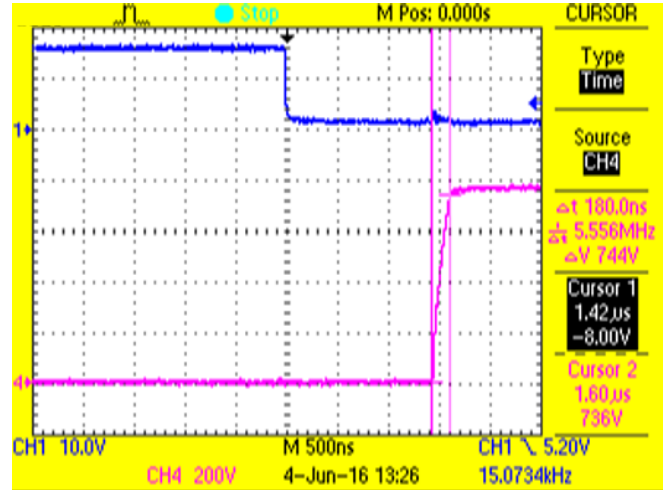


図 60. dv/dt During Sinking

6.3 Verification of ENABLE Logic

As explained in 4.9, the ENABLE logic for gate drivers is derived using a three-input AND gate and a two-input OR gate. The three inputs for the AND gates are "OVERLOAD", "GND_FAULT", and "TRIP". 61 shows that the ENABLE is active as per the timings explained in 表 11.

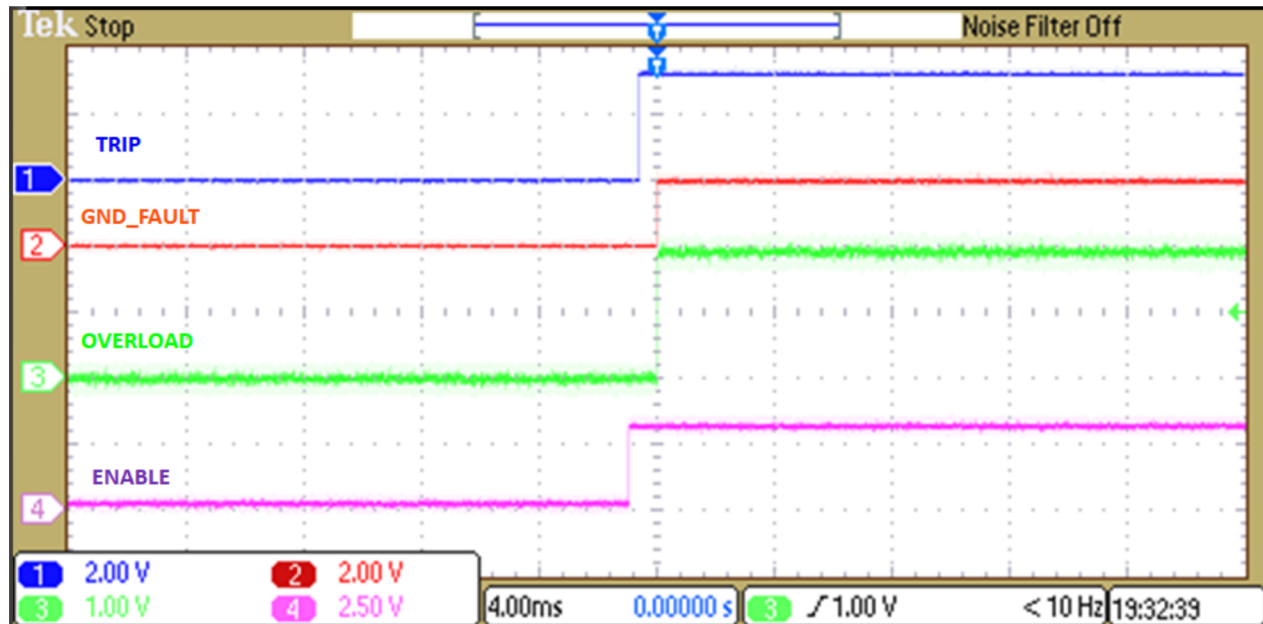


図 61. ENABLE Logic for Gate Drivers

表 11. Timings for ENABLE Logic

STATE	CONDITION	OVERLOAD	GND_FAULT	TRIP	ENABLE
t0	At the power-up (with PWM not yet started)	LOW	LOW	LOW	LOW
t1	Software makes MCUCntrl HIGH . Start-up sequence is started by software	LOW	LOW	LOW	HIGH
t2	Software make TRIP signal to go HIGH. (All faults are ignored during this time as MCUCntrl is still HIGH)	LOW or HIGH	LOW or HIGH	HIGH	HIGH
t2	MCUCntrl goes LOW. The PWMs are running, gate-drivers are enabled. Faults reach their required states	HIGH	HIGH	HIGH	HIGH

6.4 Current Measurement Propagation Delay

The propagation delay for the current measurement is captured by applying a 250-mV step input to the input of the AMC1301 (after de-soldering the 5-mΩ shunt from the PCB).

As shown in 図 62, the input of the AMC1301 (blue waveform), the output of the AMC1301 (red waveform), the output of the OPA320 (green waveform), and the output of the comparator TLC372 (pink waveform) are captured to show the step response.

図 63 shows the propagation delay from the AMC1301 input to the AMC1301 output. 図 64 shows the propagation delay from the AMC1301 output to the op amp OPA320 output. 図 65 shows the propagation delay from the AMC1301 input to the comparator TLV372 output. 表 12 shows the summary of measured delays.

表 12. Propagation Delays for Signal Chain

PARAMETER	PROPAGATION DELAY (μs)
Propagation delay from AMC1301 input to AMC1301 output	2.0
Propagation delay from AMC1301 output to op-amp OPA320 output	1.6
Propagation delay from AMC1301 input to comparator TLV372 output	4.4

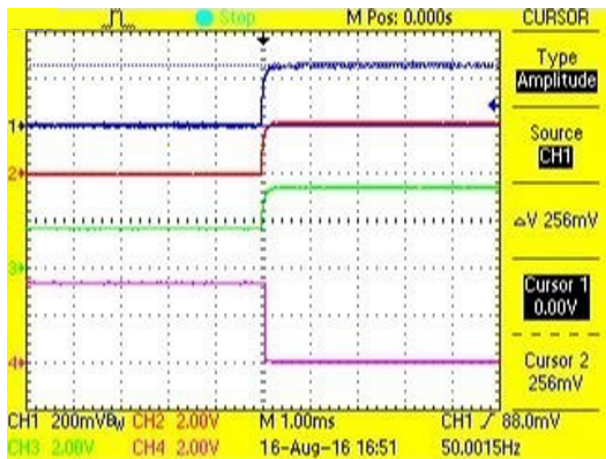


図 62. Step Response for Current Measurement Signal Chain

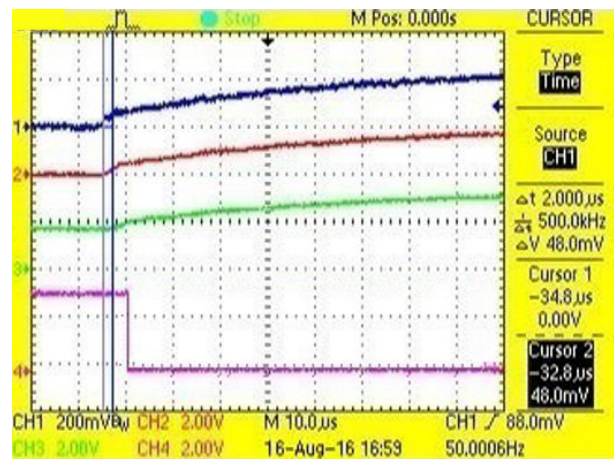


図 63. From AMC1301 Input to AMC1301 Output

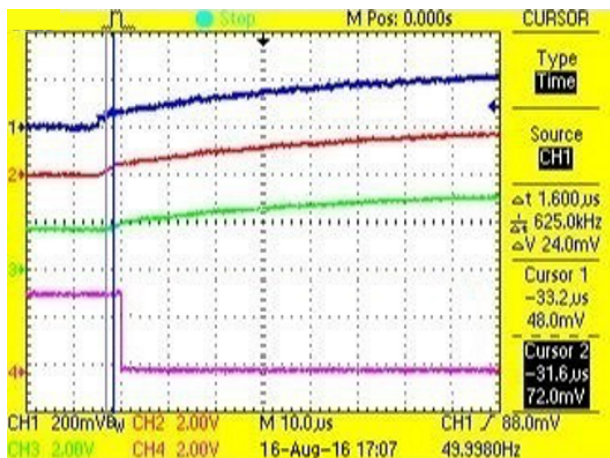


図 64. From AMC1301 Output to Op Amp Output

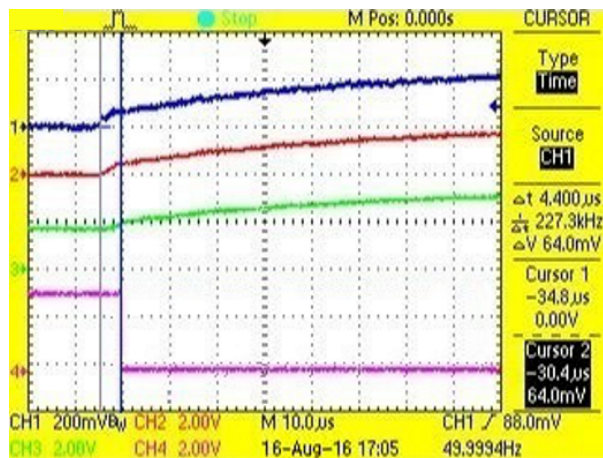


図 65. Propagation Delay From AMC1301 Input to Comparator Output

6.5 Current Measurement Accuracy

The current measurement accuracy is shown in [Figure 66](#). The measurement is done from 1 to 35 A_{RMS}, which corresponds to the 50 A_{PEAK}. As observed, the calibrated error is less than ±0.5%.

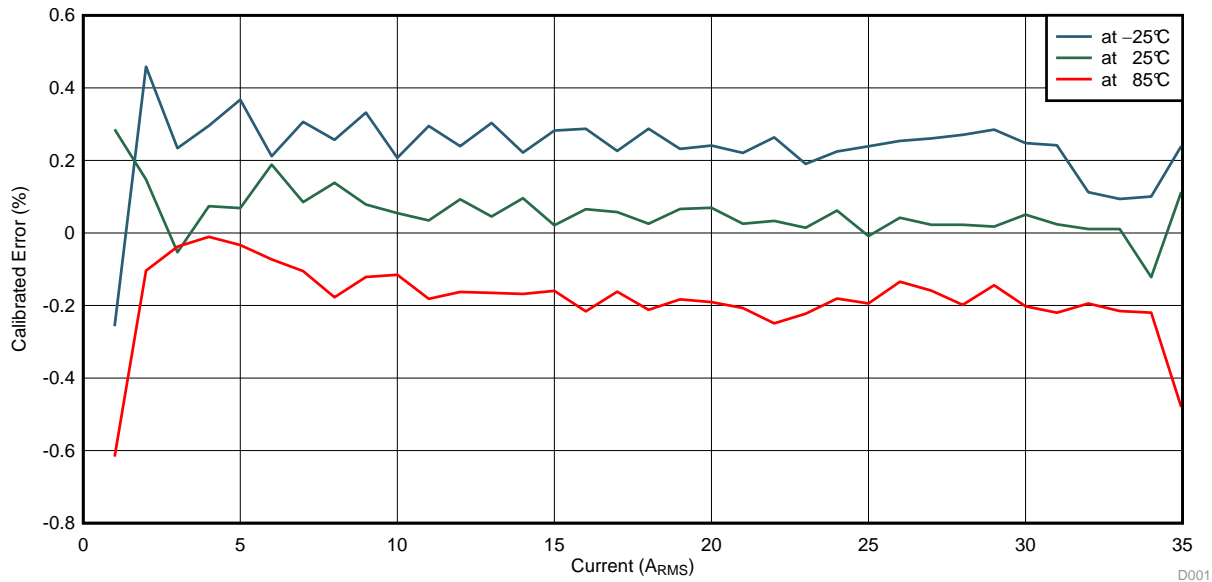


Figure 66. Current Measurement Accuracy

6.6 DC Link Voltage Measurement

6.6.1 DC Link Voltage Measurement Accuracy

The following figure shows the measurement accuracy of the DC-Link voltage., which is a graph of the percentage full-scale error versus DC-Link voltage measurement. The full scale that can be measure is 1026 V. The measurement is done by applying a DC-Link voltage between 50 V to 1000 V. During this test, the inverter is running and the motor is disconnected, which brings a switching frequency of 16 kHz. The uncalibrated error is observed to be ±1% throughout the measurement range.

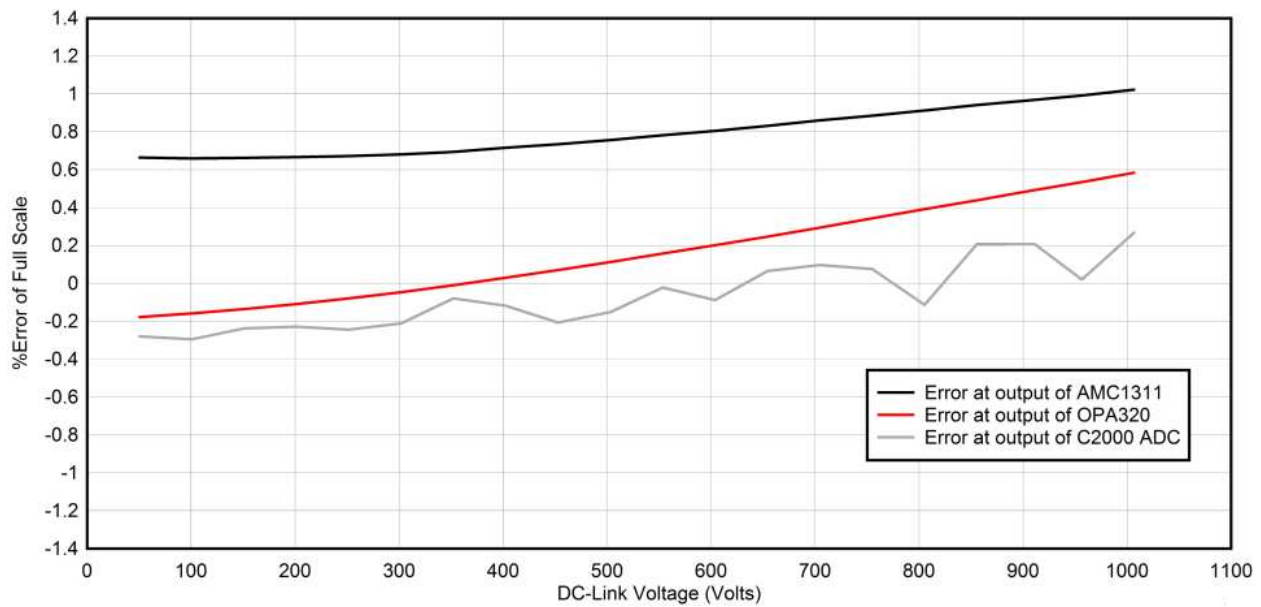


図 67. Uncalibrated Percentage Full-Scale Error vs DC-Link Voltage at No Load

The following figure shows the measurement accuracy of the DC-Link voltage when there is current in the motor. The error is measured at the output of the C2000 ADC. The test is done for a no-load current, and a current of 3 A_{RMS} and 5 A_{RMS} is sourced by the inverter into the AC induction motor. Note that the accuracy remains relatively the same throughout the range when there is a current of 3 A_{RMS}. The voltage measurement with 5 A_{RMS} into the motor is done for one reading at 600 V.

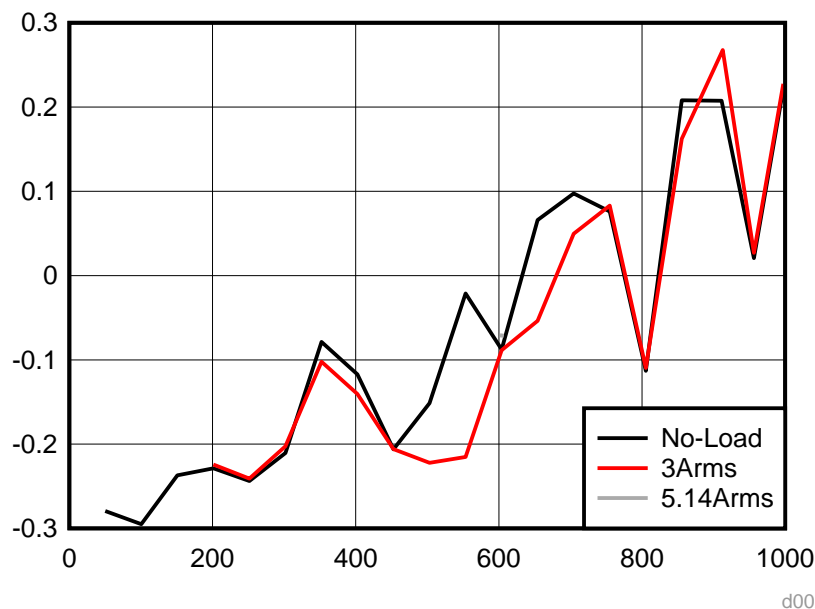
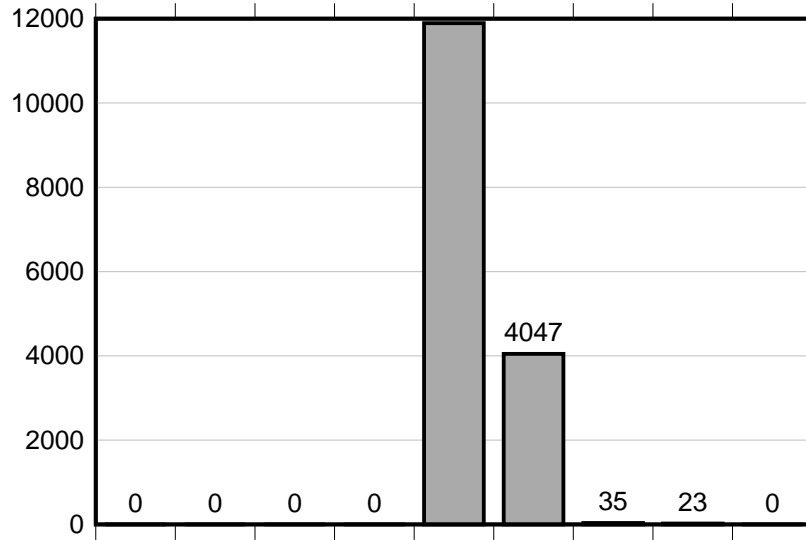


図 68. Uncalibrated Percentage Full-Scale Error vs DC-Link Voltage at No Load With Current

6.6.2 DC-Link Voltage Measurement Histogram

The histogram of the DC-Link voltage feedback signal is obtained using the 12-bit ADC of the C2000 and buffering the sample for 1 s at a sampling rate of 16 kHz. Figure 18 shows the histogram of the DC-Link feedback when the DC-Link is powered with 600 V and the invert is driving a three-phase sinusoidal current of 3 A_{RMS} into the motor. The samples differ from the center by 4 LSBs that equal to 0.1% of the full-scale range.



d001

図 69. Histogram of DC-Link Sensing Measuring 600 V With 3 A_{RMS} in Motor

6.6.3 Transfer Function

Figure 70 shows the transfer function of the DC bus voltage measurement.

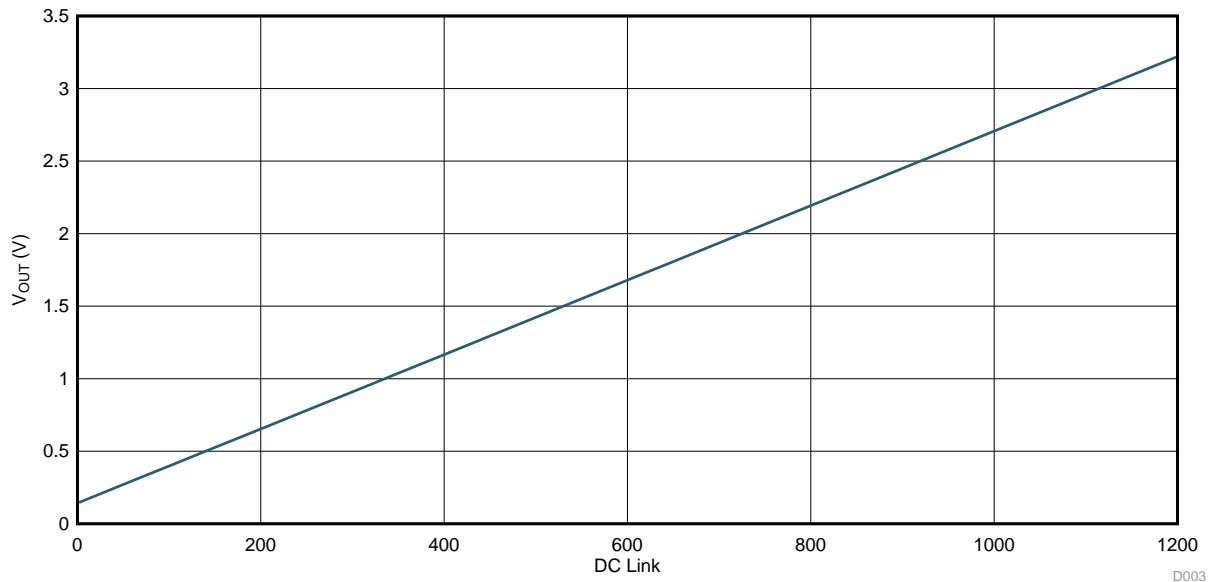


Figure 70. Transfer Function of DC Bus Voltage Measurement

6.7 IGBT Module Temperature Sensing

As explained in 4.6, the IGBT module has an internal NTC, and it is characterized for a temperature range of 0°C to 100°C. Figure 71 shows temperature versus the output of the temperature measurement signal chain.

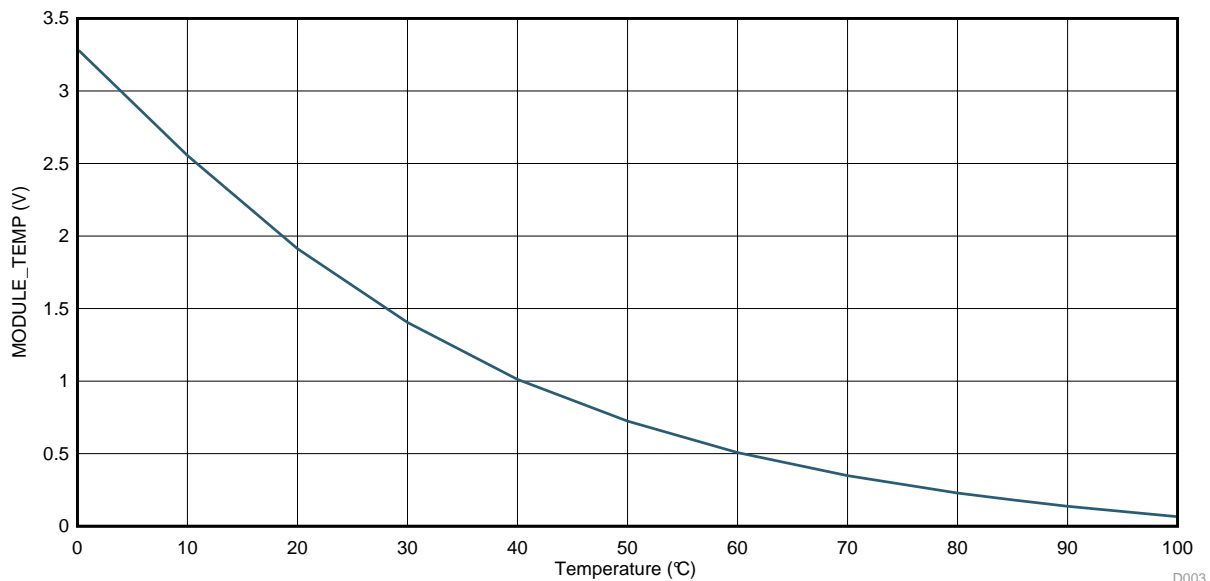


Figure 71. Transfer Function for IGBT Module NTC versus Temperature

6.8 Overload Detection

As explained in 4.7, the overload detection is implemented for all three channels, but the outputs of all overload comparators are shorted together to give single "OVERLOAD" signal.

6.8.1 Detection During Positive Half Cycle

Figure 72 shows the overload detection during a positive half cycle. The overload is detected at $49\text{ A}_{\text{PEAK}}$.

注: Blue: Current flowing through shunt, Red: OVERLOAD output from comparator

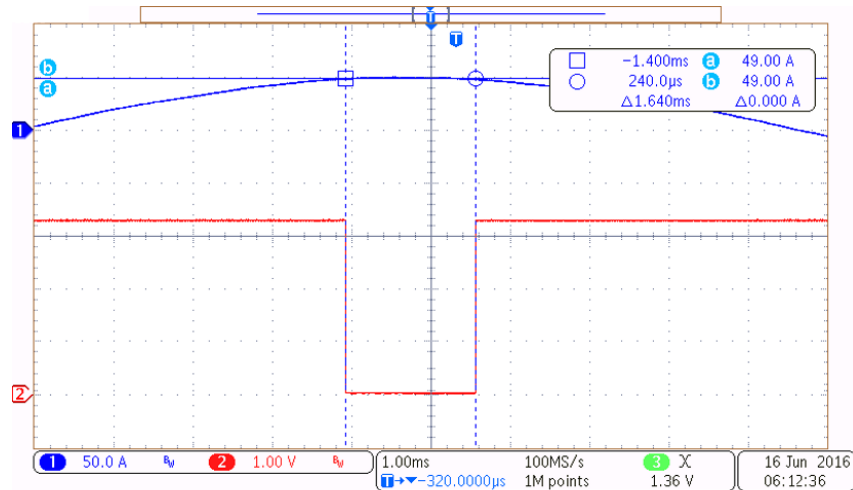


Figure 72. OVERLOAD Detection During Positive Half Cycle

6.8.2 Detection During Negative Half Cycle

Figure 73 shows the overload detection during a negative half cycle. The overload is detected at $-49\text{ A}_{\text{PEAK}}$.

注: Blue: Current flowing through shunt, Red: OVERLOAD output from comparator

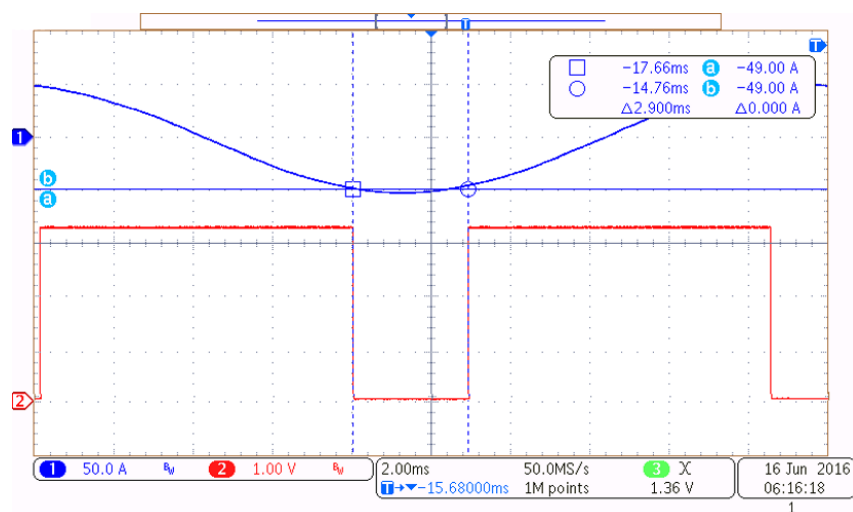


Figure 73. OVERLOAD Detection During Negative Half Cycle

6.8.3 Latching Function on TRIP Pin

The overload detect signal is latched on the TRIP pin as shown in 図 74.

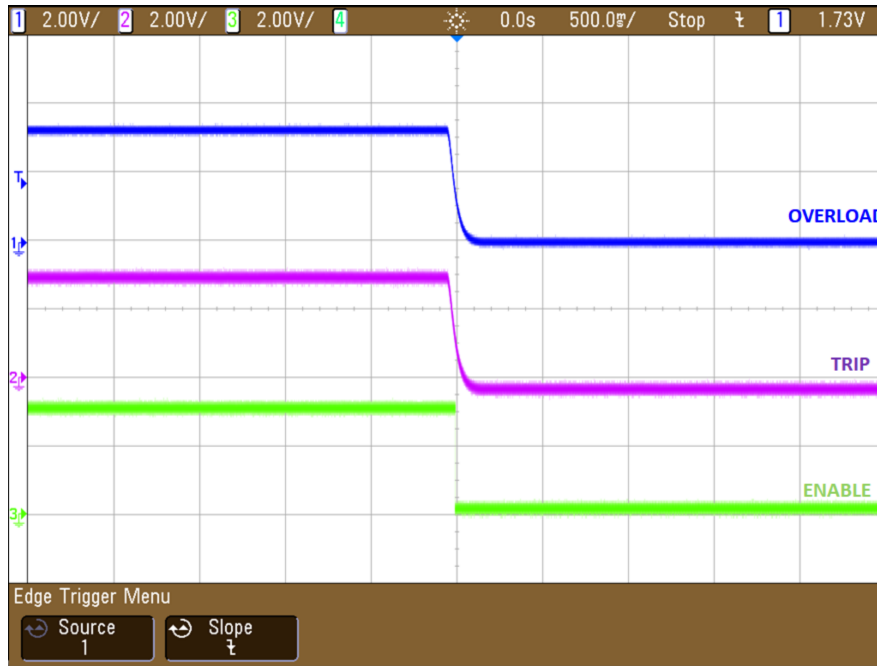


図 74. Latching of OVERLOAD Detect Signal on TRIP Pin

6.9 Ground Fault Detection

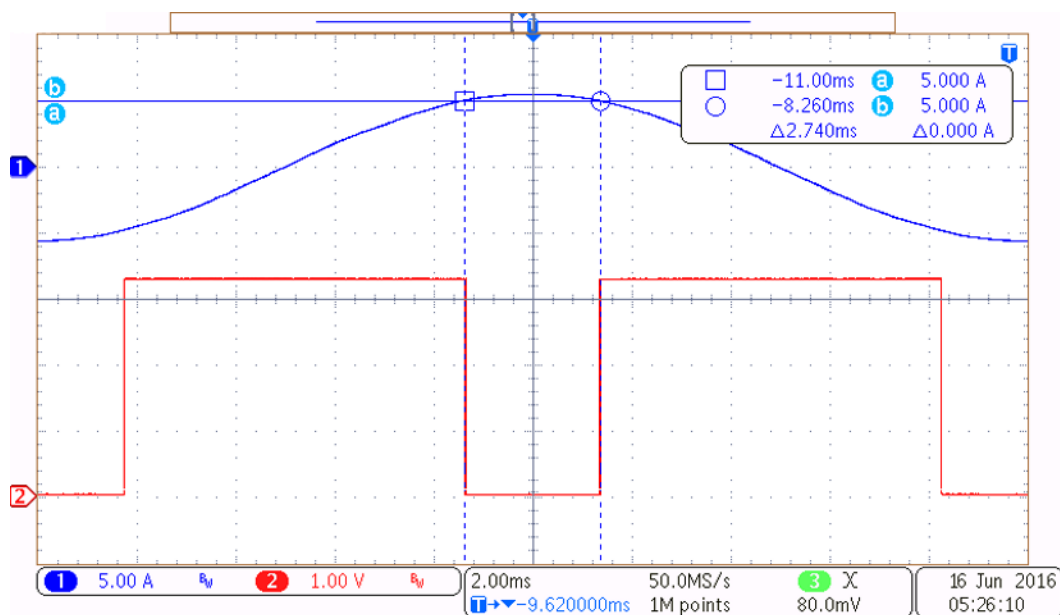
As explained in 4.8, the ground fault detection is implemented by combining the detected current for all three channels. In an ideal condition, when no ground fault has occurred, the "GND_FAULT" signal must be disabled (that is, active high). When ground fault condition occurs in any one channel (or more than one channel), the GND_FAULT detect is enabled (that is, goes low).

For capturing the ground fault occurrence, the current is passed through only one channel (V-channel) and "GND_FAULT" signal is observed.

6.9.1 Detection During Positive Half Cycle

☒ 75 shows the ground fault detection during a positive half cycle. The fault is detected at $5 A_{PEAK}$.

注: Blue: Current flowing through shunt, Red: GND_FAULT output from comparator



☒ 75. GND_FAULT Detection During Positive Half Cycle

6.9.2 Detection During Negative Half Cycle

図 76 shows the ground fault detection during a negative half cycle. The fault is detected at $-5 A_{PEAK}$.

注: Blue: Current flowing through shunt, Red: GND_FAULT output from comparator

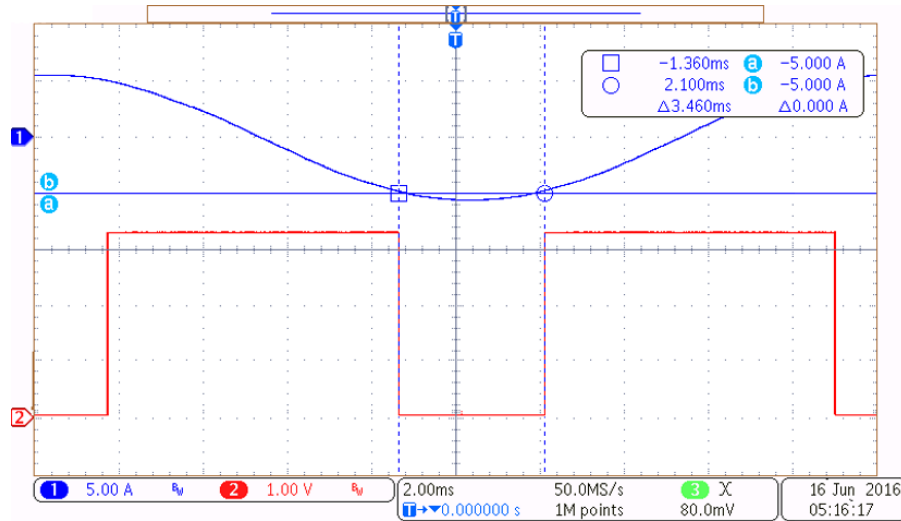


図 76. GND_FAULT Detection During Negative Half Cycle

6.9.3 Latching Function on TRIP Pin

The ground fault detect signal is latched on the TRIP pin as shown in 図 77.

注: Yellow: Ground fault, Green: TRIP, Pink: ENABLE

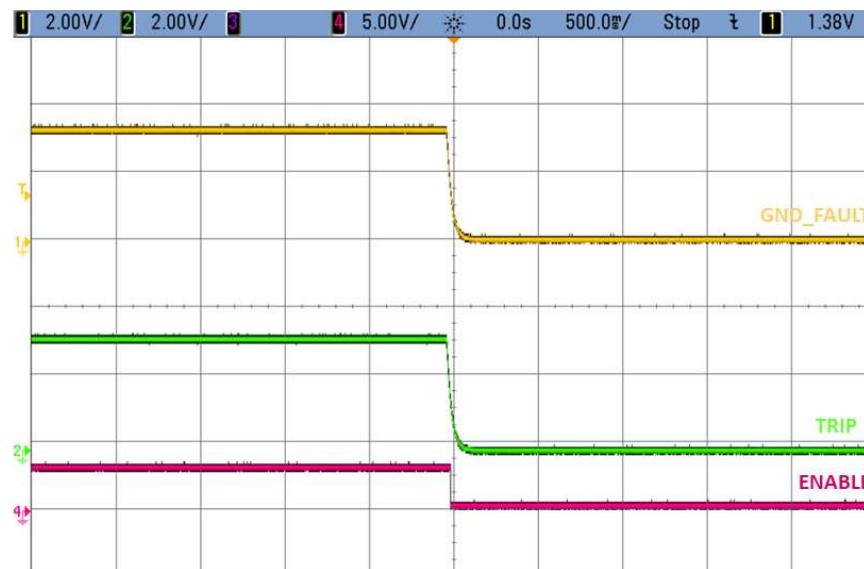


図 77. Latching of GND_FAULT Detect Signal on TRIP Pin

6.10 Testing Using Three-Phase AC Induction Motor and Load Setup

注: TI recommends that a proper heatsink must be mounted before connecting the TIDA-00366 board to the motor.

The TIDA-00366 board is connected to the 5HP Three-Phase AC Induction Motor and load setup as shown in 図 78. The motor is loaded up to 1.2 kW (limited by the load setup) and torque is applied according to the requirement.

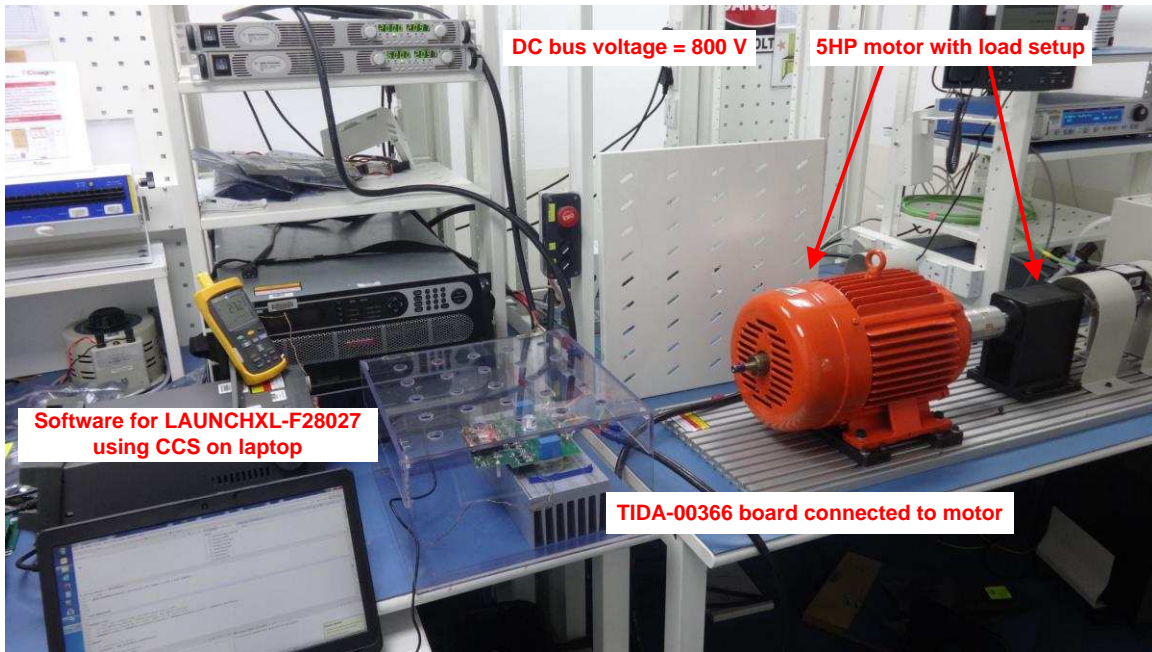


図 78. TIDA-00366 Test Using ACIM and Load Setup

表 13 shows the test results for the load test along with temperature readings observed during the test. The test conditions for the load test are as follows:

- Ambient temperature = 25.4°C
- Air flow = 400 LFM
- Freq of operation = 60 Hz
- Shunt value used for load test = 50 mΩ
- Heatsink connected to the IGBT module

表 13. Load Test Using Three-Phase AC Induction Motor

MEASURED ON MAGTROL EQUIPMENT			MEASURED ON DC SOURCE		MEASURED ON MULTIMETER	MEASURED ON OSCILLOSCOPE	MEASURED WITH THERMAL CAMERA
TORQUE	SPEED	OUTPUT (W)	VDC	IDC	AC RMS (MEASURED AT THE PHASE)	I _{RMS} (A)	MODULE TEMPERATURE (°C)
0.0	1770	10	757.6	0.425	400.7	1.559	48.7
1.0	1800	203	757.6	0.685	397.7	1.762	52.1
2.0	1800	420	757.6	0.944	395.1	2.074	56.5
3.0	1800	660	757.6	1.212	393.0	2.469	60.6
4.0	1800	860	757.6	1.485	391.3	2.933	64.1
5.0	1800	1070	757.6	1.767	390.2	3.445	68.8
5.6	1800	1220	757.6	1.984	389.5	3.862	73.4

During the load test, the current flowing through the motor terminal (W-Phase) is measured using a current probe, and the same current is observed at the MCU pin. 図 79 shows the two waveforms for the same.

注: Blue: Motor current measured with current probe, Pink: Voltage measured on MCU pin

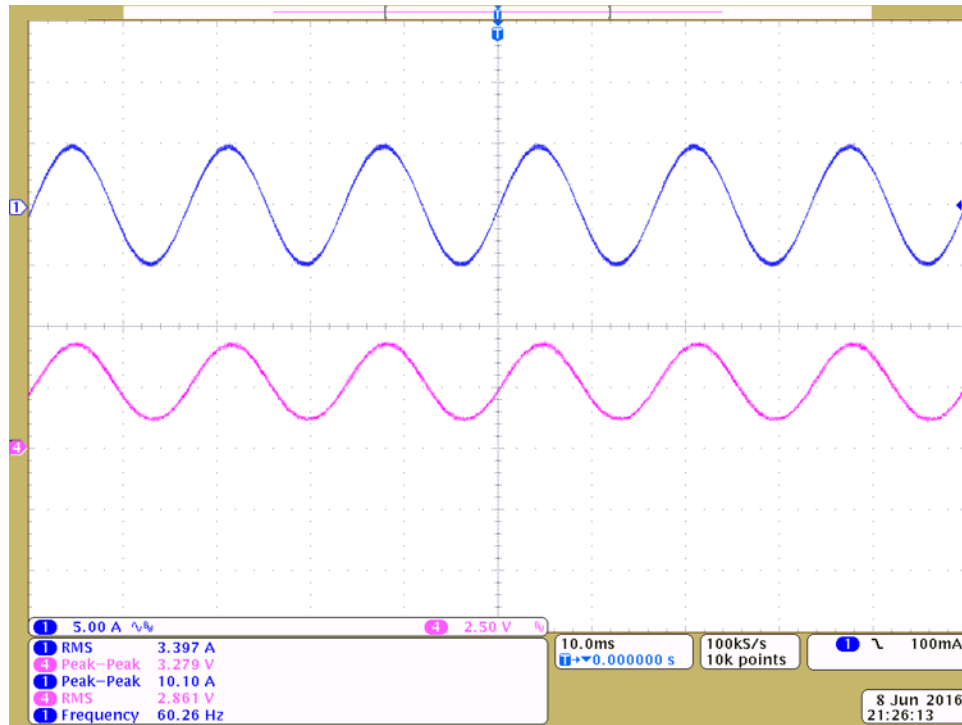


図 79. Motor Current Measurement

7 Design Files


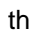
7.1 Schematics

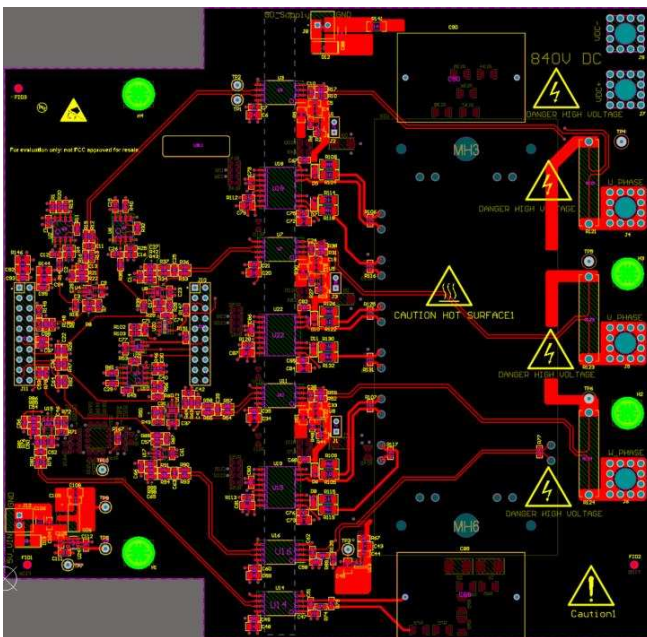
To download the schematics, see the design files at [TIDA-00366](#).

7.2 Bill of Materials

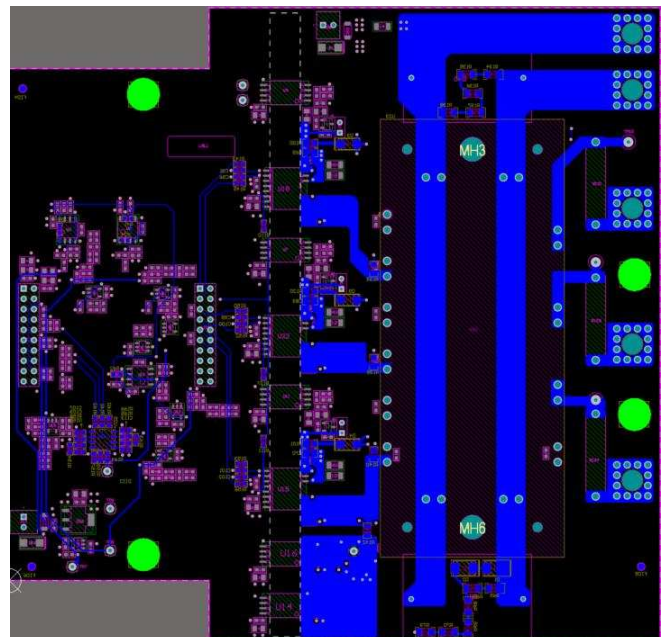
To download the bill of materials (BOM), see the design files at [TIDA-00366](#).

7.3 PCB Layout Recommendations

 80 shows the top layer and  81 shows the bottom layer of the PCB. The IGBT module is placed on the bottom layer and all the driving and sensing circuit is on the top layer.



 80. Top Layer



 81. Bottom Layer

図 82 shows the ground layer and 図 83 shows the power layer. The ground plane and power planes are cut wherever there is requirement for isolation from high-voltage side as well as between the low-side and high-side IGBT gate drivers.

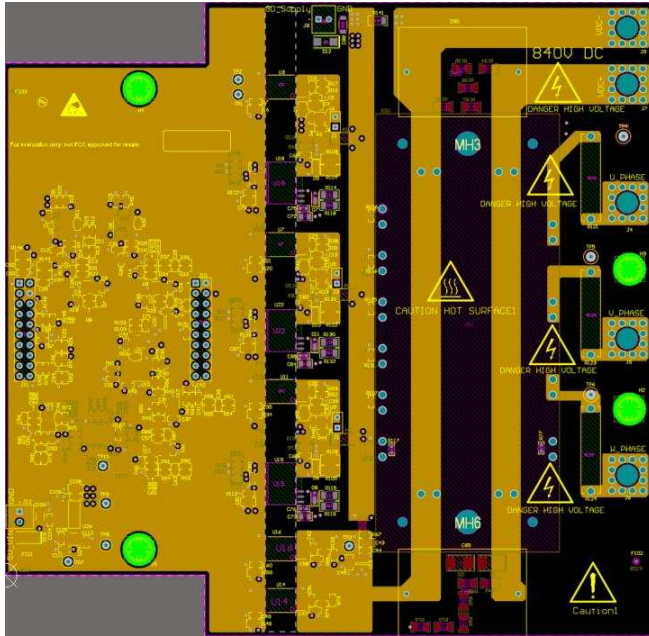


図 82. GND Layer

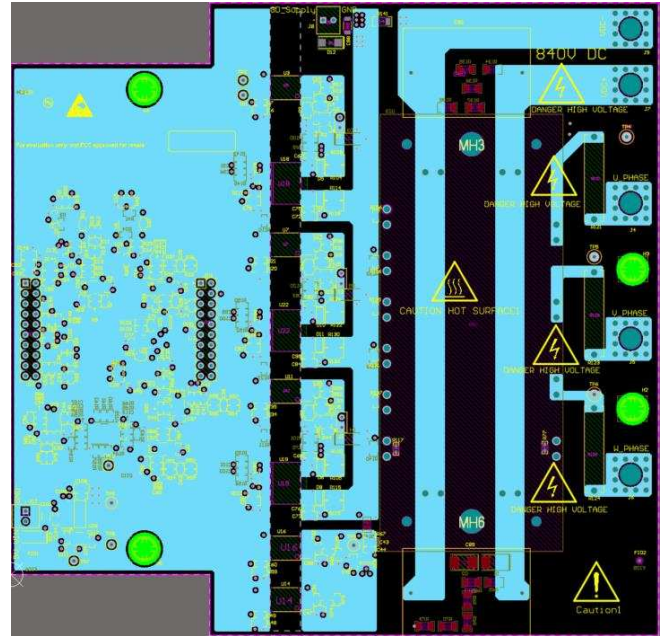


図 83. PWR Layer

Figure 84 shows the placement of components for the IGBT gate driver as well as the current sensing circuit. The figure also shows the critical placement of the decoupling capacitors that needs to be placed as close as possible to the AMC1301 while maintaining a differential routing of the input and output signals. To maintain the isolation barrier and the CMTI, keep the distance between the high-side ground (GND1) and the low-side ground (GND2) at a maximum; that is, the entire area underneath the device must be kept free of any conducting materials as shown in Figure 84. For the UCC21530, apart from placing the decoupling capacitors close to the supply pins, have multiple vias for VDD as well as VCCI supply lines. This will minimize the loop inductance of the VDD and VCCI loops.

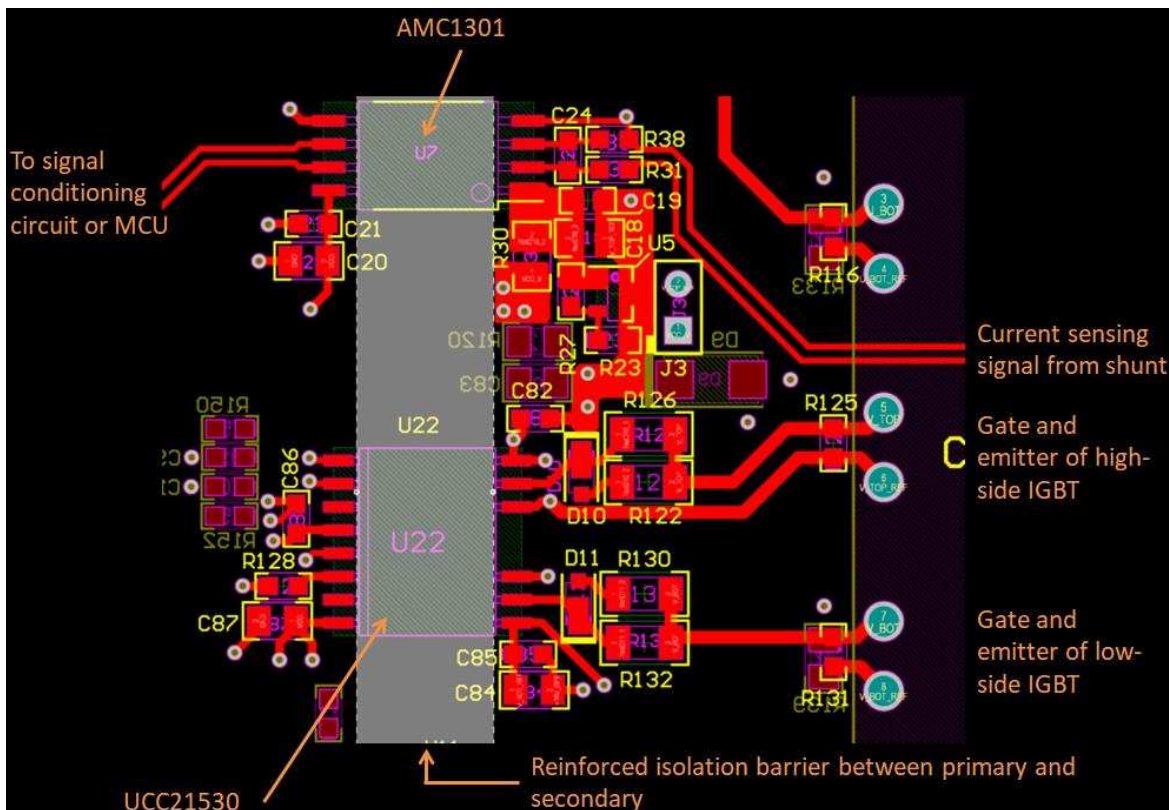


Figure 84. Gate Driver and Current Sensing Circuit

The grounding and power supply planes for the gate drivers are shown in [Figure 85](#) and [Figure 86](#), respectively. As highlighted in [Figure 85](#), the ground for the 16-V gate drive power supply (for the low-side IGBT gate driver) is isolated from the bootstrapped supply for the high-side IGBT gate-driver. Similarly, the power planes are isolated as shown in [Figure 86](#).

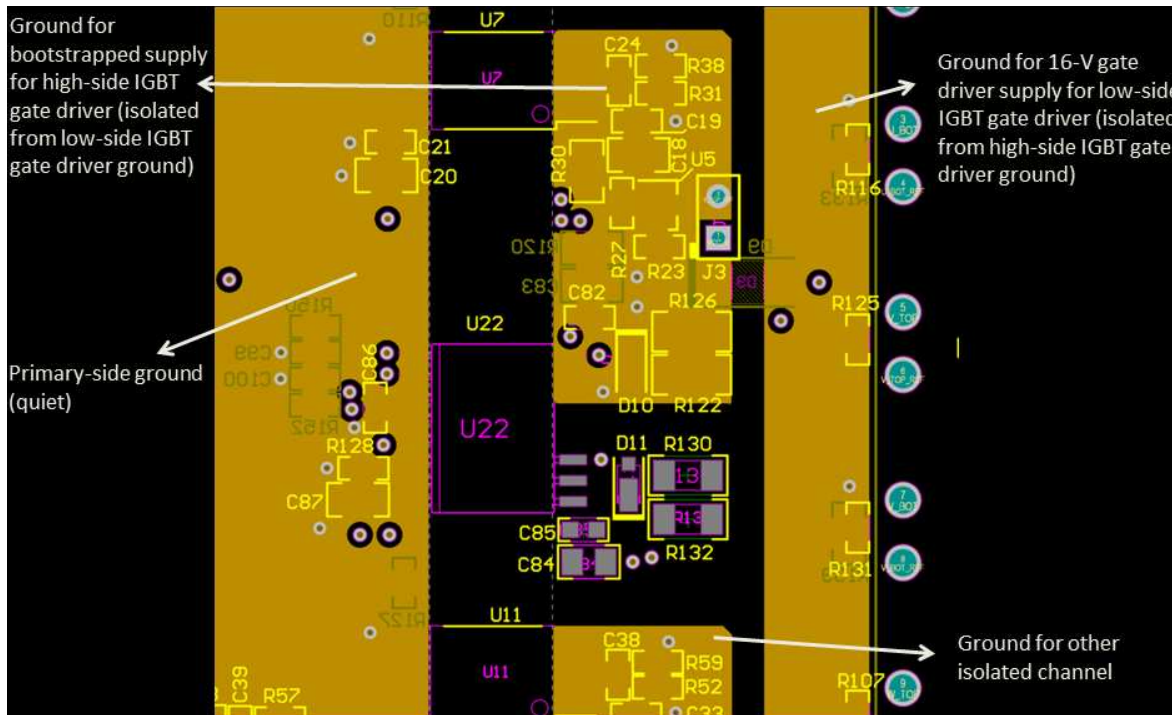


Figure 85. Grounding for High-Side and Low-Side IGBT Gate Drivers

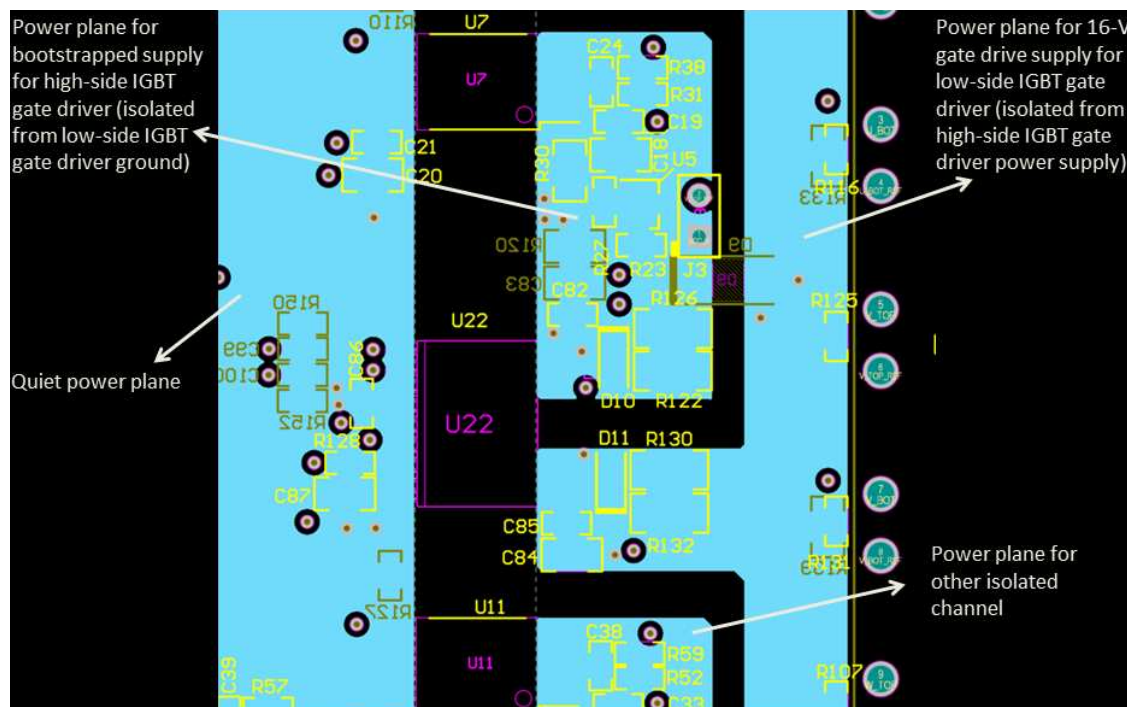


Figure 86. Power Planes for High-Side and Low-Side IGBT Gate-Drivers

図 87 shows that the return path for bottom IGBT gate signal is connected in the bottom layer. Also, the bootstrap diode is connected between the 16-V gate drive power supply (for the low-side IGBT gate driver) and the bootstrap power supply for the high-side IGBT gate driver.

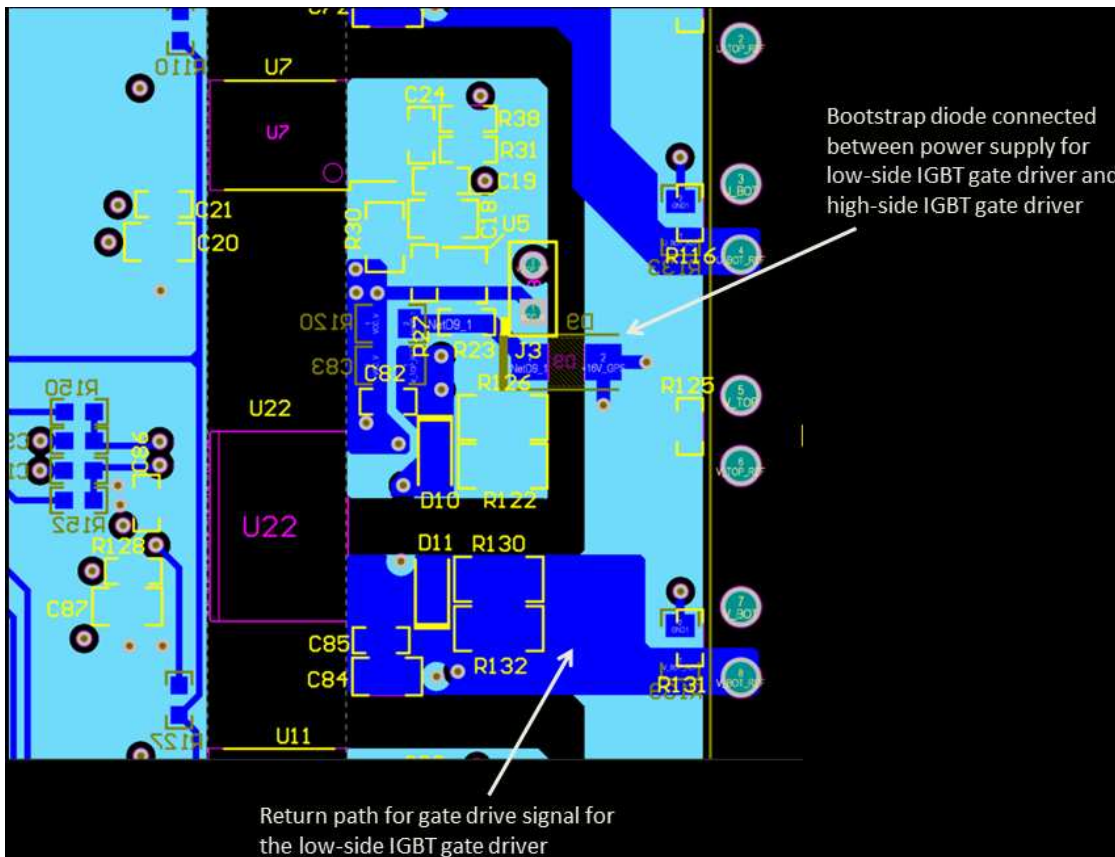


図 87. Return Path

As explained in 4.2, the grounds for all the three channels are connected to VDC- through 0-Ω resistors (shorting links). 図 88 and 図 89 show the placement of these shorting links on the board.

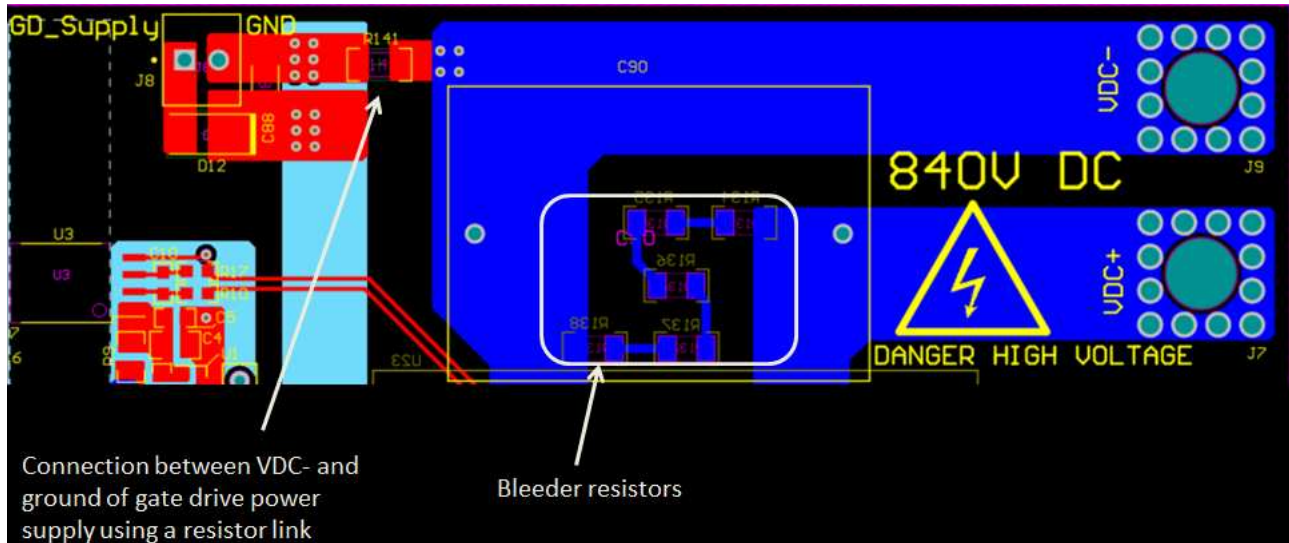


図 88. Shorting Link

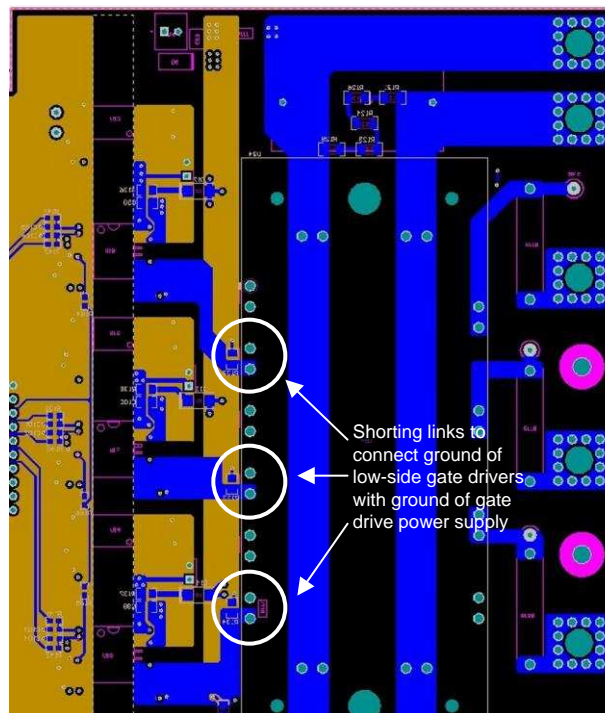


図 89. Shorting Links

Figure 90 shows the sensing circuit for DC bus voltage. The voltage sensing is done at the film capacitors as shown in Figure 90.

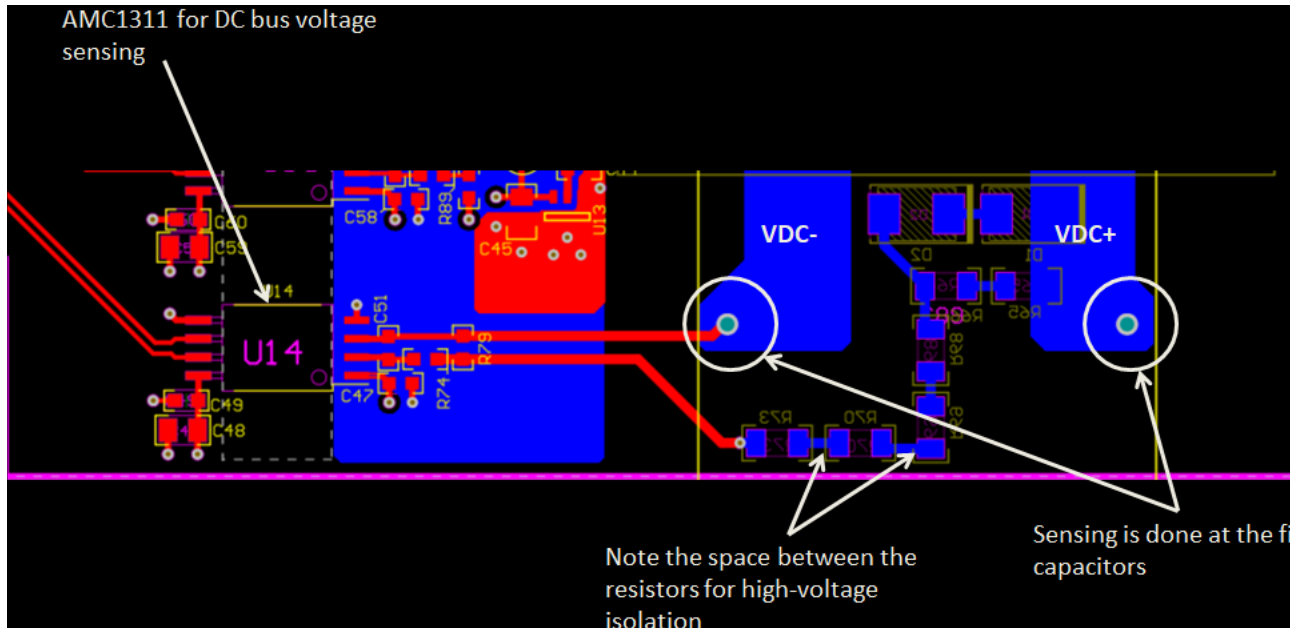


Figure 90. DC Bus Sensing Section

Since it is a high-voltage PCB, the sensing circuit cannot be in direct contact with the high-voltage planes. The sensing signals are orthogonal in the layout as shown in Figure 91.

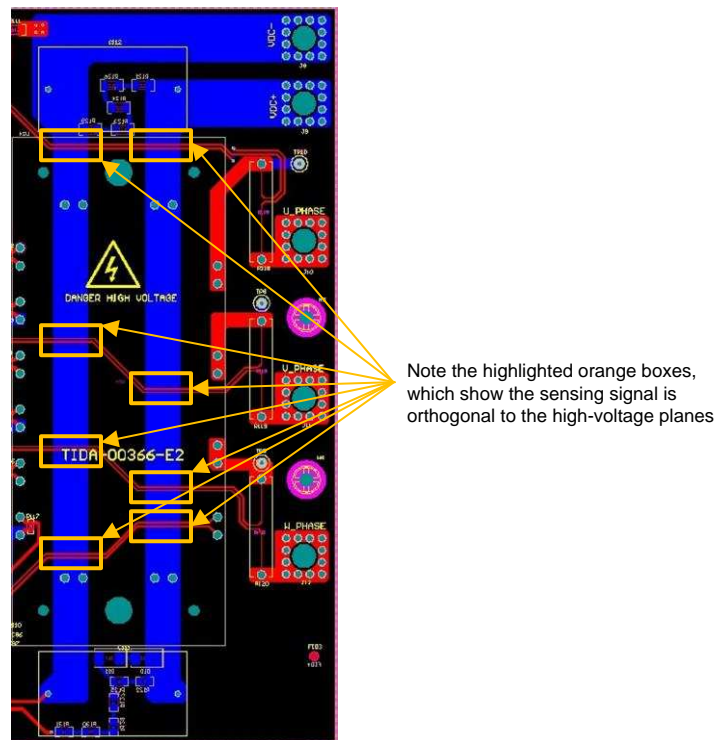


Figure 91. Sensing and High-Voltage Planes

7.3.1 Layout Prints

To download the layer plots, see the design files at [TIDA-00366](#).

7.4 Altium Project

To download the Altium project files, see the design files at [TIDA-00366](#).

7.5 Gerber Files

To download the Gerber files, see the design files at [TIDA-00366](#).

7.6 Assembly Drawings

To download the assembly drawings, see the design files at [TIDA-00366](#).

8 Related Documentation

1. Texas Instruments, [LAUNCHXL-F28027 C2000 Piccolo LaunchPad experimenter kit user's guide](#)

8.1 商標

All trademarks are the property of their respective owners.

9 Terminology

PWM— Pulse width modulation

MCU— Microcontroller unit

IGBT— Insulated bipolar gate transistor

RPM— Rotation per minute

RMS— Root mean square

NTC— Negative temperature coefficient thermistor

10 About the Authors

VAIBHAVI SHANBHAG is a systems engineer at Texas Instruments, where she is responsible for developing reference design solutions with a focus on Motor Drive segment within Industrial Systems. Vaibhavi received her bachelor of engineering in Electrical and Electronics from BITS Pilani, Goa.

N. NAVANEETH KUMAR is a systems architect at Texas Instruments, where he is responsible for developing subsystem solutions for motor controls within Industrial Systems. N. Navaneeth brings to this role his extensive experience in power electronics, EMC, analog, and mixed signal designs. He has system-level product design experience in drives, solar inverters, UPS, and protection relays. N. Navaneeth earned his bachelor of electronics and communication engineering from Bharathiar University, India and his master of science in electronic product development from Bolton University, UK.

11 Recognition

The authors would like to recognize the excellent contribution of **SANJAY PITHADIA** and **NELSON ALEXANDER** for the design and documentation of TIDA-00366 reference design.

改訂履歴

資料番号末尾の英字は改訂を表しています。その改訂履歴は英語版に準じています。

Revision B (September 2016) から Revision C に変更	Page
ドキュメント全体を通して UCC21520 を UCC21530 に変更	1
「概要」に AMC1311 を追加	1
「設計リソース」から TIDA-00195、TLV70433、SN74LVC1G10 を削除	1
「設計リソース」に TIDA-00199、TLV70450、SN74LVC1G11、SN74VC1G32 を追加	1
「特長」に広帯域幅を追加	1
paragraph to System Description 追加	3
information to Key System Specifications table 追加	4
block diagram image 変更	5
DC-Link and NTC voltage as signals measured by the AMC1301 and AMC1311 追加	6
UCC21520 to UCC21530 in Highlighted Products 変更	6
AMC1311 to Highlighted Products 追加	6
information regarding AMC1301 to Highlighted Products 追加	7
TLV70433 to TLV70450 in Highlighted Products 変更	7
SN74LVC1G10 to SN74LVC1G11 in Highlighted Products 変更	8
SN74LVC1G32 to Highlighted Products 追加	8
terminals, capacitors, and values in DC Bus Voltage Input section 変更	9
DC Input image 変更	9
Bleeder Resistors image 変更	9
current carrying capacity from 75 A to 85 A 変更	11
MG1250H XN2MM to MIXA60W1200TED 変更	11
Littlefuse Inc. to IXYS throughout document 変更	11
IGBT Module Connections image 変更	11
resistors that connect the reference points 変更	11
Grounding Scheme image 変更	11
information in Isolated IGBT Gate Driver section 変更	12
Functional Block Diagram of UCC21530 image 変更	12
Gate Driver UCC21530 and Related Components and Circuits image 変更	13
Gate Driver Power Supply image 変更	14
Gate Resistors image 変更	17
information in Isolated Current Sensing Circuit section 変更	18
Reinforced Isolated Amplifier AMC1301 image 変更	18
Power Supply Generation Using TL431B image 変更	19
Differential-to-Single Ended Signal Conversion image 変更	21
information in DC Bus Voltage Sensing Circuit section 変更	22
DC Bus Voltage Sensing Circuit image 変更	22
Calculation of Gain for Differential to Single Ended Conversion for Voltage Sensing section 追加	22
Component Selections section 追加	23
information in NTC Temperature Sensing Circuit section 変更	24
NTC Temperature Sensing Circuit image 変更	24
resistors for setting the threshold 変更	25
Overload Protection Circuit image 変更	26
information in Ground Fault Protection section 変更	26
Ground Fault Detection Circuit image 変更	27
information in Gate Logic for ENABLE Signal section 変更	28
ENABLE Logic Generation image 変更	28
20-Pin Connector to Connect With Connectors J6 and J2 on LAUNCHXL-F28027 image 変更	30
20-Pin Connector to Connect With Connectors J1 and J5 on LAUNCHXL-F28027 image 変更	31
information in Power Supplies section 変更	31

• 3.3-V Generation From 5-V Input image 変更	34
• 5-V Generation From 16-V Gate Drive Power Supply Input image 変更	35
• 1.65-V and 3.3-V Reference Generation image 変更	35
• Top View of PCB for TIDA-00366 image 変更	36
• information in Connectors table 変更	37
• information in Test Data section 変更	39
• 5-V Rail Generated Using TLV70450 image 変更	40
• Ripple on 5-V Rail Generated Using TLV70450 image 変更	40
• PWM at the Gate Driver Output image 変更	44
• PWM at Gate Driver Output—Dead Time (Rising Edge) image 変更	45
• PWM at Gate Driver Output—Dead Time (Rising Edge) image 変更	45
• Startup Sequence (PWM at Gate Driver Output) image 変更	46
• Low-Side Gate Driver UVLO image 変更	47
• High-Side Gate Driver UVLO image 変更	47
• information in Verification of ENABLE Logic section 変更	52
• ENABLE Logic for Gate Drivers image 変更	52
• information in Timings for ENABLE Logic table 変更	52
• Accuracy of Measurement section 削除	55
• Uncalibrated Percentage Full-Scale Error vs DC-Link Voltage at No Load image 変更	56
• Uncalibrated Percentage Full-Scale Error vs DC-Link Voltage at No Load With Current image 変更	56
• Histogram of DC-Link Sensing Measuring 600 V With 3 A _{RMS} in Motor image 変更	57
• Latching of OVERLOAD Detect Signal on TRIP Pin image 変更	60
• Latching of GND_FAULT Detect Signal on TRIP Pin image 変更	62
• Top Layer image 変更	65
• Bottom Layer image 変更	65
• GND Layer image 変更	66
• PWR Layer image 変更	66
• Gate Driver and Current Sensing Circuit image 変更	67
• Grounding for High-Side and Low-Side IGBT Gate Drivers image 変更	68
• Power Planes for High-Side and Low-Side IGBT Gate-Drivers image 変更	68
• Return Path image 変更	69
• Shorting Link image 変更	70
• DC Bus Sensing Section image 変更	71

Revision A (July 2016) から Revision B に変更
Page

• PROPAGATION DELAY of 表 12 変更	53
• 図 62 変更	53
• 図 63 変更	53
• 図 64 変更	53
• 図 65 変更	53
• paragraph and 図 67 under 6.6.1 変更	55
• 図 67 変更	56
• 図 67 変更	56
• 図 67 変更	57

2016年6月発行のものから更新
Page

• プレビュー・ページから 変更	1
------------------------	---

重要なお知らせと免責事項

TI は、技術データと信頼性データ(データシートを含みます)、設計リソース(リファレンス・デザインを含みます)、アプリケーションや設計に関する各種アドバイス、Web ツール、安全性情報、その他のリソースを、欠陥が存在する可能性のある「現状のまま」提供しており、商品性および特定目的に対する適合性の黙示保証、第三者の知的財産権の非侵害保証を含むいかなる保証も、明示的または黙示的にかかわらず拒否します。

これらのリソースは、TI 製品を使用する設計の経験を積んだ開発者への提供を意図したものです。(1) お客様のアプリケーションに適した TI 製品の選定、(2) お客様のアプリケーションの設計、検証、試験、(3) お客様のアプリケーションに該当する各種規格や、その他のあらゆる安全性、セキュリティ、規制、または他の要件への確実な適合に関する責任を、お客様のみが単独で負うものとし、

上記の各種リソースは、予告なく変更される可能性があります。これらのリソースは、リソースで説明されている TI 製品を使用するアプリケーションの開発の目的でのみ、TI はその使用をお客様に許諾します。これらのリソースに関して、他の目的で複製することや掲載することは禁止されています。TI や第三者の知的財産権のライセンスが付与されている訳ではありません。お客様は、これらのリソースを自身で使用した結果発生するあらゆる申し立て、損害、費用、損失、責任について、TI およびその代理人を完全に補償するものとし、TI は一切の責任を拒否します。

TI の製品は、[TI の販売条件](#)、または [ti.com](https://www.ti.com) やかかる TI 製品の関連資料などのいずれかを通じて提供する適用可能な条項の下で提供されています。TI がこれらのリソースを提供することは、適用される TI の保証または他の保証の放棄の拡大や変更を意味するものではありません。

お客様がいかなる追加条項または代替条項を提案した場合でも、TI はそれらに異議を唱え、拒否します。

郵送先住所 : Texas Instruments, Post Office Box 655303, Dallas, Texas 75265

Copyright © 2022, Texas Instruments Incorporated